ÇUKUROVA UNIVERSITY
INSTITUTE OF NATURAL AND APPLIED SCIENCE

MSc THESIS

Can Onur TOKUNÇ

MODELING OF A SHUNT ACTIVE POWER FILTER WITH EPLL BASED CONTROL METHOD FOR MITIGATION OF POWER QUALITY PROBLEMS CAUSED BY INDUCTION FURNACES

DEPARTMENT OF ELECTRICAL AND ELECTRONICS ENGINEERING

ADANA, 2010

ABSTRACT

MSc THESIS

MODELING OF A SHUNT ACTIVE POWER FILTER WITH EPLL BASED CONTROL METHOD FOR MITIGATION OF POWER QUALITY PROBLEMS CAUSED BY INDUCTION FURNACES

Can Onur TOKUNÇ

ÇUKUROVA UNIVERSITY
INSTITUTE OF NATURAL AND APPLIED SCIENCES
DEPARTMENT OF ELECTRICAL AND ELECTRONICS ENGINEERING

Supervisor : Asst. Prof. Dr.K. Çağatay BAYINDIR
: Year: 2010, Pages:147
Jury : Asst. Prof. Dr.K.Çağatay BAYINDIR
: Prof. Dr. Mehmet TÜMAY
: Yrd. Doç. Dr. Ramazan ÇOBAN

Modern induction furnaces become popular with the development of power electronic converters. Current source coreless induction furnaces are used in metal melting processes because of the advantage of power circuit for high power applications. Besides the advantages, current source coreless induction furnace has unfamiliar power quality problems such as varying harmonics and interharmonics.

In this thesis a current source coreless induction furnace is modeled and power quality problems are presented. A shunt active power filter with EPLL based control method together with detuned harmonic filters for reactive power compensation is proposed to mitigate the power quality problems caused by current source coreless induction furnace.

Performance of the proposed method is evaluated with case studies using PSCAD / EMTDC.

Key Words: Three phase shunt active filter, Induction furnace, enhanced phase locked loop, power quality, interharmonics

ÖZ

YÜKSEK LİSANS

İNDÜKSİYON OCAKLARININ NEDEN OLDUĞU GÜÇ KALİTESİ PROBLEMLERİNİ AZALTMAK İÇİN PARALEL AKTİF GÜÇ FİLTRESİNİN EPLL TABANLI KONTROL METODU İLE MODELLENMESİ

Can ONUR TOKUNÇ

ÇUKUROVA ÜNİVERSİTESİ
FEN BİLİMLERİ ENSTİTÜSÜ
ELEKTRİK ELEKTRONİK MÜHENDİSLİGİ ANABİLİM DALI

Danışman : Yrd. Doç. Dr.K. Çağatay BAYINDIR
: Yıl: 2010 Sayfa:147
Jüri : Yrd. Doç. Dr.K. Çağatay BAYINDIR
: Prof. Dr. Mehmet TÜMAY
: Yrd. Doç. Dr. Ramazan ÇOBAN

Güç elektroniği dönüştürücülerinin gelişmesiyle modern indüksiyon ocakları popüler hale gelmektedir. Akım beslemeli çekirdeksiz indüksiyon ocakları büyük güçteki uygulamalarda güç devresinin avantajından dolayı metal eritme proseslerinde kullanılmaktadır. Akım beslemeli indüksiyon ocakları bu avantajlarının yanında alışkın olunmayan değişken harmonikler ve ara harmonikler gibi güç kalitesi problemleri vardır.

Bu tezde akım kaynaklı çekirdeksiz indüksiyon ocağı modellenmekte ve güç kalitesi problemleri sunulmaktadır. Akım beslemeli çekirdeksiz indüksiyon ocağından kaynaklanan güç kalitesi problemlerini azaltmak için EPLL kontrol metotlu paralel aktif güç filtresi ile reaktif güç kompansazyonu için pasif harmonik filtresi önerilmektedir.

Önerilen metodun performansı PSCAD/EMTDC programında farklı durum çalışmalarıyla değerlendirilmektedir.

Anahtar Sözcükler: Üç faz aktif filtre, indüksiyon ocağı, geliştirilmiş faz kilitlemeli döngü, güç kalitesi, ara harmonik

ACKNOWLEDGEMENTS

First of all it is a pleasure to thanks both Prof. Dr. Mehmet Tümay and Asst. Prof. Dr. K.Çağatay Bayındır who made this thesis possible with their understanding and giving me a chance to choose subject in parallel with my working area and unforgettable contribution.

I would like to express my deepest gratitude to my supervisor Asst. Prof. Dr. K.Çağatay Bayındır not only for his guidance, criticism, encouragements and also for his useful suggestions and continuous confidence in me. He has made available his support in a number of ways to improve and finalize this thesis.

I owe special thanks to Adnan Tan for his companionship and cooperation during my study. I could have never completed this thesis without his support and generous help.

I would like to thanks for accepting to be the members of examining committee for my thesis.

I would like to show my gratitude also to my manager Mr. N. Savaş Seçen, chief engineer Mr. Harun Tokmak and colleagues for their understanding, patience and continuous support during my study.

I would like to thank MSc. Ahmet Teke, Mehmet Uğraş Cuma for their suggestions, encouragement and valuable technical discussion.

I wish to thanks to my closest friends for their understanding and support during my hard times.

Finally I would like to express my dippiest thanks to my lovely family my mother Semra Tokunç and my father Hakkı Tokunç and my brother Okan Tokunç without whose support I would have never been able to aspire for this level of education .

CONTENTS **PAGE**

LIST OF TABLES **PAGE**

LIST OF FIGURES **PAGE**

LIST OF SYMBOLS

V_c	Capacitor voltage
V_{max}	Maximum voltage
f_o	Operating frequency
Ic	Compensating current
I_L	Load current
P_1	Instantaneous Real power
q_1	Instantaneous Imaginary power
α	Alfa component
β	Beta component
I_S	Source current
i_a	Phase A current
i_b	Phase B current
i_c	Phase C current
Va	Phase A voltage
Vb	Phase B voltage
Vc	Phase C voltage
$\bar{p}$	D.C. component of real power
$\tilde{p}$	A.C component of real power.
$\bar{q}$	D.C. component of imaginary power
$\tilde{q}$	A.C. component of imaginary power
i_F	Current reference signal
i_L^+	Positive sequence current
i_L^-	Negative sequence current
i_L^0	Zero sequence current
i_d	d-q frame d component current
i_q	d-q frame q component current
V^f_a	Phase A voltage fundamental component
V^-_a	Phase A voltage negative sequence component

V^{h}_{a}	Phase A voltage negative harmonic component
V^{+}	Instantaneous positive-sequence components of the voltage
I^{+}	Instantaneous positive-sequence components of the current
Ø	Phase displacement between voltage and current
i_a^{+}	Active component of fundamental current
i_r^{+}	Reactive component of fundamental current
F_a	Phasors of phase A
V_{DC}	Capacitor voltage of active filter
Qc	Capacitive power
V	Nominal line voltage
Xc	Capacitive impedance
F_L	Line frequency
C	filter capacitor
F_R	Resonance frequency
L	filter inductance
A	Amplitude
V_{REF}	Reference value of capacitor voltage

LIST OF ABBREVATIONS

DRI	Direct Reduced Iron
EAF	Electric Arc Furnace
BOF	Basic Oxygen Furnace
AC	Alternating Current
DC	Direct current
EU	European Union
IF	Induction Furnace
LMF	Ladle melt furnace
PQ	Power Quality
IEC	International Electrotechnical Commission
UPS	Uninterruptable Power Supply
IEEE	The Institute of Electrical and Electronics Engineers
PCC	Point of common coupling
SCR	Short Circuit Ratio
TDD	Total demand distortion
IGBT	insulated gate bipolar transistor
APF	Active Power Filter
DVR	Dynamic voltage restorer
UPQC	Unified Power Quality Conditioner
PWM	Pulse Width Modulation
GTO	Gate Turn Off THYRİSTOR
SAPF	Shunt active power filter
NPC	neutral-point-clamped
PLL	Phase locked loop
FFT	Fast Fourier Transform
IRP	Instantaneous Reactive Power Compensation
HPF	High Pass Filter
LPF	Low Pass Filter
SVM	Space vector modulation

DFT	Discrete Fourier Transform
EPLL	Enhanced Phase Locked Loop
SC	Symmetrical component
VSI	Voltage Source Inverter
RMS	root mean square
pu	per unit
PI	Proportional Integral

1. INTRODUCTION

Steel is crucial to the development of any modern economy and is considered to be the backbone of human civilisation. The level of per capita consumption of steel is treated as an important index of the level of socioeconomic development and living standards of the people in any country. It is a product of a large and technologically complex industry having strong forward and backward linkages in terms of material flows and income generation. All major industrial economies are characterized by the existence of a strong steel industry and the growths of many of these economies have been largely shaped by the strength of their steel industries in their initial stages of development.

The Turkish iron and steel sector, in existence since the late 1930's, is growing rapidly, swiftly making Turkey one of the largest producers of crude steel in the world. In 2006, Turkey reached an annual production of 23.3 million tons of crude steel, which increased to 25.6 million tons in 2007 – enough to place it as the 11^{th} largest producer worldwide and third in Europe.

The new level of crude steel is 78 percent higher than it was in 2001, representing a huge boon for the industry. Turkey has also proven to be a good consumer of iron and steel, with consumption up to 18.5 million tons – a 110 percent increase since 2001(Istanbul Chamber Of Commerce,2008).

The steel industry is the largest energy-consuming industry in the world. Currently, energy represents about 20% of the total cost of producing steel and is rising. The increasing cost of energy and even its current and future availability have led to the need to refocus attention on energy intensity in steel production (American Iron And Steel Industry Institute, 2005).

The iron and steel sector covers the production of crude steel via the primary and secondary production routes, including the pre-production steps coke making, sintering and pelletisation, as well as further processing of ferrous metals.

The production of crude steel is in principle carried out via two routes, differing as well in the metallurgical process, energy input and process emissions as in the quality and application purpose of the products. Starting from iron ore, BOF

crude steel is produced via the production of hot metal in a blast furnace and its following conversion to crude steel in a basic oxygen furnace, while EAF steel is produced by the smelting of scrap or direct reduced iron in an electric arc furnace.

The production of BOF steel requires two preceding processes, namely coke making and sintering. The process of coke making is the conversion of coal to coke by heating of coal in absence of air (or oxygen) to remove the volatile components and other substances like tars, which will be contained in coke oven gas. In the sintering process, iron ores of different grain size are agglomerated together with additives to create a material feed for the blast furnace with improved permeability and reducibility. Hot metal is most commonly produced in blast furnaces that are fed with sinter, coke and additives. To make best possible use of the heat of roughly 1600°C, hot metal is conveyed as fast as possible to the basic oxygen furnace, where its conversion to crude steel takes place. Oxygen is blown through molten hot metal in the BOF in order to drive out the carbon content. Scrap is added to the BOF to be able to control the reaction and keep the temperature within limits.

Alternatively to the blast furnace process iron ore can also be converted into metallic iron in a direct reduction process. The product yielded is often referred to as “direct reduced iron (DRI)” or “sponge iron”. Direct reduced iron is used instead of scrap as input for electric arc furnaces (ECOFYS, 2009).

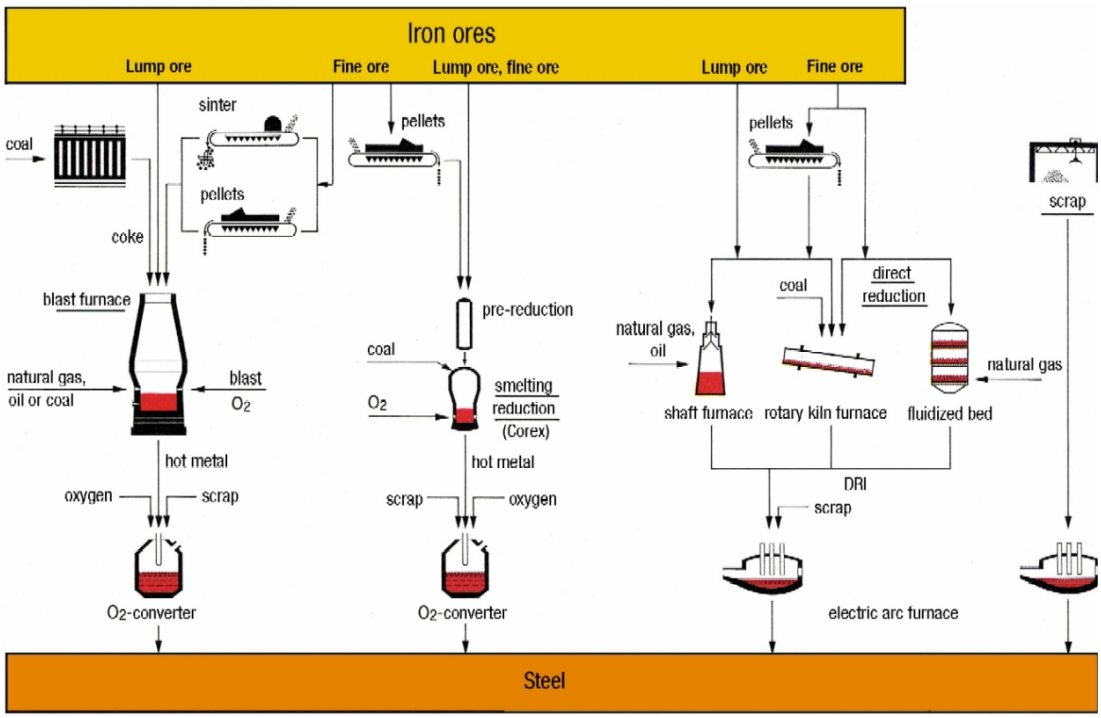

Figure 1.1 Crude steel production processes (ECOFYS, 2009)

In the electric steel process, the heat required is obtained not by oxygen combustion of the accompanying elements in the pig iron, but from electrical energy. The conversion of electrical energy into heat can be achieved by an electric or, induction furnace. Electric steel processes are based on the use of scrap, with small amounts.

Over 90 % of all electric steel produced is by the use of the A.C. electric arc furnace. Three graphite electrodes carry the current through the furnace roof into the charge of metal. The electric arc formed melts the charge at temperatures up to 3500°C. The Furnace has the following essential components: the vessel or shell with a furnace door and a tapping hole; the roof which can be removed for charging; electrode arms which support the electrodes; tilting equipment for emptying the furnace; the furnace transformer; and the measuring and control equipment (Quass et.al, 2007). The flicker and harmonics generated by electric arc furnaces present a problem that is well known to both the steel industry and electrical utilities. The familiar methods to completely resolve that power quality problems are to install a dynamic static reactive power compensation device (SVC).

One of the most economic ways of producing steel is made through the use of induction furnaces. Usually a typical induction furnace is designed with a topology formed by an AC – DC converter (rectifier), a filter and a DC – AC converter (inverter). Converters are highly used in industrials. Often these converters that are used in the induction heating furnaces have a three phase rectifier and a single phase inverter. In these converters, load is coil of induction heating furnace that can be controlled in the form of parallel and series with a capacitor bank. If changing current of switches of inverters are varied by changing current load naturally. The block diagram of induction furnace is shown in Figure1.2.

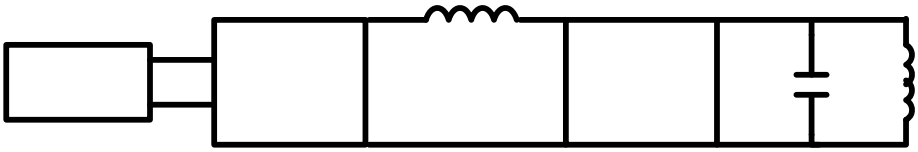

Figure 1.2 Block diagram of an actual induction heating furnace

The problem with this kind of furnaces, from an electrical point of view, is the creation of a considerable harmonic distortion. The cause of the distortion is within the induction furnace design and operation. An induction furnace works melting the scrap using a medium frequency magnetic field created by a coil. The coil is fed by the medium frequency AC current supplied by an inverter which is fed by a DC current converter connected to the AC distribution network supply.

As the created distortion is very high and affects the voltage supplied by the distribution network, it is highly possible that other loads supplied from the same network will be affected. In this case, it is necessary to have corrective actions in order to fulfill the legislation concerning voltage harmonic distortion.

Some power electronic loads are capable of producing currents over a whole range of frequencies, which has brought about increased interest in interharmonics. The electronically-controlled induction furnace is, perhaps, the epitome of such a load. This type of furnace has also become popular with small- to medium-sized casting operations that can be served from distribution systems. Traditional methods for solving harmonic problems did not work. Power quality analyzers not designed to

3 phase source Uncontrolled rectifier

display interharmonics gave confusing readings. Significant utility and consulting manpower was required to diagnose and solve the problem.

In the literature induction furnace isn't modeled in detail. Although there are many papers about design and electromagnetic analysis of modern coreless induction furnaces, it is seen that there are fewer papers that focus on power quality problems and solution of these problems in modern induction furnaces. Various solutions of these problems for induction furnaces are clearly discussed in (Dugan et al., 1999). The other effective paper is (Rudnev et al., 1999) which introduces the differences between current source and voltage source induction furnaces and power quality problems of furnaces. Moreover, the interharmonics and voltage fluctuation power quality problems of current source furnaces are presented and different solutions are discussed. In (Zamora et al., 2003) the model of steel plant which contains both voltage source and current source furnaces and the model of active power filter which is designed to solve the power quality problems of furnaces are presented. However, only the odd harmonic problems of furnaces are indicated. There is no explanation about the interharmonics problem of current source furnaces. In (Unnikrishnan et al., 2006) a three level STATCOM is set up for the solutions of 12 pulse current source induction furnace in India. Although the paper presents an experimental study, the interharmonic problems of induction furnace are not discussed.

In this thesis, the current source induction furnace is modeled in PSCAD/EMTDC and the varying harmonics and interharmonics power quality problems of furnace are presented clearly. Harmonics and interharmonics are produced by the induction furnace in wide spectrum. To solve the power quality problems of current source induction furnace, a power quality compensation system which is consists of from shunt APF and shunt passive filter combination is proposed. The classical control methods of shunt APF such as d-q method, discrete FFT method aren't remedied. Shunt APF is designed for compensating the varying harmonics and interharmonics problems and reactive power compensation of current source induction furnace with using effective controller based on EPLL. Passive

filter which is formed from 4 - step is designed for reactive power compensation to reduce the ratings of shunt APF.

The content of the thesis is arranged as follows:

After this introductory chapter, Chapter 2 Steel Production Methods and Turkey Iron and Steel Industry are discussed.

In chapter 3, Induction furnace operation, power quality problems and solutions are deeply explained.

In chapter 4, Operation principles of induction furnace are deeply discussed and modeling of induction furnace is presented.

In chapter 5, Operation principle of shunt active filter and detuned passive filter are explained, proposed control algorithm is deeply analyzed, proposed shunt active filter and passive filter are modeled.

In chapter 6, Simulation results and different case studies are presented.

In chapter 7, the important conclusions of the study are explained.

2. STEEL PRODUCTION METHODS AND TURKEY IRON AND STEEL INDUSTRY

2.1. Steel Production Methods

Steel is used widely in all sectors of modern society, which could not exist without steel. Steel is also a globally manufactured and traded commodity. Production levels have been quite stable in industrialized countries, but demand has increased massively in developing countries. Annual production of steel increased to more than 1000 million tones for the first time in 2004. The year 2004 was also noteworthy because, Chinese steel production and use surpassed production and use in the second biggest market, the European Union (EU).

Globally, the construction sector is the biggest steel user followed by other structural steelworks, mechanical engineering, car manufacturing and metal goods. The construction sector has a large share especially in urbanizing developing economies. Despite current global regression, most sectors using steel are still growing and the general market situation for the steel sector on a global scale is positive.

Approximately one-third of all manufactured steel is internationally traded, but transfer distances are usually not long due to relatively high transfer costs. Low value products are least profitable to transfer, but highly specified products can be traded across very long distances. This is why most of the new capacity is built near where there is new demand.

Steel production technology is mature and well-established. During the last decades, there have been no major innovations, and it is likely that the next generation of steel producing technologies will require more than 20 years of research. At the same time, other drivers have changed quickly. The most significant changes have been sharply increasing steel demand, the beginning of greenhouse gas emission regulation and soaring prices of both raw material and products.

Other materials can replace steel in certain products, e.g., aluminum in cars or wood in buildings, but currently these options are minor and the steel industry have replied to these challenges by designing specific steel alloys for these purposes.

Overall, customer-specific steel quality and products are the competitive advantage of many western steel mills (Lindroos, 2009).

Currently, there are two main routes for the production of steel: production of primary steel using iron ores and scrap and production of secondary steel using scrap as the main raw material. A wide variety of steel products are produced by the industry, ranging from slabs and ingots to thin sheets, which are used in turn by a large number of manufacturing industries (Price et al.,2001).Steel production requires several steps that can be accomplished with different processes. Both the input material of each step and the process substantially affect the total energy consumed during production.

Different parts of steel manufacturing processes are usually very closely integrated at a plant level. Every installation has a unique combination of process integrations, fuels, raw materials, etc. This intricate issue can again be simplified. To sum up, steel can be produced by two processes: basic oxygen furnace (BOF) or electric arc furnace (EAF). Figure 2.1 shows the general block diagram of the steel production (Lindroos, 2009).

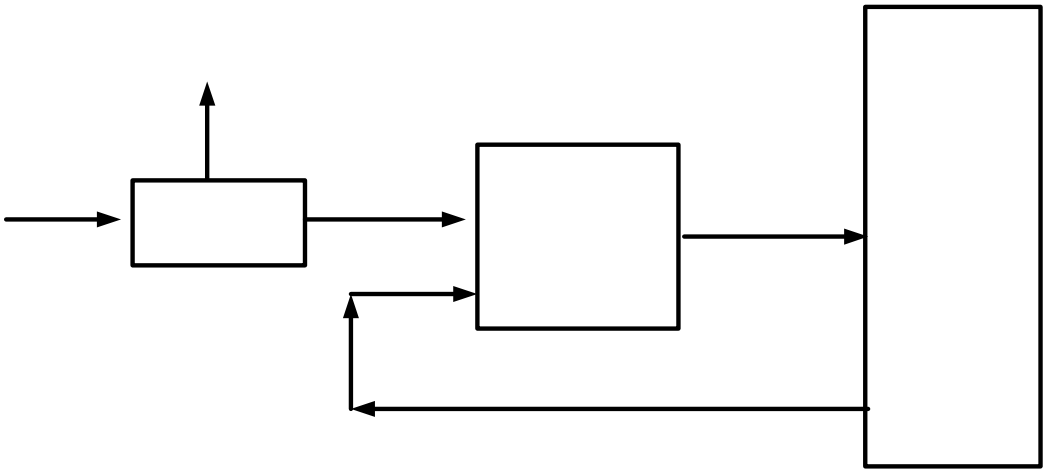

Figure 2.1 General Block diagram of the steel production

2.1.1. The Primary Steel Production

In essence, all primary iron and steel production processes are based on the same chemical reactions. In iron ore, iron is presented in its oxidized form. In iron

reduction processes, a reducing agent, based on carbon or hydrogen, removes the oxygen from the iron. This removal can take place either above or below the melting point of the ore and the reduced iron.

Reduction above the melting point results in pig iron. Above the melting point, most of the gangue materials segregate from the liquid iron, and float upon it. Because of the high temperature and the liquid state of the iron, carbon readily dissolves in the pig iron, resulting in typical carbon contents between 4 and 6%. Reduction and dissolution of some of the gangue material may result in silicon and manganese contents of about 1%, depending on the ore composition and process conditions. In addition, pig iron contains some sulphur and phosphorus.

Oxygen blowing converts the pig iron to steel by oxidation of the carbon, silicon, and phosphorus. The carbon escapes mainly as carbon monoxide, while the oxidized silicon, sulphur and phosphorus segregate into the slag. This segregation process is enhanced by addition of flux materials, such as lime.

Reduction below the melting point results in directly reduced iron (DRI), which retains the original shape of the ore, and includes the gangue material present in the ore. At the temperature of reduction, the carbon of the reducing agent hardly dissolves in the iron; therefore DRI contains virtually no carbon. For conversion of DRI to steel, removal of the gangue material is necessary. Moreover, the carbon content has to be adjusted to the required amount. Therefore, melting the DRI is necessary to convert the DRI to steel.

Although the chemical reactions involved in the various steel production methods are very similar, steel producing installations and the flows therein are very different. Therefore, the various production routes have different demands with regard to resources. Iron ore occurs as lump ore and fine ore, and the latter is often processed into sinter or pellets. Both natural gas and coal are used as reducing agents. The blast furnace requires the conversion of an important share of the coal to coke. The demands with regard to the resources and necessary pre-processing steps strongly influence costs, energy-use and emissions of the various routes leading from ore to steel.

Figure 2.2 shows processes for steel production.

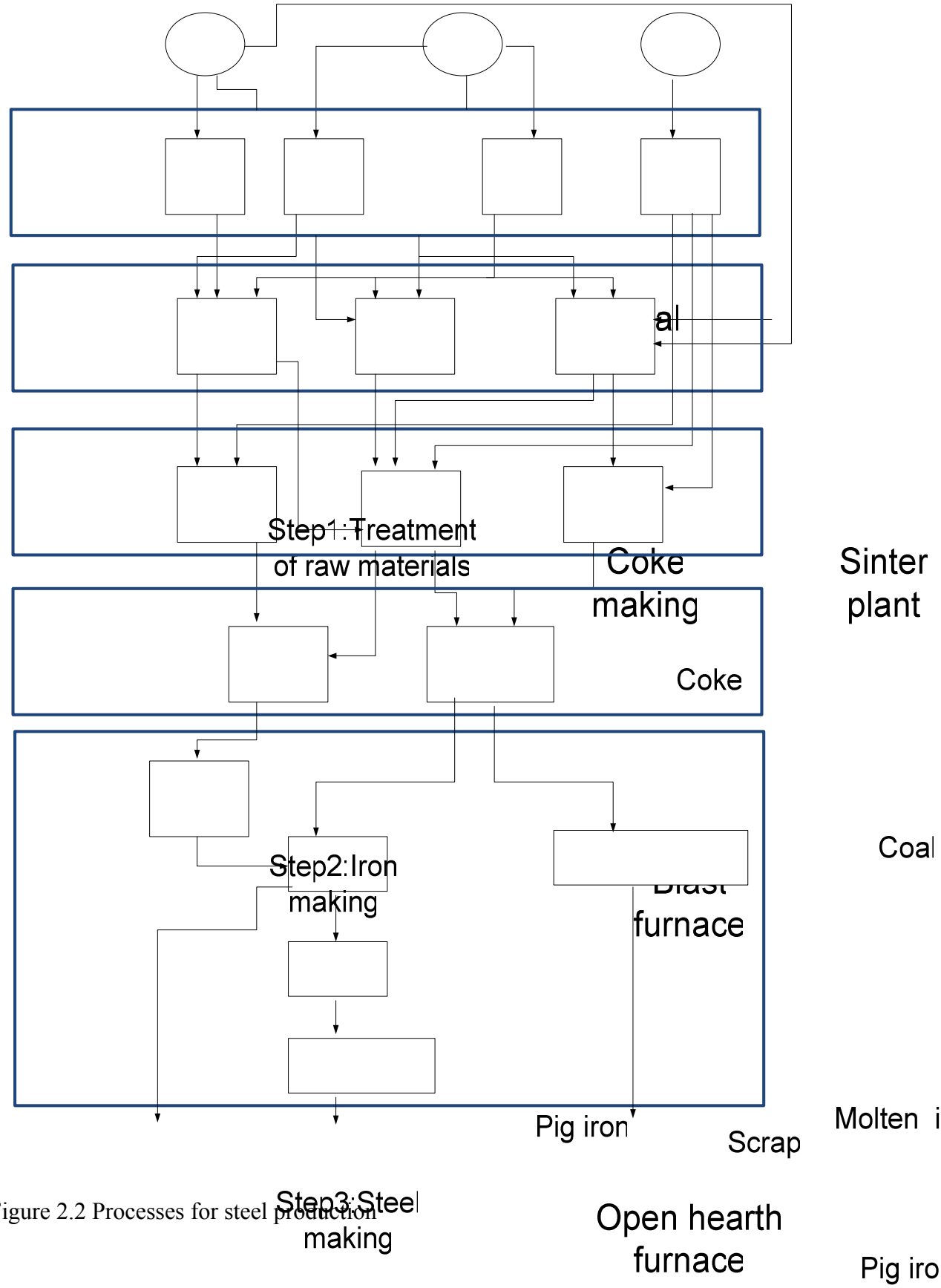

Figure 2.2 Processes for steel production

The oxygen steel production chain starts from iron ore, which is pelletized or sintered and fed into the blast furnace with coke and air. Iron ore is a mixture of iron and oxygen, and the most common form of iron ore is hematite (Fe2O3). Taking the oxygen out of iron is called reducing. There is theoretical minimum for required reduction agents, but it can be made with fuels containing only carbon or hydrogen.

In modern technology, the reducing is done mostly with carbon monoxide (CO), which burns with oxygen from iron ore and forms carbon dioxide (CO2). One source of the study concluded that the theoretical minimum of CO2 emissions from the reduction of iron ore without hydrogen is 1415 kgCO2/ tone of reduced iron. The emissions of the best available technology were around 1500 kgCO2/ tone of reduced iron.

Small amounts of carbon monoxide can be replaced with hydrogen from oil or natural gas. Hydrogen and oxygen from iron ore form only water, which allows smaller emissions than represented emission limits with only coal.

After a blast furnace, reduced iron (pig iron) is shifted to a basic oxygen furnace (BOF), where it is converted to steel. In order to change or improve the properties of steel, various additives are fed in alongside the hot metal. Stainless steel, for example, contains chromium at least 11.5% of its mass. Basic oxygen furnaces can use also scrap steel to replace some pig iron. After the steel converter, liquid steel is cast, rolled and finished for use.

In the oxygen steel process, the blast furnace is, by far, the largest CO2 emitter. The reduction process of iron ore is a source of over 90% of oxygen steel greenhouse gas emissions. Future technologies will be more efficient, but existing blast furnaces will be the dominant technology for at least 20 or 30 years. There are also several other possibilities to decrease emissions below announced limits, for example natural gas or charcoal.

Figure 2.3 presents a more detailed scheme of the oxygen steel process, but it still lacks many processes, inputs and other details. Installations may include only a part of, or the entire, processes chain: for example, they may buy or produce the coke or iron pellets, and the installation may handle further processing itself or sell the crude steel. In addition, blast furnace gas and coke oven gas are burned to produce

power and heat, but the power plant may be owned by the steel producer or other company, and the steel installation may use all or just a part of the produced power and heat. These variations create a multitude of installation boundaries and a problematic definition of a sector boundary in sectoral approaches (Lindroos, 2009).

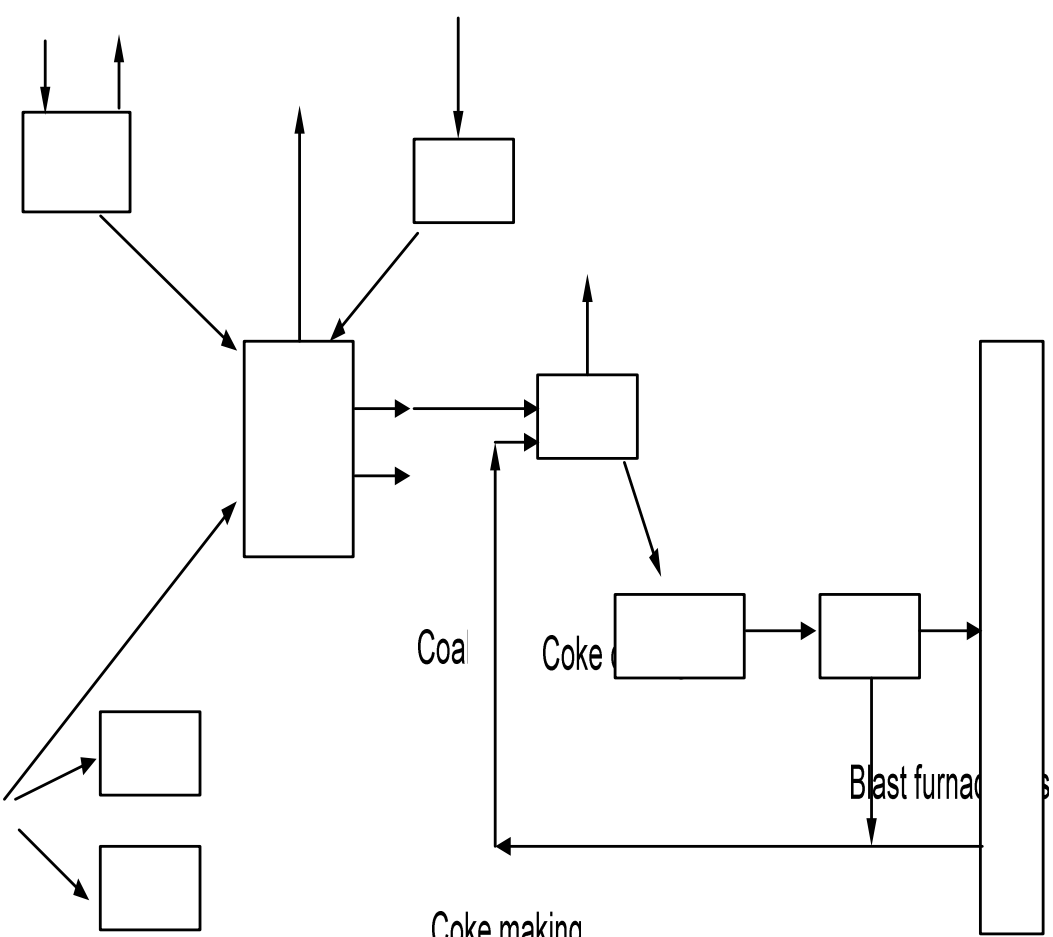

Figure 2.3 more detail scheme of the oxygen steel process chain

The blast furnace is the most energy-intensive step in an integrated steel mill and requires about 11-15 GJ per tones of pig iron produced. Of this amount approximately 7 GJ is used for the chemical reduction of iron ore to pig iron. In addition, energy input is required to raise the temperature to a level at which the chemical reduction can thermodynamically proceed at a sufficient rate. Carbon (from energy sources such as coal or coke) is used both as the reducing agent and as the energy input. The reducing agent (feedstock energy use) may constitute up to 50% of

the total energy demand of an integrated steel mill. Accounting for which proportion of energy input results in energy-related emissions and which results in process related emissions is ongoing (ANNEX I EXPERT GROUP, 2001).

2.1.2. The Secondary Steel Production

Secondary, or scrap based, production of steel is very straightforward. Melting steel scrap results in liquid steel, which can be shaped in the desired forms by casting, rolling and finishing (Lankford, 1985). Secondary steel is produced in an electric arc furnace (EAF) or in an induction furnace (IF) using scrap. The secondary steel industry includes so-called “mini-mills”, which make relatively simple products from low-priced scrap. In secondary steel production, the scrap is melted and refined, using a strong electric current. Several process variations exist, using both AC or DC currents, and fuels can be injected to reduce electricity use. Steel making based on external scrap (scrap from outside the steel sector) requires less than half as much primary energy as steel made from ore(Price et al.,2001).

2.1.2.1 Electric Arc Furnace

Electric arc furnaces (EAFs) are widely used in steelmaking and in smelting of nonferrous metals. The EAF is the central process of the so-called mini-mills, which produce steel mainly from scrap.

The electrical components in an EAF are fairly straightforward. The basic alternating current (AC) EAF consists of an EAF transformer and three carbon electrodes. These electrodes are connected to the EAF transformer secondary bus via short multiple runs of large conductor. Also, there are two variations of the EAF that see frequent usage today. The basic AC EAF now often has a multi-tapped series reactor in the circuit connected to the EAF transformer high-side connections. The other possible configuration is a direct current (DC) EAF. This version has a thyristor controlled power converter connected to the secondary of the EAF transformer and the output of this converter is connected between a single furnace

electrode and a plate in the bottom of the furnace shell. Most DC EAF's use a 12-pulse power converter but there are some exceptions.

One additional furnace type is the ladle melt furnace (LMF). This type furnace is used strictly for adjusting the molten metal temperature and/or metal chemistry. An LMF almost always has just a basic configuration. All these possible configurations are illustrated in Figure 2.4.

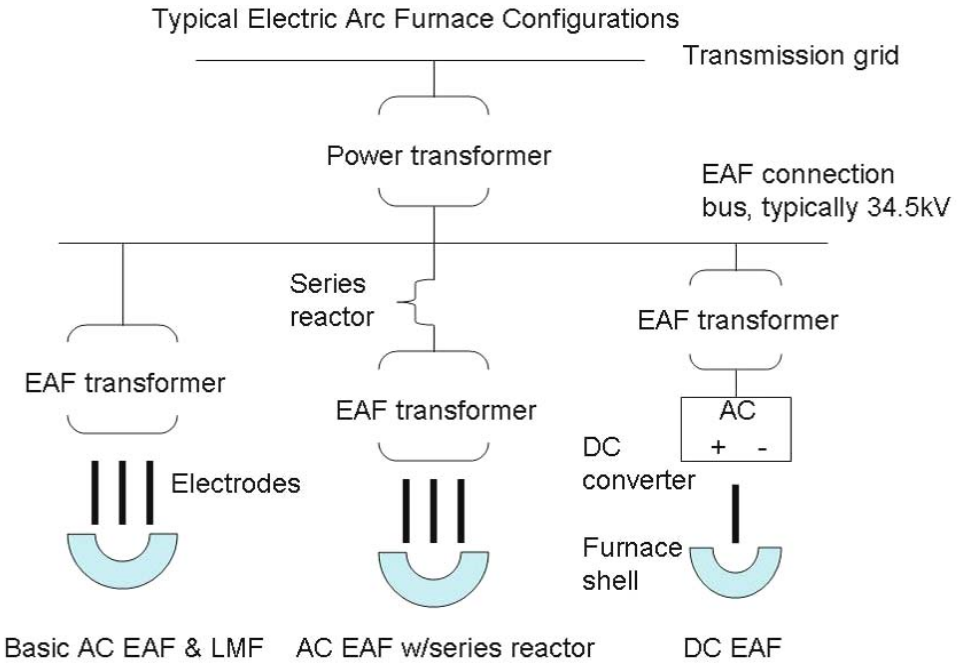

Figure 2.4 Single-lines of various EAF types (Burch, 2008).

Regardless of the configuration used, the actual operation of the EAF is the same. A graphical representation is illustrated in Figure 2.5. Scrap metal is placed in the furnace shell and the electrodes (or electrode in the case of a DC EAF), are lowered into the shell. The scrap metal completes the electrical circuit between the three phases causing basically an intentional short-circuit. The resulting heat due to this short circuit in turn melts the scrap into a molten state. This initial phase of melting is called the bore-in stage. During bore-in, the scrap starts out as various

assorted sizes placed in a random fashion into the shell. As the scrap melts, the remaining scrap collapses into the molten metal causing further melting. It is these collapses, called cave-ins, that contribute to the worse flicker caused by an EAF. As the scrap caves in, the scrap will move far enough from one or more electrodes such that the arc is extinguished. Each furnace electrode can be independently controlled hydraulically by a current sensing circuit. Once this circuit senses a loss or drop in current through that electrode, the hydraulics will move the electrode toward the scrap to reignite the arc. This action of striking an arc, extinguishing the arc, and re-striking the arc occurs over and over in a random manner for each electrode during the bore-in phase of melting. From an electrical perspective, this same process is the source of wide power swings on the utility grid which translate into potentially large voltage swings resulting in flicker.

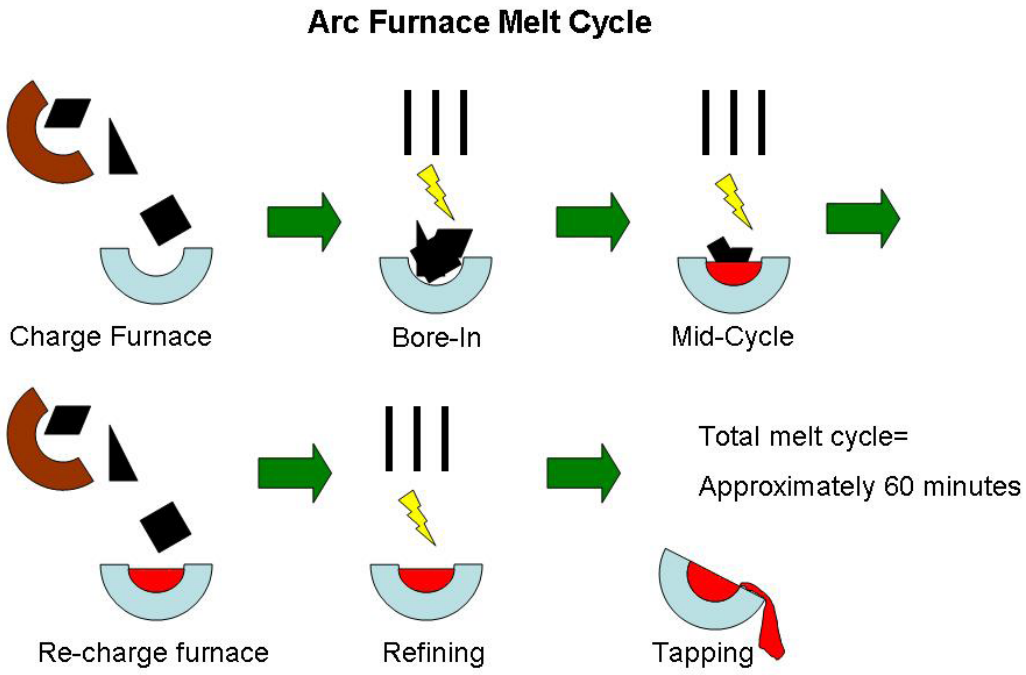

Figure 2.5 Typical melt cycle components (Burch, 2008)

Once the initial load of scrap, or charge, has melted some two things happen. The power swings will settle down as more molten metal is in the shell. This results in a much smoother operation. Also, the furnace shell will now accommodate a

second charge or load of scrap. When the second charge is added, there will again be an initial period of bore-in to reduce the new scrap to molten metal. Once all the scrap is molten, the EAF enters what is called the refining stage of the melt. Sometimes this is referred to as the flat bath stage. During this stage, the power level if fairly constant and the resulting voltage swings and flicker will be at a minimum.

While the above process is typical of all EAF's, the type of EAF used can limit both the power swings and the resulting flicker. By placing a series reactor in series with the EAF, as explained above, the power swings can be reduced during the bore-in phase. This is the predominate practice now for AC EAF operation. Also, the use of DC converter technology to provide DC power to the furnace electrode also reduces the resulting power swings and flicker (Burch, 2008).

2.1.2.2 Induction Furnace

The electric induction furnace differs from the electric arc furnace in that the metal is heated by induced electric current within the charge rather than by an arc. Induction furnaces are generally smaller than electric arc furnaces, and often they are used in iron and steel foundries and for special purposes such as melting under vacuum or in an inert atmosphere, and melting of relatively high-purity charge materials. The induction furnace is also used in combination with the cupola or EAF for increasing the metal temperature and as a holding furnace. Induction furnaces are used to a limited extent for melting special grades of steel. Steel castings also are made by some producers of steel ingots (Fenton, 2005).

The two most common induction melting furnace designs are the coreless and channel furnaces.

Channel type induction furnaces basically consist of a vessel to which one or more inductors are attached. The inductor is actually a transformer whereby the secondary winding is formed with the help of a loop of liquid metal confined in a closed refractory channel. In the furnace the energy is transformed from the power system at line frequency through a power supply to the inductor and converted into heat. One advantage of this type of furnace is that the vessel or upper case can be

built in any practical size & shape to suit the application. Figure 2.6 shows the typical channel type induction furnace

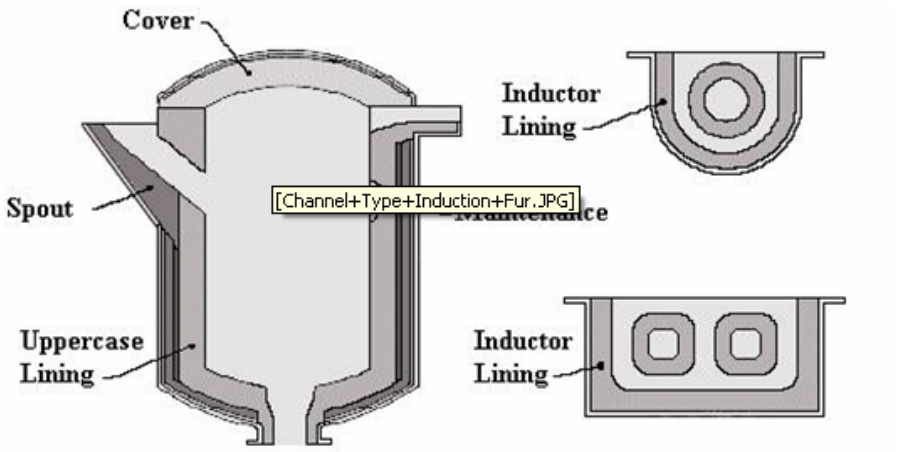

Figure 2.6 Channel type induction furnace (Web)

Coreless melting furnaces use a refractory envelope to contain the metal, and surround that by the coil. These furnaces are designed like a cylindrical crucible surrounded by a power coil in which energy is supplied either directly from the network (line frequency) or through a frequency converter. The magnetic field generated by the coil carries the energy to the charge. Figure 2.7 shows the coreless type induction furnace. Operating on the same basis as a transformer, the charge acts as a single secondary turn, thereby producing heat through eddy current flow when power is applied to the multi turn primary coil. When the metal melts, these electromagnetic forces also produce a stirring action. Mixing and melting rates can be controlled by carefully selecting frequency and power (Kiyoumarsi, 2008).

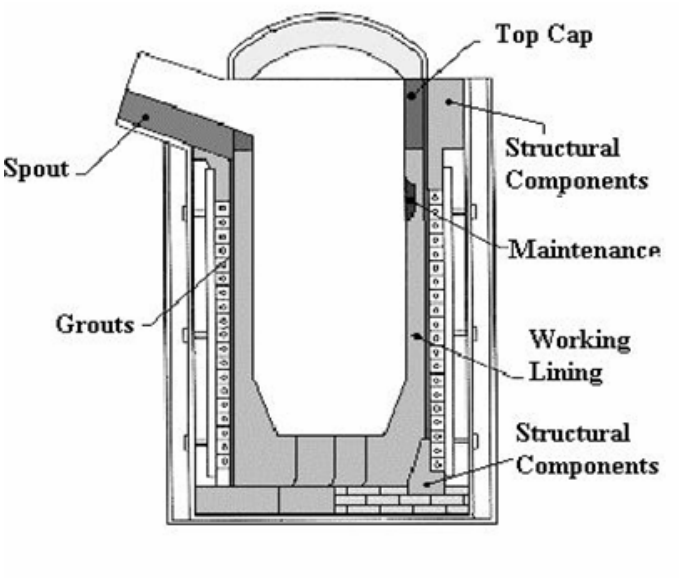

Figure 2.7 Coreless Type Induction Furnace (Web)

2.2. Turkey Iron And Steel Industry

Turkish steel industry, which has born when the first integrated iron and steel plant of the country Karabuk Iron and Steel Works (KARDEMIR) has started operation in 1939, has gain acceleration after Eregli Iron and Steel Works (ERDEMİR) and Iskenderun Iron and Steel Works (ISDEMIR) started to operate in years 1965 and 1975, respectively. Takeover of ISDEMIR by ERDEMIR on condition to transformation to flat production was the highest noteworthy development of the sector in the latest years. While the establishment of electrical arc furnace plants, which were started to be established with the affect of economical liberation moves starting from 1980's, form the most important building structure of the sectorial development, Turkish iron and steel industry shows big development in the last 20 years by means of both production and quality and become one of the most important steel producer countries. Turkey, which has produced 2.4 million tons of steel in 1980, increased its production to 9.3 million tons in 1990 and 14.3 million tons in 2000. Turkey has produced 25.75 million tons of steel in 2007 and it has become the 11th largest steel producer country of the world. Turkey, as a fast growing country in steel sector, has maintained its high growing rate in 2008 despite the effects of world financial crisis and the country increased its production by 4,1%

to 26.81 million tons. Turkish steel exports has reached 2.5 billion USD record value in August 2008, and then became 2.2 billion in September, 1.2 billion in October, 824 million in November, 860 million in December.

Turkey was the world's 11th steel producer with a total production of 20.9 million tonnes in 2005, accounting for 2.0% of total world steel production. It ranked 12th in 2004 with a total production of 20.5 million tones and a growth rate of 12% over 2003. In the early 1980s, three government-owned integrated steel producers controlled a substantial majority of the capacity. Over the past two decades, significant capacity has been added through private mini-mill investments. As a result, Turkey has become one of the major players in the global steel market.

The industry consists of three main types of players: Integrated steel producers, mini-mills using electrical arc furnaces (EAF) and processors. Currently, 3 integrated plants and 16 electrical arc furnaces operate in the sector. Processors import semis or purchase them from integrated steel producers and mini-mills. With the exception of one cold rolling company that produces flat products and a few companies producing specialized products such as spring steel, most of these players are sub-scale rolling mills supplying low-value-added, often very substandard, long products to the construction industry (Anonymous, 2006).

Today its electricity demand is nearly one tenth of the installed generation capability of 40 GW in the country. Steel production in Turkey is based on extensive use of arc and ladle furnaces in most of the plants, which is the cause of power quality problems at those locations of the Turkish Electricity Transmission System.

Power quality (PQ) of electric arc furnaces (EAF) has been investigated previously by some other researchers Arc furnace characterization of one plant has been achieved in terms of PQ parameters given in the IEC standard 61000-4--30.

Major Iron and Steel Plants are marked on the map of the Turkish Electricity Transmission System in figure 2.8. Steel production in only four of these plants is based on blast furnaces. At three points or regions of the Turkish Electricity System, multi-furnace operation takes place. Power quality of all of those plants has been

investigated based on the field measurements carried out according to IEC 61000-4-30 for Class B performance by using the mobile monitoring systems((Salor et al., 2010).

By the end of year 2009, 50 MVAR STATCOM prototype has been made ready for commissioning at Sincan Transformer Substation. And also medium voltage active filter prototype has been successfully commissioned at TEİAŞ Denizli-2 Transformer Substation. Measurements with transient events and harmonics measurement systems have been started.

Figure 2.8 Location of iron and steel plants on the Turkish Electricity Transmission System

3. INDUCTION FURNACE OPERATION, POWER QUALITY PROBLEMS AND SOLUTIONS

3.1. Induction Furnace Operation

Today, power quality studies are becoming a growing concern. The most important parameters which affect power quality are harmonics, voltage instability and reactive power burden. They cause low system efficiency, poor power factor, cause disturbance to other consumers and interference in the nearly communication networks. The increased problems in power networks impose to identify the sources of power quality deterioration (Iagar et al., 2009).

As technology advances, the electrical loads are multiplying in numbers and complexity. This throws tremendous challenge to the quality of power supply system. Power electronic converters are examples of such types of loads. Steel mills, which employ induction furnaces for melting scrap iron is one of the industrial areas where the use of such power converters is inevitable. The tuned filters or passive compensators are the traditional solution for harmonics issues. Since they are tuned for a fixed frequency they are not affective for varying harmonics spectrum. The induction furnace is a typical example of load, which generates harmonics in different spectrum based on the configuration of the controlled rectifier i.e., 12-pulse for heating mode or 6-pulse for sintering mode. Passive filters are also susceptible to sinking the harmonics injected by other loads in the grid. To overcome these shortcomings of passive filters various active power filter configurations have been reported (Unnikrishnan et al., 2006).

When capacitors are placed on distribution systems, there will always be one or more frequencies at which the system could resonate. While there are often harmonic-producing loads on the systems, there have been relatively few instances where severe resonances have occurred. Only I-2% of all feeders have harmonic voltage distortion exceeding limits. The solution to resonances is generally to change capacitor sizes or move the banks so that the system is tuned away from troublesome harmonics.

Induction heating is a well established widespread technology, which finds application in a large variety of industrial production processes. Since the basic principles of the technology are well known for many years, the competition in the market is very strong and the success among competitors is determined by the improvement of processes for obtaining better quality, higher fabrication rate of products and the reduction of cost of the installations (Lupi, 2003). Induction heating equipments do not introduce dust and noise emissions in operation, but cause power quality problems in the electric power system.

Since the 1970s, induction has been the number one method of melting in non-ferrous metal foundries and an important tool in iron foundries. New technology is improving induction power supplies, furnace refractory linings, heat recovery, and overall system control. In the last ten years, the use of induction melting has increased by as much as 20% per year, making it the fastest growing electric technology in metals production. Over time, induction may even surpass conventional use of electric arc furnaces in both tons of production and kilowatt-hours of energy use (Rudnev et al., 1999). The problem with this kind of furnaces, from an electrical point of view, is the creation of a considerable harmonic distortion. The cause of the distortion is within the induction furnace design and operation.

An induction furnace works melting the scrap using a medium frequency magnetic field created by a coil. The coil is fed by the medium frequency AC current supplied by an inverter which is fed by a DC current converter connected to the AC distribution network supply. The principle of an induction furnace is based on the principle of a transformer. The induction coil represents the primary winding and the melting material represents the secondary winding of transformer (Zamora et al., 2003).

Modem induction furnaces use electronic power converters to supply a variable frequency to the furnace induction coil. Figure 3.1 shows the block diagram of the modern induction furnace. The frequency at the melting coil varies to match the type of material being melted and the amount of material in the furnace. The furnace coil and capacitor basically form a resonant circuit and the dc-to-ac inverter drives the circuit to keep it in resonance. Thus, all the reactive power for the coil is

supplied by the capacitor. The inductance of the coil varies depending on the type, temperature, and amount of material. This results in a varying operating frequency for the furnace. The typical range of frequencies for a steel- melting furnace of the type encountered in this case is 150 - 300 Hz (Dugan et al., 1999).

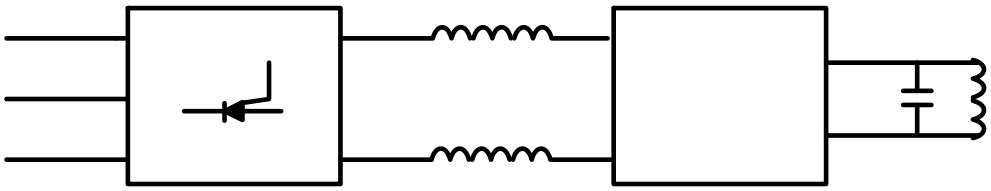

Figure 3.1 Block diagram of a modern induction furnace with a current- source inverter

The power supply of an induction-melt furnace provides both the power and control required to properly melt metal. Early induction melting was carried out at line frequency, with power provided by a special transformer and tuning circuits. Switching capacitors provided power factor adjustment, and changing transformer taps regulated the power level. For maximum melting power, the resonant frequency of a tuned LC circuit had to be matched to the line frequency. This condition limited the coil current and therefore the efficiency of the furnace because the 50-Hz line frequency results in relatively high penetration into the melt and excessive stirring. Also, early induction-melt furnaces were single-phase loads, which draw heavily from only one phase of a three-phase system and limit the power available from the utility service (Rudnev et al., 1999).

The advent of large-scale solid-state power supplies has greatly improved induction melting. Three-phase converters can be operated at a high power factor, thereby increasing the practical power ratings in a typical application. These power supplies also precisely control frequency and the depth of penetration to efficiently melt the material without over-stirring. The process is more efficient because the variable frequency power supplies are able to match the varying electrical characteristics of different metals during melting. The electronic power supply that is

used on the modern furnace has opened the way for batch operation by eliminating the need to maintain a molten heel. Figure 3.2 shows a typical furnace and its electronic power supply.

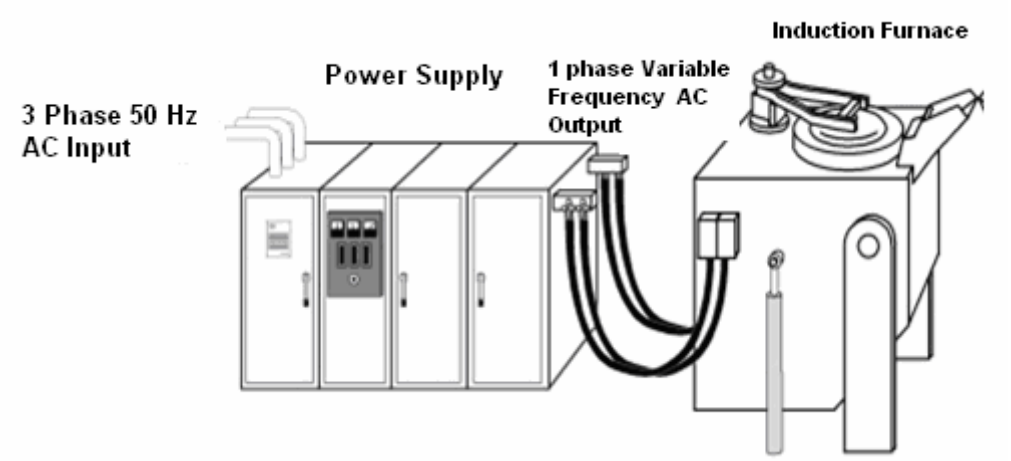

Figure 3.2 Typical Electronic Power Supply and Induction-Melt Furnace (Rudnev et al., 1999).

Electronic power supplies control current and frequency for efficient induction melting. Most electronic power supplies rectify the AC line current to provide a DC source of energy. This DC is then inverted at a frequency to obtain the desired induction from the furnace resonant circuit. The two main types of solid-state power supplies are the current fed power supply (parallel furnace resonant circuit) and the voltage-fed power supply (series furnace resonant circuit),both of which are used in medium frequency induction melting systems.

The voltage-fed power supply, which is the newer of the two designs, takes advantage of switching technology that is capable of handling high currents. As shown in Figure 3.3, it employs a simple input diode rectifier to produce DC, and a parallel connected DC capacitor for energy storage and filtering. The output inverter controls melting power by its commutation frequency and can fully regulate the current to the series tuning capacitor and the furnace. Consequently, the inverter is exposed to the full current and partial voltage of the furnace. The DC capacitor provides or absorbs excess energy for starting and stopping the inverter.

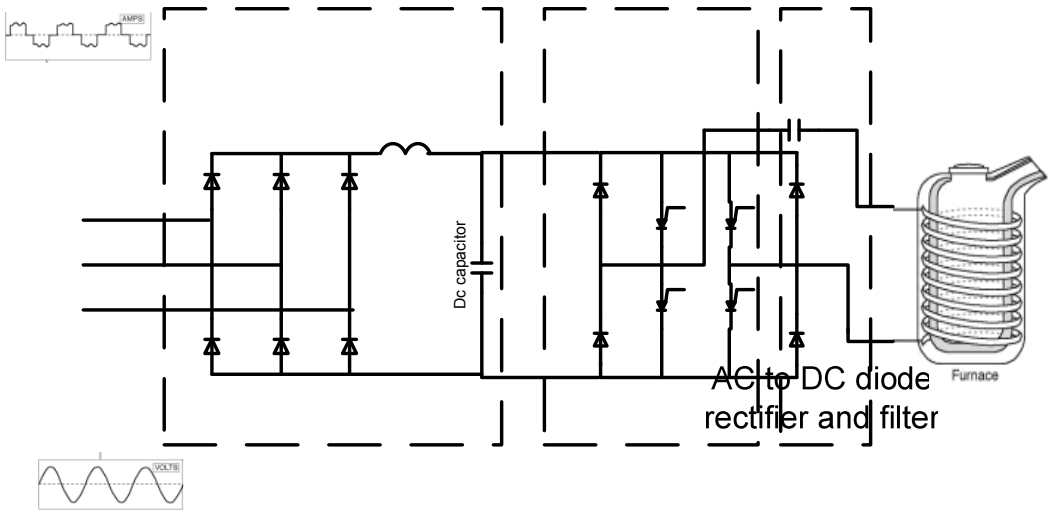

Figure 3.3 Voltage-Fed Power Supply Driving a Series-Resonant Furnace Circuit

As shown in Figure 3.4, the basic current-fed converter uses a phase-controlled rectifier to convert AC to DC and to regulate the voltage on the DC link. When current is flowing in the DC link, the two series connected inductors provide energy storage and filtering. Consequently, a starter circuit is needed to energize these inductors, and a crowbar circuit is used to discharge them when the melt is complete. The inverter commutates or reverses the current to obtain the desired output frequency, which, along with varying the rectifier output voltage, controls the melting power.

Current-fed designs have been around longer and take advantage of rugged and economical switching-device technology. The inverter is exposed to the full furnace voltage. However, it only sees about 10% of the furnace resonant current because the reactive component of the furnace current bypasses the inverter via the parallel tuning capacitor. Consequently, the current-fed power supply has less control over the furnace current than the voltage-fed power supply.

One side effect of using a phase-controlled rectifier in the current-fed power supply is voltage notching. The line voltage is notched because a momentary line-to-line fault occurs as each phase rectifier device is turned on before the other phase device has commutated off. Depth of the notch depends on the circuit impedance between furnace transformer and the rectifier. Width depends on the timing between turn-on and turn-off. Notches are more severe near the converter, as illustrated in the

voltage waveform shown in Figure 3.4. Notching can cause equipment operating problems when propagated in a plant electrical system. The most common problem caused by notching is tripping of other power supplies and DC drives (Rudnev et al., 1999).

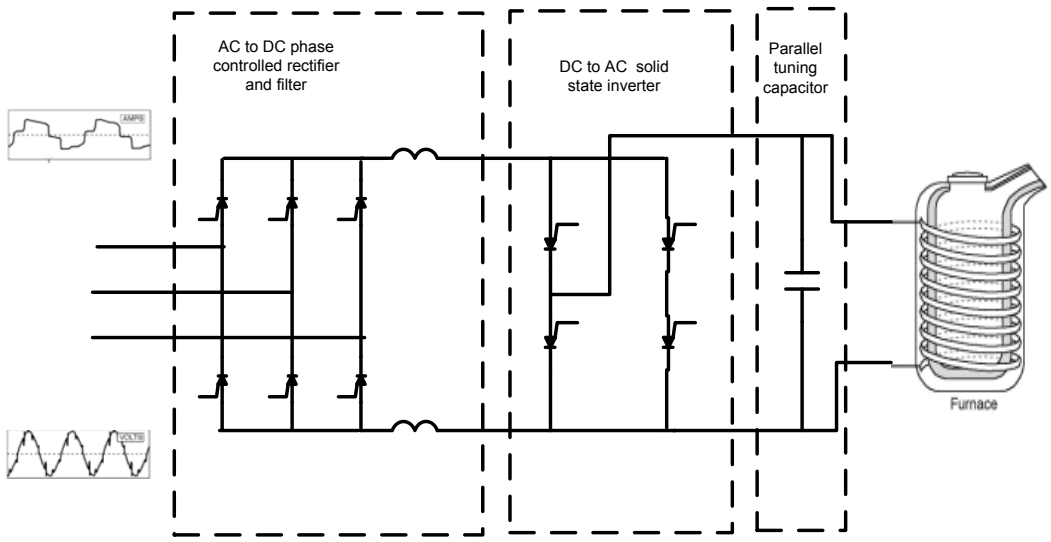

Figure 3.4 Current-Fed Power Supply Driving a Parallel-Resonant Furnace Circuit

A typical parallel resonant inverter circuit for induction furnace is shown in Figure 3.5.The phase controlled rectifier provides a constant DC current source. The H-bridge inverter consists of four thyristors and a parallel resonant circuit comprised capacitor bank and heating coil. Thyristors are naturally commutated by the ac current flowing through the resonant circuit.

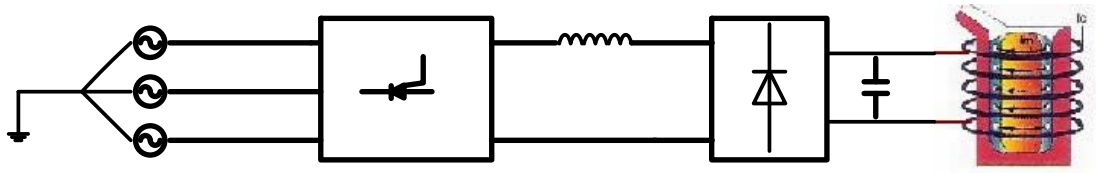

Figure 3.5 Block diagram of induction furnace system

It is important to select the proper power rating for the system. There are many factors that influence the selection of furnace power. The first is the capacity to be melted, the type of the material to be melted (Iron, Aluminum, Tin ...) and the desired melt cycle time. To raise the temperature of a solid material to the pouring

temperature, energy must be put into it based upon the characteristics of its solid specific heat, latent heat of fusion, and liquid specific heat. An improperly designed system that has an undersized power supply will reduce the efficiency of the overall system and reduce the weight of metal that can be melted per kWh applied. This could result in the inability for the system to reach the required pour temperature

There are two types of induction furnaces. The first is coreless and the second is called channel. The coreless induction furnace has copper coils that are protected by a steel and magnetic shield and kept cool by water circulating from a special tower. A layer of refractory, or difficult to melt material, is placed above the coils and heated to the desired temperature. A crucible, which is a melting pot made of heat resistant material, is above the refractory. The metal to be melted is placed inside the crucible and the heat produced by the electromagnetic charge melts the scrap.

The channel induction furnace can also be called a core induction furnace. It functions very similarly to the coreless furnace, except for the addition of a heated core. Channel furnaces were originally used as molten metal holders, but have been found useful in the melting of lower melt temperature metals.

Both types of induction furnaces produce a natural stirring motion when the metal is molten. The pull of the magnetic fields and electrical currents cause the materials to sway in different directions. This stirring is essential to maintaining the integrity of the metal. The coreless furnace creates a more violent stirring, while the channel is known to have less turbulence at the surface.

The principle of melting in induction furnace is that the electrical coil surrounding the cylindrical crucible acts as primary and the metallic charge as secondary. When an electrical current is passed through the primary coil the electromagnetic field causes induced current to flow through the metallic charge making it melt.

When the electrical current is switched on, the eddy currents developed between primary copper coil and heavier secondary current in the metallic charges melt in the charge to the desired temperature. The charge is placed in this crucible and it acts as the secondary winding. The crucible is surrounded by several turns of water cooled copper tubing which carries the high frequency primary current. The

charge consists of sponge iron, pig iron, Ms-scrap. After reaching temperature the gangue material present in the charge comes out in the form of slag and float in the molten bath. The slags are removed through tapping and manually.

The coreless induction furnace consists basically of a crucible, inductor coil, and shell, cooling system and tilting mechanism.

The crucible is formed from refractory material, which the furnace coils is lined with. This crucible holds the charge material and subsequently the melt. The choice of refractory material depends on the type of charge, i.e. acidic, basic or neutral. In this design a neutral refractory is used and based on effectiveness, availability and practical application in Nigerian foundries, zirconium oxide (ZrO_2) is implored. The durability of the crucible depends on the grain size, ramming technique, charge analysis and rate of heating and cooling the furnace (Ahmed, 2009). Figure 3.6 shows typical components of a coreless induction furnace.

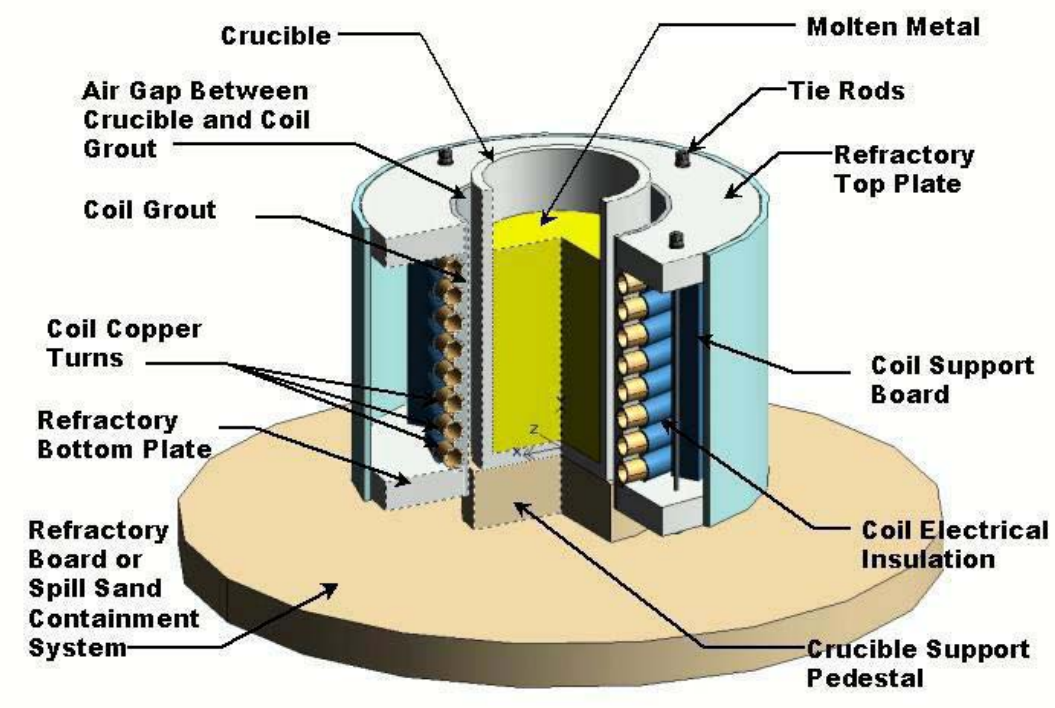

Figure 3.6 Typical Components of a Coreless Induction Furnace (Ahmed, 2009).

The inductor coil is a tubular copper coil with specific number of turns. An alternating current (A.C) passes through it and magnetic flux is generated within the conductor. The magnetic flux generated induces eddy currents that enable the heating and subsequently the melting process in the crucible. In order to eliminate electrical breakdown the turns are insulated by wrapping with mica tape, this serve as a good insulator.

The shell is the outer part of the furnace. This houses the crucible and the inductor coils, and has higher thermal capacity. It is made of rectangular parallel piped with low carbon steel plate and joined at the corners by edge carriers from angular pieces and strips of non-magnetic metal.

The cooling system is a through-one-way- flow system with the tubular copper coils connected to water source through flexible rubber hoses. The inlet is from the top while the outlet is at the bottom. The cooling process is important because the circuit of the furnace appears resistive, and the real power is not only consumed in the charged material but also in the resistance of the coil. This coil loss as well as the loss of heat conducted from the charge through the refractory crucible requires the coil to be cooled with water as the cooling medium to prevent undue temperature rise of the copper coils.

Tilting of the furnace is to effect pouring of the melt as a last operational activity before casting. Since this furnace is of small capacity, a manually operated tilting mechanism is adopted. The furnace is hinged on at the spout edge with a shaft and bearings. At one side to the bearing is pinion and gear system to give a gear reduction, so that when the handle is turned clockwise, the furnace is tilted to achieve a maximum angle of 90 degrees for complete pouring of the molten metal (Bala, 2005).

Rather than just a furnace, a coreless induction furnace is actually an energy transfer device where energy is transferred directly from an induction coil into the material to be melted through the electromagnetic field produced by the induction coil.

The geometric shape of the furnace is shown in figure 3.7. The shape of the crucible is cylindrical. The internal diameter of the crucible (the diameter of melt) and the height of melt are determined by the furnace capacity (Ahmed, 2009).

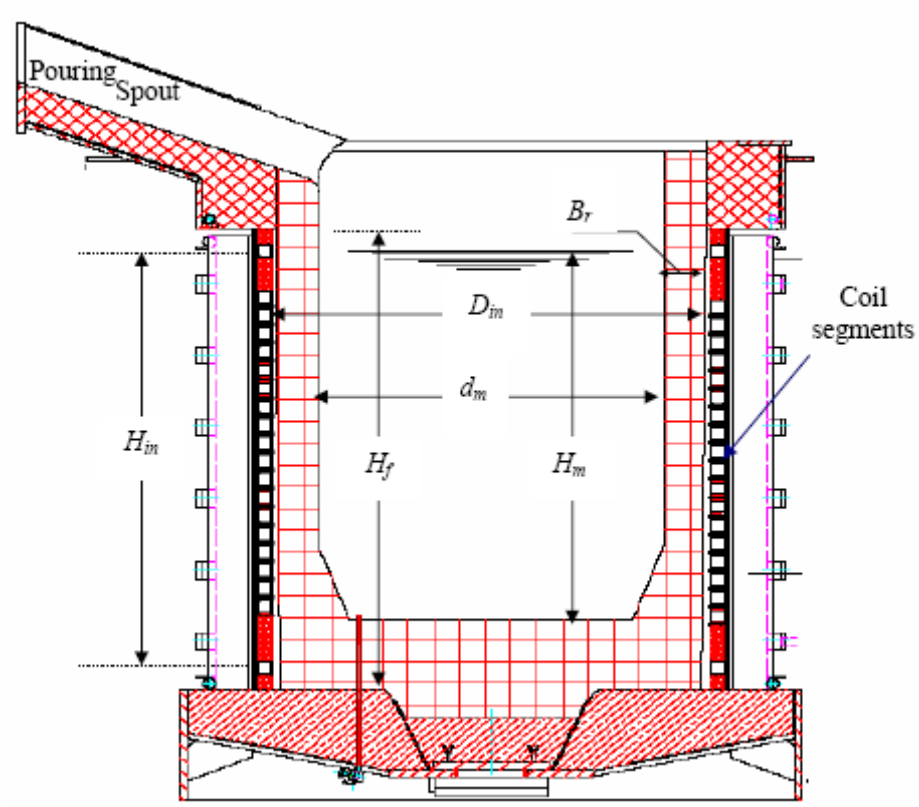

Figure 3.7 The geometric shape of the furnace (Ahmed, 2009)

3.2 Power Quality Problems And Solutions

3.2.1 Power Quality Problems

Sometimes thought to be a panacea for the induction melting process, modern solid state power supplies have actually been a mixed blessing for achieving compatibility with the electric utility system. Large three-phase power supplies for furnaces, while providing economies of scale with higher productions levels, also bring large fluctuating load currents with varying levels of harmonic distortion. These varying furnace currents can affect distribution line-voltage regulation and quality.

Both current- and voltage-fed inverters generate harmonics back into power lines in the process of rectifying AC to DC. In the larger furnaces, it is popular to provide more than one rectifier bridge, along with phase-shifting transformers. This reduces the amount of current per bridge and the level of harmonics in the combined current drawn from the utility. Each three-phase bridge requires six devices, and one positive and one negative pole for each phase. A single bridge, such as shown in Figures 3.3 and 3.4, is called a six-pulse rectifier and two bridges are called a 12-pulse, as shown in Figure 3.8.

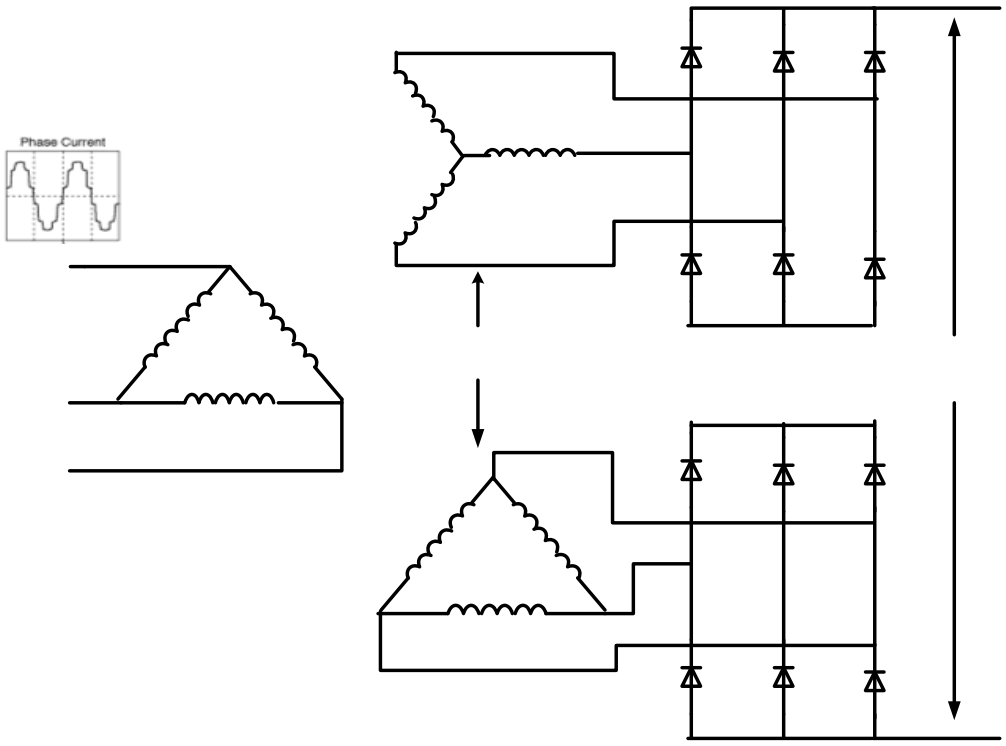

Figure 3.8 Typical 12-Pulse Bridge Rectifier Configuration with Phase- Shifting Transformers

Increasing the number of rectifier bridges add more steps in the waveform of the line current, making it more sinusoidal.

The term “power factor” is well defined for 50-Hz systems as the phase difference between the fundamental current and voltage. In the presence of harmonics, power factor is best defined as the ratio of the watts over the total kVA

for all frequencies. Distorted systems have limited power factors even when the fundamental voltage and current are in phase. For example, when the current is 21.5% distorted, as with the practical case of a six-pulse rectifier, the maximum power factor is 0.98 instead of 1.0. At 60% distortion, the maximum power factor is about 0.86. The expected power factors for 6-, 12-, and 24-pulse bridge rectifiers in full-wave rectification mode are relatively high. The greater the number of pulses the greater the expected power factor. Compared to the full-wave rectifier in voltage-fed power supplies, the phase controlled rectifier in current-fed power supplies uses a delay in turning on switches to control power levels and to regulate the DC bus voltage. It should be noted that the power level and power factor in a phase-controlled rectifier drops rapidly with the increase of delay angle. At a delay angle of 30°, the maximum is 0.95, at 90° it is less than 0.7, and at 120° it drops to 0.46. Therefore, if the power supply is current-fed, low power factors can be expected when the power supply reduces power to the furnace.

In addition to the harmonics that are normally expected from different pulse rectifiers large furnaces operating at a few hundred hertz can generate significant non-characteristic harmonics. These harmonics, which fluctuate with the frequency of the furnace resonant circuit, are usually not multiples of the supply frequency, making them difficult to filter. This phenomenon, known as interharmonics, can overload power system capacitors, introduce noise into transformers, cause lights to flicker, instigate UPS alarms, and trip adjustable speed drives (Rudnev et al., 1999).

The typical scenario for the generation of inter-harmonics is a relatively large furnace with a current-fed power supply operating between 100 and 5000 Hz on a distribution feeder. If the inverter is operating at frequency, f_0, the dc link ripple current frequency is $2f_0$, with its own integer harmonics of $2f_0$. The controlled rectifier switches the inverter $2f_0$ on and off with the 500 Hz ac mains. The resulting line current contains pairs of current components at frequencies of

$2f_0 \pm 50$, $4f_0 \pm 50$, …

Where f_0 = furnace operation frequency

If the furnace operating frequency is 160 Hz, then the first pair of distorting currents, equal in magnitude, will appear at 270 Hz and 370 Hz; the second pair, of

lesser magnitude, will be at 590 Hz and 690 Hz. A monitor must sample several cycles of power frequency currents to correctly observe these frequencies. They will often not appear in single-cycle samples. A typical spectrum from a 6-cycle sample, yielding 10 Hz increments, is shown in figure 3.9.

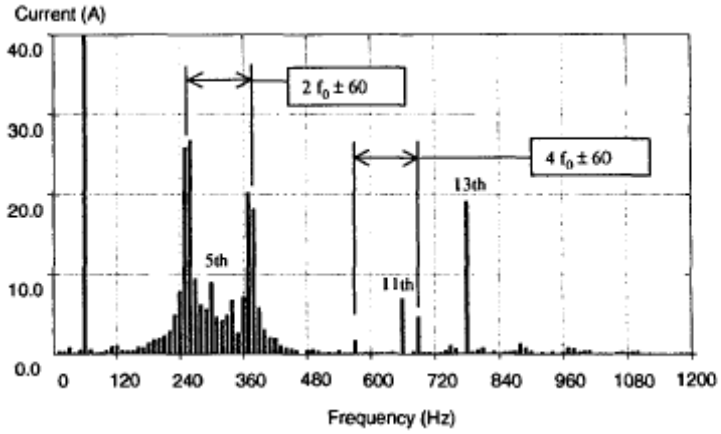

Figure 3.9 Typical spectrum of induction furnace current (Dugan et al., 1999)

The magnitude of the first pair typically was 10% of the fundamental. This was greater than the 5^{th}, 11^{th}, and 13^{th} harmonic currents. The 5^{th} is a non-characteristic harmonic but was found in significant amounts in nearly all measurements. Keep in mind throughout the remainder of the paper that the frequency pairs from the inverter move slowly through a wide frequency range as the furnace completes its melt and pour cycle. It can be at one frequency for a time ranging from several seconds to several minutes. For the first pair, the frequency would range from about 250 Hz to 650 Hz. It can be assumed that for all practical purposes any frequency within this range can be produced by the furnace (Dugan et al., 1999).

The interaction level depends on the relative size of the furnace, its operating frequency, and loading. Also, the effect might be aggravated by resonance in the system, which causes amplification of the inter-harmonic frequencies at certain points in the power system.

Inter-harmonic is a relatively new classification of power system distortion. Its effect on the power system is unique, as are the methods for measuring inter-

harmonics and mitigating its effects. Inter-harmonics can be thought of as voltage or current components that are not related to fundamental frequency or to integer-harmonic components of the system. As furnace power supplies become more sophisticated, the frequencies of the current they draw are less likely to be limited to harmonics of the fundamental.

The equipment that causes inter-harmonics includes induction furnaces, static-frequency converters, cycloconverters, induction motors that drive shakers, and DC arc furnaces. Generally, any equipment that draws a load current that pulsates asynchronously with the fundamental power system frequency generates inter-harmonics. In the case of induction melting, the variable frequency of the furnace is likely to cause interharmonics in the power system. The typical impacts on other equipment are flickering lights or computer screens, tripping of certain power electronic equipment, and heating in the power system similar to the heating caused by harmonic currents.

Standards are still emerging on this subject. IEEE 519-1992 indirectly addresses interharmonics in the discussion on cycloconverters. A future IEEE standard is expected to provide general technical descriptions of the phenomenon, methods of measurement, and guidelines for limits. The IEC 61000-2-1 currently defines the inter-harmonic environment, and IEC 61000-4-7 describes a measurement technique. Even with these standards, agreement among popular harmonic monitors does not exist. If a monitor can detect inter-harmonics, the most common result is an under-registration of the inter-harmonic levels (Rudnev et al., 1999).

Another international standards and conformity assessment body, International Electro technical Commission (IEC), produced a standard, IEC 61000-3-6, which also provides guidelines to address harmonics issue with sets of steady state limits. Both standards are in common where the limits were derived based on a basic principle of insuring voltage quality and shared responsibility between utility and customer. Both lay the responsibility on consumer to limit the penetration of current harmonic into power system while utility company is responsible to limit harmonic voltage at point of common coupling (PCC). According to IEEE definition,

point of common coupling is a point anywhere in the entire system where utility and consumer can have access for direct measurement and the indices is meaningful to both(Izhar et al.,2003)(Halpin,2005).

IEEE has come out with a guidelines and standard regarding harmonics in the IEEE standard 519-1992 “IEEE Recommended Practices and Requirements for Harmonic Control in Electrical Power Systems”. The Standard is a guide in designing of power systems with nonlinear loads. The limits set are for steady-state operation and recommended for worst case scenario. The quality of power is observed at point of common coupling (PCC) which is the interface between source and loads.

The standard generally provide information and guidelines on sources of harmonics, resonant condition due to harmonics, frequency response and modeling for transmission and distribution system, effect of harmonic, balanced and unbalanced system, measurements and steady state limits. The voltage distortion limits are used as a system design values set for worst case scenario in a normal condition. However, the worst case scenario is normally referred to maximum current harmonic penetration. Fluctuation of harmonic impedance in the system can also cause an increase in harmonic voltage. This study looks at varying factors of harmonic impedance within a distribution network and compare with harmonic voltage distortion limit at point of common coupling using design components values and maximum current harmonic penetration from a single source. Table 3.1, 3.2 and 3.3 are the harmonic current and voltage limits from IEEE 519-1992 standard.

Table 3.1 Basis for harmonic current limits based on IEEE 519-1992

SCR at PCC	**Maximum individual Frequency Harmonic voltage (%)**
10	2.5-3.0%
20	2.0-2.5%
50	1.0-1.5%
100	0.5-1.0%
1000	0.05-0.10%

Table 3.2 Current distortion limit for general distribution systems (120V through 69000V)

I_{SC}/I_L	<11 [%]	11≤h<17 [%]	17≤h<23 [%]	23≤h<35 [%]	35≤h [%]	TDD [%]
<20	4.0	2.0	1.5	0.6	0.3	5.0
20<50	7.0	3.5	2.5	1.0	0.5	8.0
50<100	10.0	4.5	4.0	1.5	0.7	12.0
100<1000	12.0	5.5	5.0	2.0	1.0	15.0
>1000	15.0	7.0	6.0	2.5	1.4	20.0
Even harmonic are limited to 25% of the odd harmonic limits above						

Table 3.3 Voltage Distortion Limits

Bus Voltage at PCC	Individual Voltage Distortion (%)	Total Voltage Distortion (%)
69kv and below	3.0	5.0
69.001kv through 161kv	1.5	2.5
161.00kv and above	1.0	1.5

Another standard for harmonic is IEC 61000-3-6. A paper by Halpin (2005) provides comparisons between IEEE and IEC standards, both similarities and differences. The paper touched on areas such as driving principle, harmonic voltage limits, current harmonic limits, even-order harmonic, non-characteristic harmonic, time-varying harmonic and inter-harmonic. Both standards aim at a similar goal which is to ensure voltage quality with the main principle of shared responsibility between utility and customer. IEC provide comprehensive limits on time-varying harmonic compared to IEEE. The IEC time-varying harmonic limit is based on percentiles, e.g. 95th and 99th for very short time (3 second) and short time (10 minute) aggregate measurements (Halpin, 2005).

3.2.2 Solutions

When an induction furnace is causing power quality problems, other customers are often involved. Both end user and power provider want to consider all practical solutions. Tools for avoiding and resolving typical problems include measurement and assessment methods, application of standards, changes in the furnace or utility power supply, special operating procedures, and power conditioning. Pre-installation planning and post-installation problem-solving for a specific foundry case will demonstrate options for preventing and resolving power quality problems (Rudnev et al., 1999).

3.2.2.1 Passive Filtering

Passive filters consisting of capacitors, inductors and/or resistors can be classified into tuned filters and high-pass filters. They are connected in parallel with nonlinear loads such as diode/thyristor rectifiers, ac electric arc furnaces, and so in. Figure 3.10 and 3.11 show circuit configurations of the passive filters on a per-phase base.

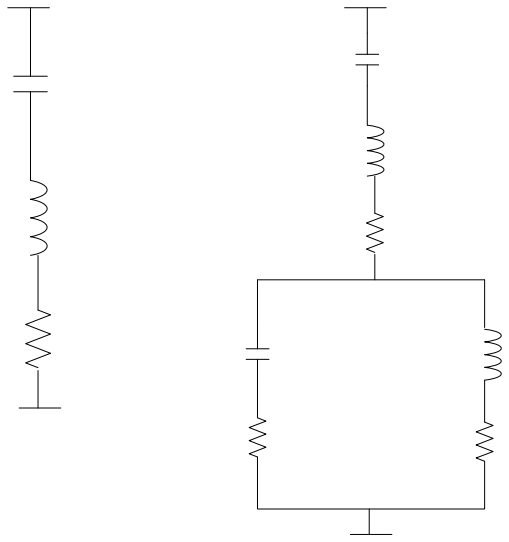

Figure 3.10 Passive tuned filters: (a) single tuned, and (b) double tuned

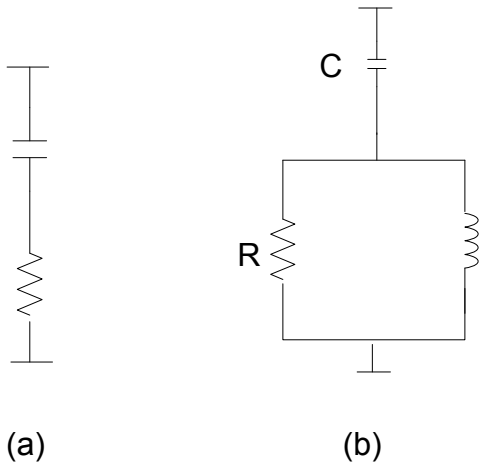

Figure 3.11 Passive high-pass filters: (a) first-order, (b) second-order

The normal filtering approach for harmonic producing loads is to place at least one series-tuned resonant shunt near the source of the harmonics. If only one filter is used, it is usually tuned at the lowest characteristic harmonic. This would be the 5^{th} harmonic. Often this will suppress the largest harmonic and, at least, de-tune the system for the remainder of the harmonics. Common additions to this scheme are to place another filter at the 7^{th} with, perhaps, a high-pass filter at the 11^{th} or 13^{th} harmonic. This scheme will not work well for an induction furnace like the one filter. Just below the notch frequency of these filters is a sharp parallel resonant peak. For a 5^{th} harmonic filter, the resonant peak will be near the 4^{th} (250Hz). The furnace is capable of exciting this resonance when operating in its low frequency range. This will very likely result in filter failure.

Another approach is to place enough capacitors on the service supplying the melting facility to tune the whole system to a lower frequency than the furnace produces. The capacitor bears no relation to the size of the load, but rather to the short circuit impedance of the system. Thus, the capacitor could be very large relative to plant load. The system is tuned to less than the 4^{th} harmonic. Above the resonant frequency, this scheme actually results in less current injected into the distribution system than without any capacitors at all (compare with base line). This is most of the $2f_o$ operating band. This works well, but the trick is to keep the furnace $2f_o$ current frequencies higher than the frequency to which the system is now tuned. Very large currents were injected when the furnace frequency slipped too low.

The drawbacks of this approach are cost of the capacitors and very poor voltage regulation. Also, the utility may not be able to accommodate the excess reactive power. This approach may be ruled out if other loads of this service bus will not tolerate the voltage variation.

This introduces more cost to provide a sizable 3-phase reactor, but has the advantage of providing isolation from the service bus so that other loads are relatively unaffected. The capacitor required would be smaller, which offsets some of the increased cost. However, the voltage regulation at the furnace will still be poor, if not worse than placing one very large capacitor on the service bus. Fortunately, current source inverters are less sensitive to voltage than other types of loads. One might be able to work with the manufacturer at design time to adjust the design of the converters and dc link to operate over a wider voltage range.

If the utility cannot accept the excess reactive power from this filtering arrangement, one modification could be to add a shunt reactor that cancels the 50 Hz component of the capacitor current. It would have a minor effect on the tuning of the system, so this would also have to be taken into account.

3.2.2.2 Choose a Different Type of Furnace Power Supply

Not all induction furnace power supply designs operate in the manner described. It is more appropriate when connected to a high capacity source, such as directly to the transmission system. For distribution systems with many capacitors, a design with better isolation of the furnace frequencies is more appropriate. The end user had the option of two different kinds of furnaces. Whether this is accurate or not, it produced only harmonic currents, which, in retrospect, would have been much easier to deal with on a distribution system (Dugan et al., 1999).

3.2.2.3 Active Filtering

As the created distortion is very high and affects the voltage supplied by the distribution network, it is highly possible that other loads supplied from the same

network will be affected. Then, it is necessary to have corrective actions in order to fulfill the legislation concerning voltage harmonic distortion.

Among these corrective actions, active filters are one of the most effective. This solution presents many advantages over other alternatives:

- The steel plant is composed of loads that vary fast their consumption changing the harmonic composition. The connection and disconnection of power electronic components changes the harmonic composition too. The filter has to be fast.

- The active filter overcomes the resonance problems associated with the power factor correction capacitors. Moreover, the filter can work as a dynamic compensator of reactive power, depending on the instantaneous needs of reactive power of the steel plant.

- The active filters can perform a load compensation of the three phases, removing the neutral current in unbalanced systems.

Before taking any corrective action, it is necessary to evaluate the distortion introduced by the installation into the distribution network. In this stage, simulation has been proved to be a useful tool when evaluating the harmonic distortion. It allows quantifying the harmonic distortion created by a system and, when a corrective action is introduced, simulation shows the reduction in the distortion. Hence, simulation can be used as a tool for the design of the active filter (Zamora et al., 2003).

3.2.2. 4 Reconfiguring Feeders

An interim solution was achieved by reconfiguring the feeders to provide an express feed without capacitor banks to a strong substation bus where there is little impact on other customers. Commercial and industrial customers with computer networks and power factor correction capacitors, with one exception, were moved to other feeders. This solution was not completely satisfactory.

Reasons this approach might not work include: 1) it is not possible to construct a configuration that avoids problems; 2) the substation bus is not

sufficiently stiff and other feeders are affected; 3) load growth cannot be accommodated; 4) emergency reconfiguration not possible.

There is also the valid concern that the operation of the feeder may be turned over to another entity in the future and the knowledge of this special feeder will be lost.

3.2.2. 5 Modify Induction Furnace

A distribution engineer would like to see the operating frequency of the furnace restricted to a very narrow range. This would provide much more leeway for placing capacitors on the distribution system. One thing that can be done at design time is to provide for more automatic switching steps in the furnace capacitor.

For the current-source inverter, increasing the dc link inductance causes a directly proportional decrease in the magnitude of the distorting currents reaching the ac side. There are design limitations, but this can result in a furnace design that is much more tolerable from the perspective of the utility distribution system.

3.2.2.6 Feed from Transmission

There are potentially fewer difficulties when an induction furnace is fed directly from transmission lines rather than through a distribution feeder. The great advantage is that the transmission system is a much stiffer system and can absorb the harmonic currents without causing as much voltage distortion. Induction furnace loads are frequently very small compared to transmission capacity. Of course, this is why some utilities choose to serve them through distribution facilities -- the load size does not seem to justify a transmission substation. However, if the operating difficulties are taken into consideration, the justification may be easily achieved.

Transmission systems are not impervious to problems from this type of load. Capacitors are becoming more common at transmission levels. While the tuning of systems today are typically fairly high so that they are not in the range that might be excited by the furnace frequencies, other distribution substations fed from the transmission are tuned to frequencies in the 5^{th} - 9^{th} harmonic range. Therefore, it is

possible that an induction furnace might excite a distribution system via the transmission system. A radial transmission feed from a station that contains a distribution substation would seem a good candidate for trouble.(Dugan et al., 1999).

4. INDUCTION FURNACE MODELING

4.1 Induction Furnace Modeling

In this thesis the coreless induction furnace is modeled. In this type of furnace the coil is hallow and metal scrap is charged in it for melting. Core is not present for flux linkage between primary and secondary and hence the name. The heart of the coreless induction furnace is the coil, which consists of a hallow section of heavy duty, high conductivity copper tubing which is wound into a helical coil. Coil shape is contained within a steel shell and magnetic shielding is used to prevent heating of the supporting shell. When the charge material is molten, the interaction of the magnetic field and the electrical currents flowing in the induction coil produce a stirring action within the molten metal. The degree of stirring action is influenced by the power and frequency applied as well as the size and shape of the coil and the density and viscosity of the molten metal. The stirring action within the bath is important as it helps with mixing of alloys and melting of turnings as well as homogenizing of temperature throughout the furnace (Al–Shaikhli et al., 2009). The coreless induction furnace is commonly used to melt all grades of steels and irons as well as many non-ferrous alloys.

The power circuit of 10MVA current source induction furnace circuit is shown in figure 4.1. It consists a phase shifting transformer with two secondaries, 12 pulse controlled rectifier, DC link inductance, H-bridge inverter, inverter output inductance, parallel resonance capacitors and coil inductance. The primary of the transformer fed from 31.5kV 50 Hz power network.

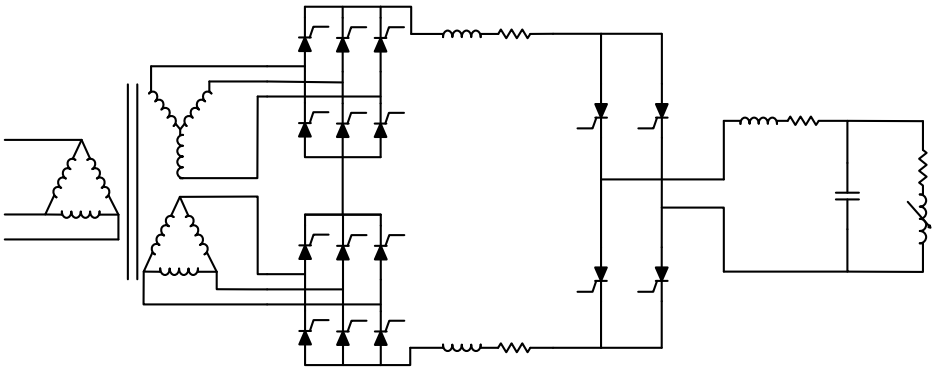

Figure 4.1 The Power Circuit of 10MVA Current Source Induction Furnace

Table 4.1 shows the power circuit specifications of current source induction furnace.

Table 4.1 The Power Circuit Specifications

Transformer	12 MVA, 31.5 kV/1.2 kV -1.2kV, Δ/ Δ-Y
L_{DC}	1 mH
R_{DC}	1.5 Ω
L_S	0.0125 mH
R_S	0.5 Ω
C	5.28 mF
R_f	0.015 Ω
L_f	0.053 – 0.21 mH

The power control of furnace is achieved by controlled rectifier. Firing angle of thyristors determine furnace power. H-bridge inverter keeps parallel resonance circuit in the resonance by changing the operating frequency.

As shown in figure 4.1 the capacitor and the furnace coil is parallel connected in current source circuit. To keep the parallel LC circuit in figure 4.1 at the resonance.

$$X_L = -X_C \tag{4.1}$$

$$\omega L = \frac{1}{\omega C} \tag{4.2}$$

$$\omega = \frac{1}{\sqrt{LC}} \tag{4.3}$$

In this thesis, the main purpose of modeling current source induction furnace is to indicate the power quality problems of induction furnace. Thus, simple controller is developed for the furnace. It is seen from equation (4.1) the resonance frequency of furnace is related the values of capacitor and furnace coil. The parallel resonance capacitor value is constant. The furnace coil is varied depending on the type, temperature, and amount of charging material. According to assigned furnace coil values, furnace frequencies are determined and furnace is operated at linearly increasing frequencies. After the operation frequency is determined, the classical PWM method is used for trigger IGBT of H bridge inverter According to furnace operation scenario, furnace starts operating at 150 Hz and operation frequency of furnace reaches to 300 Hz.

The coreless induction furnaces are electrically analogous to the transformers. The equivalent circuit approximation of transformer is used for induction furnace calculations (Tremayne,1983). The equivalent circuit of a transformer is shown in figure 4.2.

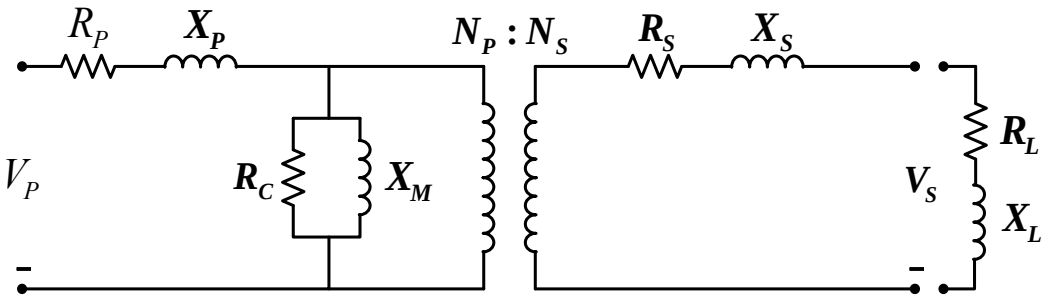

Figure 4.2 Equivalent Circuit of Transformer

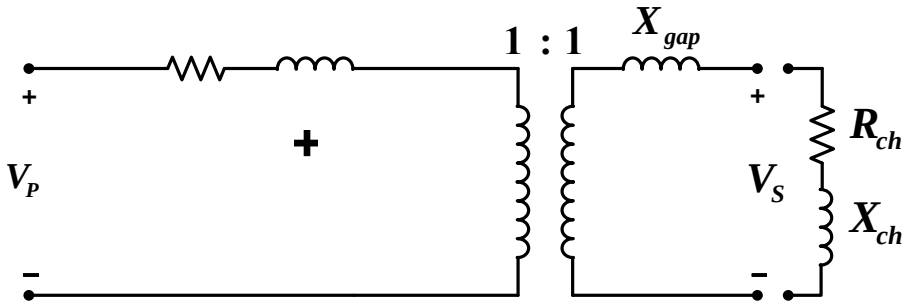

Figure 4.3 Equivalent Circuit of Coreless Induction Furnace

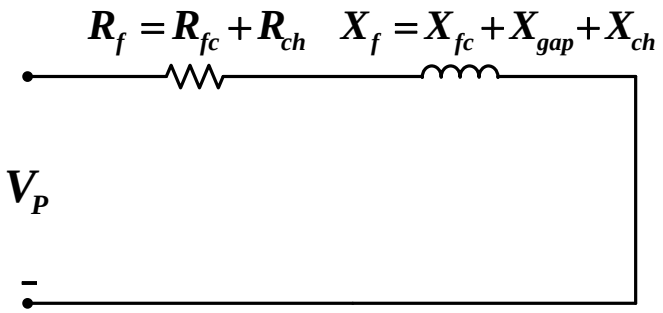

Figure 4.4 Coreless Induction Furnace Equivalent Circuit

R_P and X_P are the primary winding resistance and reactance of transformer. R_C is the core resistance and X_M is the magnetizing reactance of transformer. N_P is the primary winding turn ration and N_P is the secondary winding turn ratio. R_S and X_S are the secondary winding resistance and reactance of transformer. R_L and X_L are the load resistance and load reactance. When this transformer model is applied to coreless induction furnace R_P and X_P are the coil resistance R_{fc} and reactance X_{fc} of furnace. R_C and X_M can be neglected in the furnace model. Because of the coreless structure, their effects are very less. N_P is equal to coil turn number and N_S is equal to 1. R_S and X_S are not used in furnace model because the secondary winding is absent in the coreless furnace. X_{gap} is the reactance of insulation material and gap

between coil and inside of crucible. The load resistance R_L and reactance X_L are equal to the charge resistance R_{ch} and reactance X_{ch} of coreless induction furnace. The approximate equivalent circuit of coreless induction furnace is shown in figure 4.3. and the equivalent circuit of furnace referred to primary side is shown in the figure 4.4. R_f is the furnace resistance which is equal to the sum of coil resistance and charge resistance referred to primary side. X_f is the furnace reactance which is equal to the sum of furnace coil reactance, gap reactance and load reactance.

In this thesis the simulation has been carried out using PSCAD/EMTDC. Blocks for the simulation of the induction furnace and for calculation and visualization of the harmonic content have been developed. Figure 4.5 shows the PSCAD model of induction furnace. If an AC current is fed through a coil, the electromagnetic field that is produced is constantly changing. This changing magnetic field induces electrical current (AC) in another circuit that is held close. This induced secondary current can be utilized to generate heat in the circuit of the second conductor by exploring the electrical losses due to the current. These losses are due to Hysteresis and Eddy current.

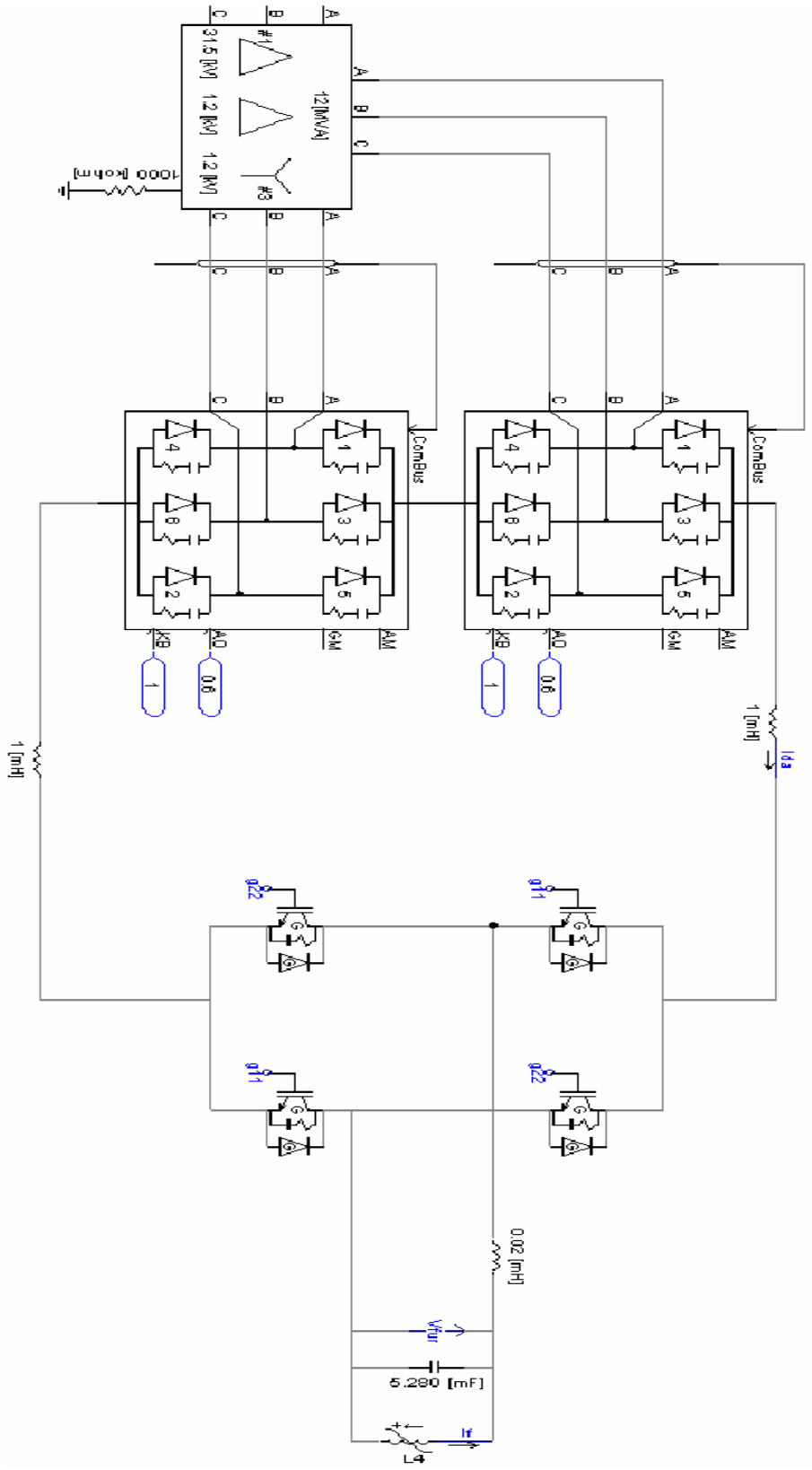

Figure 4.5 PSCAD model of induction furnace

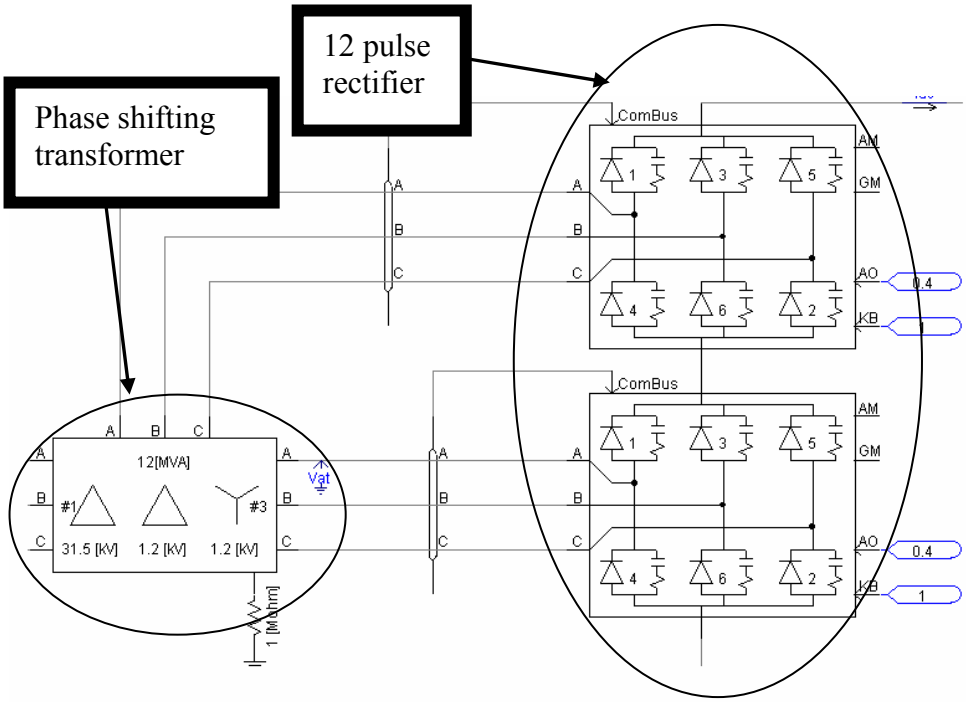

Figure 4.6 12-Pulses Bridge Rectifier Configuration with Phase- Shifting Transformers of induction furnace model

Incoming mains 3 phase supply from furnace transformer is rectified by full control bridge rectifier. Six identical thyristor which are connected in bridge configuration to convert incoming AC to corresponding DC. Thyristors are used in phase control mode and therefore by varying firing angle, the output power can be varied from lower level to higher level. Figure 4.6 shows the typical 12-Pulse Bridge Rectifier Configuration with Phase shifting transformers of induction furnace model of the PSCAD model. In the larger furnaces, it is popular to provide more than one Rectifier Bridge, along with phase-shifting transformers. This reduces the amount of current per bridge and the level of harmonics in the combined current drawn from the utility.

Figure 4.7 show the basic current-fed converter of PSCAD model uses a phase-controlled rectifier to convert AC to DC and to regulate the voltage on the DC link. When current is flowing in the DC link, the two series connected inductors provide energy storage and filtering.

The inverter is responsible for converting high voltage DC to AC to feed it to the load circuit. It is a single phase bridge connection of four current carrying arms. Configuration used is called parallel inverter, as load induction melting coil and capacitors are parallel to each other. IGBT are connected in four arms. Each arm has serially stack IGBT in range of 3-4 depending of output voltage designed. IGBT in diagonal pair are fired in each half cycle of medium frequency, this frequency is determine by parallel resonant LC circuit.

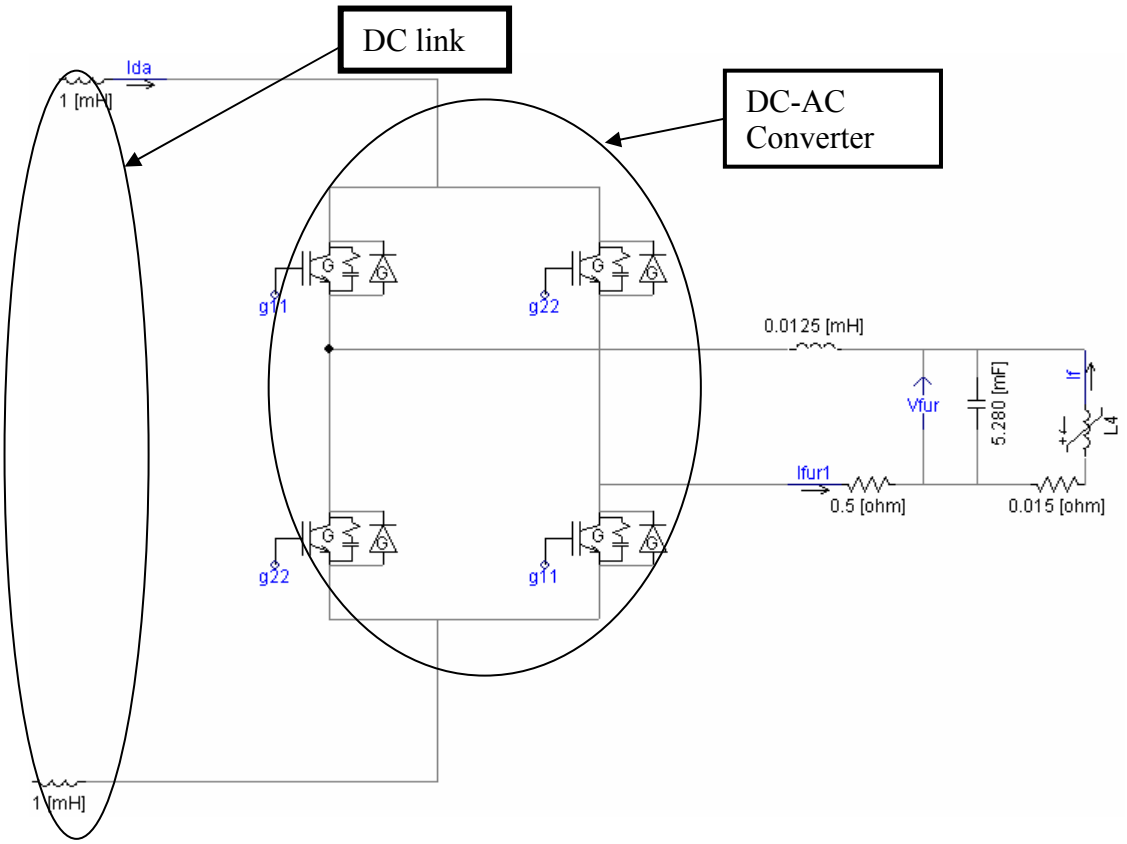

Figure 4.7 Current fed converter of PSCAD model

Figure 4.8 shows the parallel resonance capacitor and variable inductance of furnace of the PSCAD model.

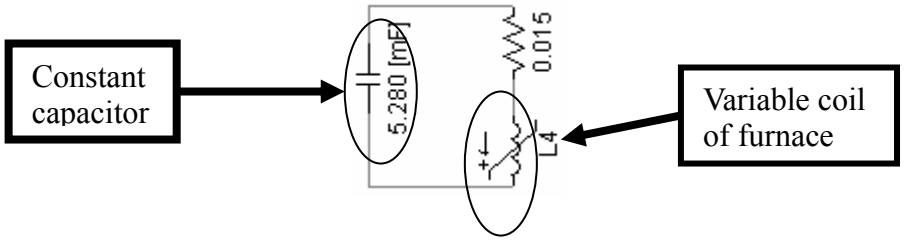

Figure 4.8 PSCAD model of parallel resonance circuit

Figure 4.9 shows the dc-ac inverter control blocks of PSCAD model. These PSCAD blocks generate pulse to control the dc-ac inverter .In this model PWM method is used for control DC-AC inverter. It controls the dc ac inverter according to the changing of furnace coil. In figure 4.9 furnace coil blocks modify the furnace coil according to simulation time. Furnace coil block and inverter frequency control block works coordinated. Depending on varying of simulation time, furnace coil value and operation frequency of inverter changes. As the simulation time progress, the coil value of the furnace decreases. Also operating frequency of the inverter varies according to the resonance frequency formulas. So the inverter keeps to circuit in resonance. This results in a varying operating frequency for the furnace.

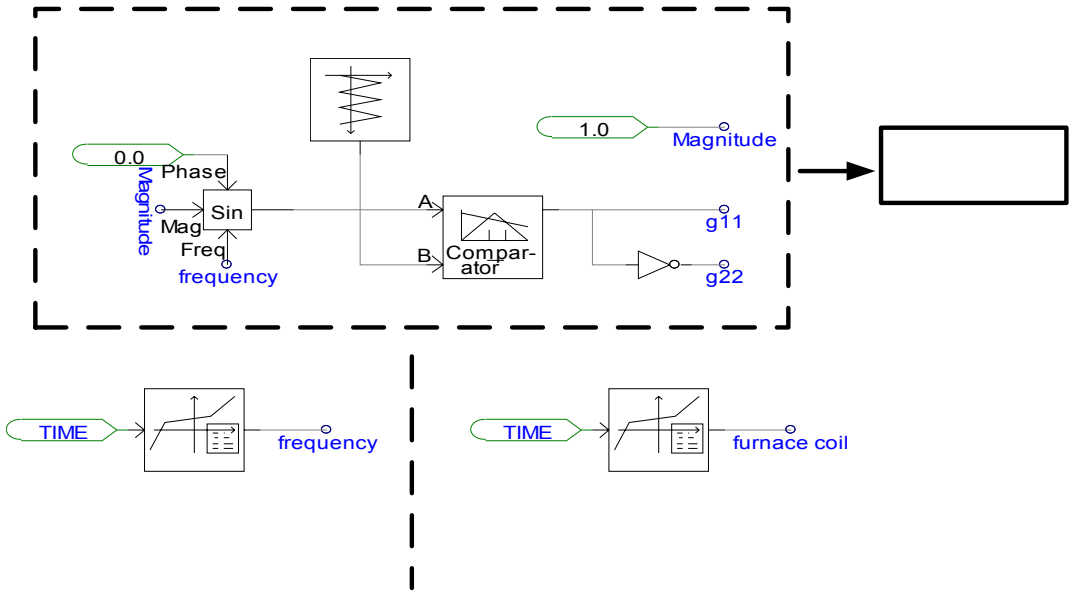

Figure 4.9 DC-AC Inverter control blocks

4.2 Simulation Results of Induction Furnace

In this part of thesis simulation results of proposed 10MVA current source coreless induction furnace are presented. The induction furnace is working without compensation system. Figure 4.10 shows the input current of the furnace. It is shown that the furnace current is not pure sinusoidal. These current contains harmonic component.

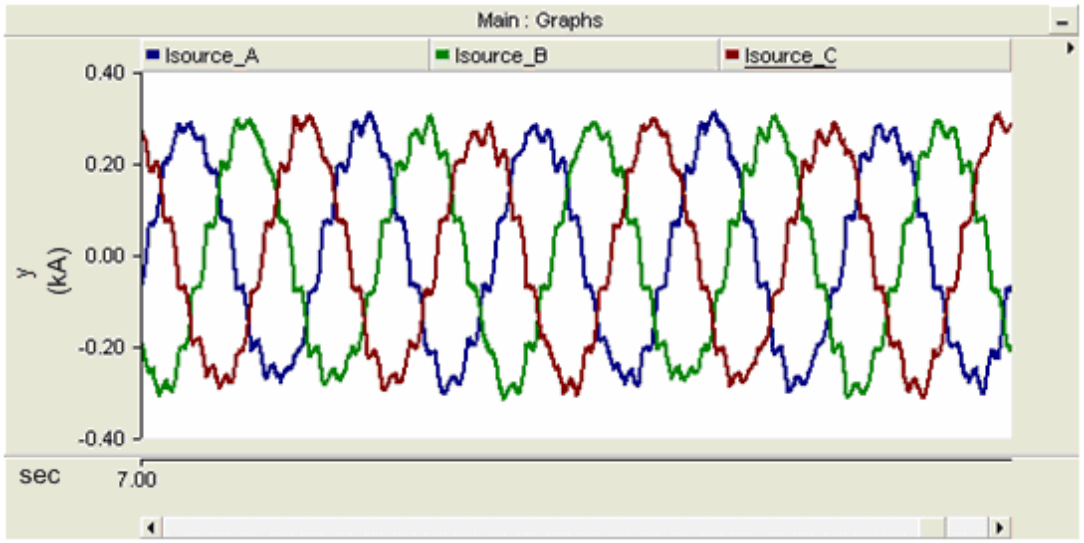

Figure 4.10 Three phase source current of the network

The three phase input voltage of the induction furnace is shown in figure 4.11.It is seen that there is no distortion in the voltage signal.

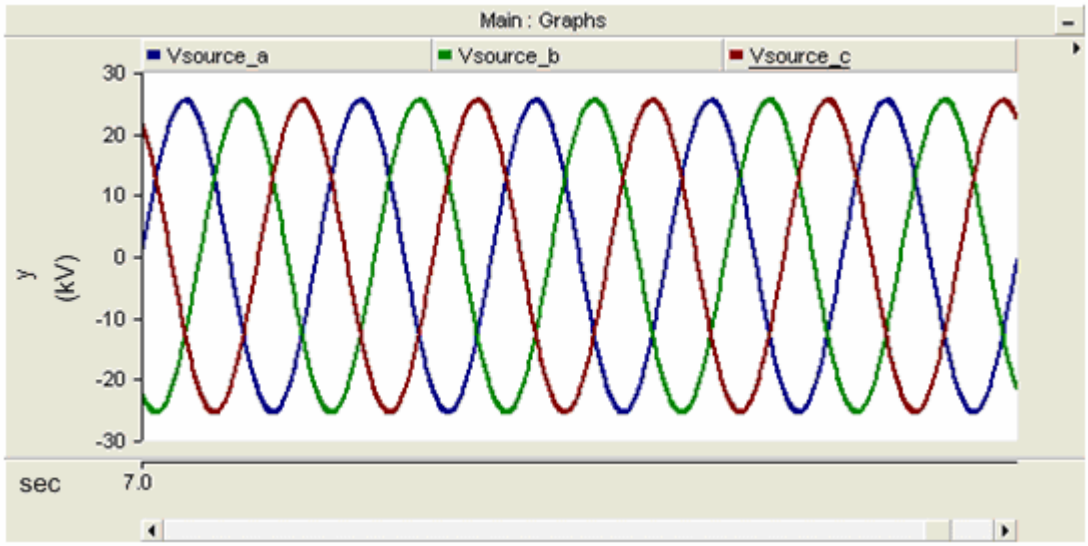

Figure 4.11 Three phase source voltage of the network

Phase A source current and voltage are shown respectively in figure 4.12 and figure 4.13.

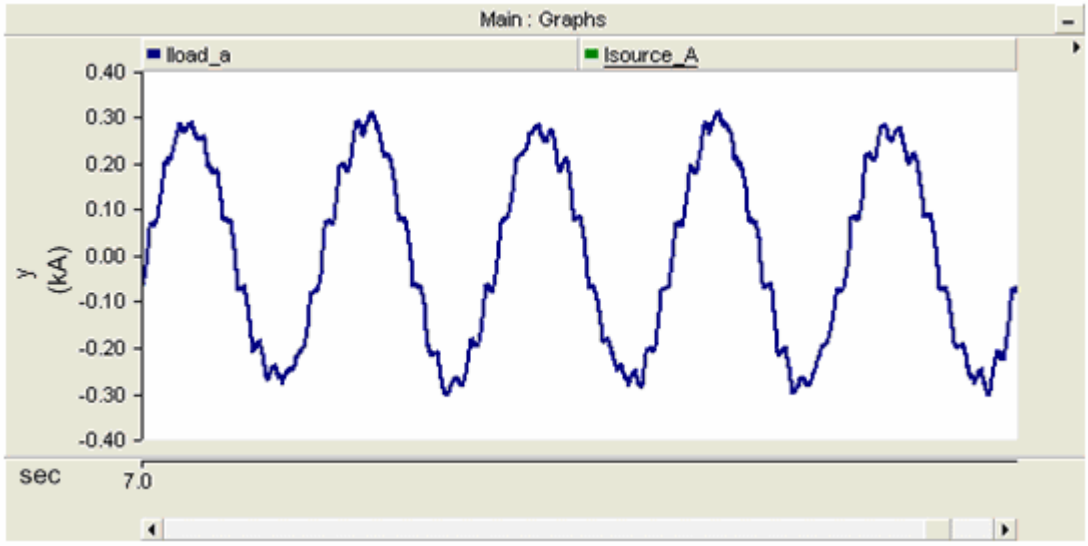

Figure 4.12 Phase A source current of the network

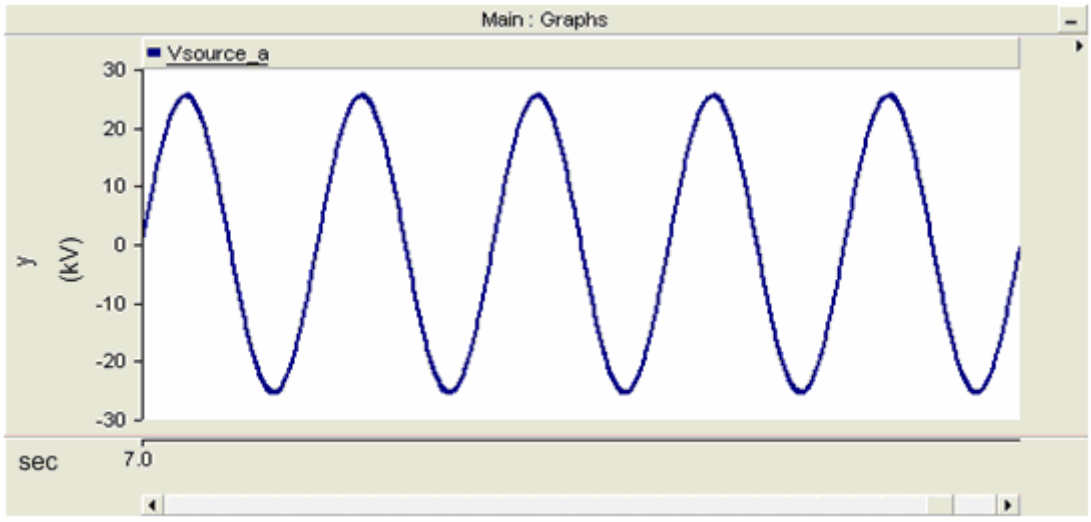

Figure 4.13 Phase A source voltage of the network

Figure 4.14 shows the apparent power of induction furnace. It is shown that the furnace apparent power increase from 6MVA to 10MVA.It means that the furnace is started to charge up to full load capacity. Figure 4.15 and figure 4.16 show the induction furnace current and voltage respectively. It is seen that the furnace current is approximately 30 kA and furnace voltage is approximately 3kV.The furnace voltage is smaller than the furnace current. It means that the furnace coil and capacitor in resonance.

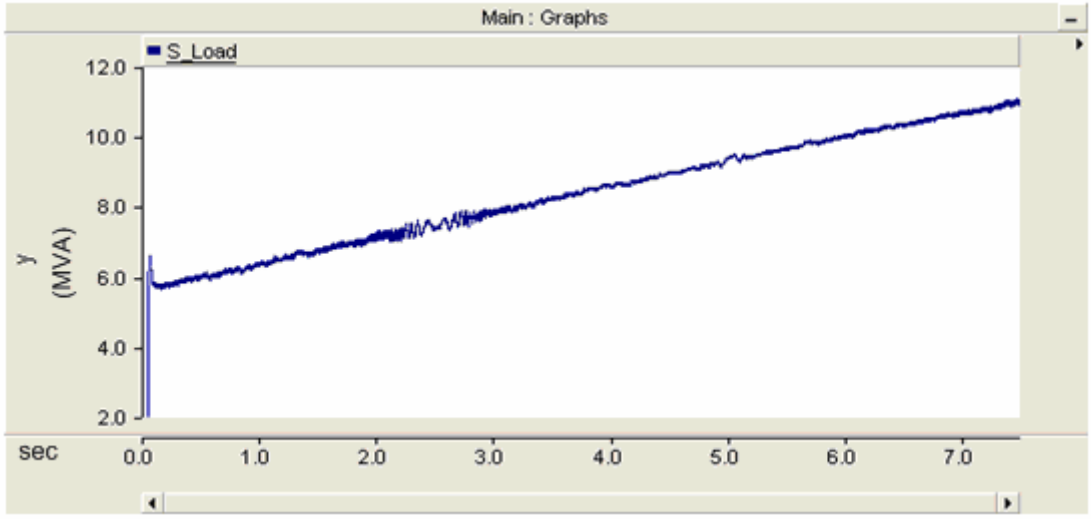

Figure 4.14 Induction furnace apparent power (MVA)

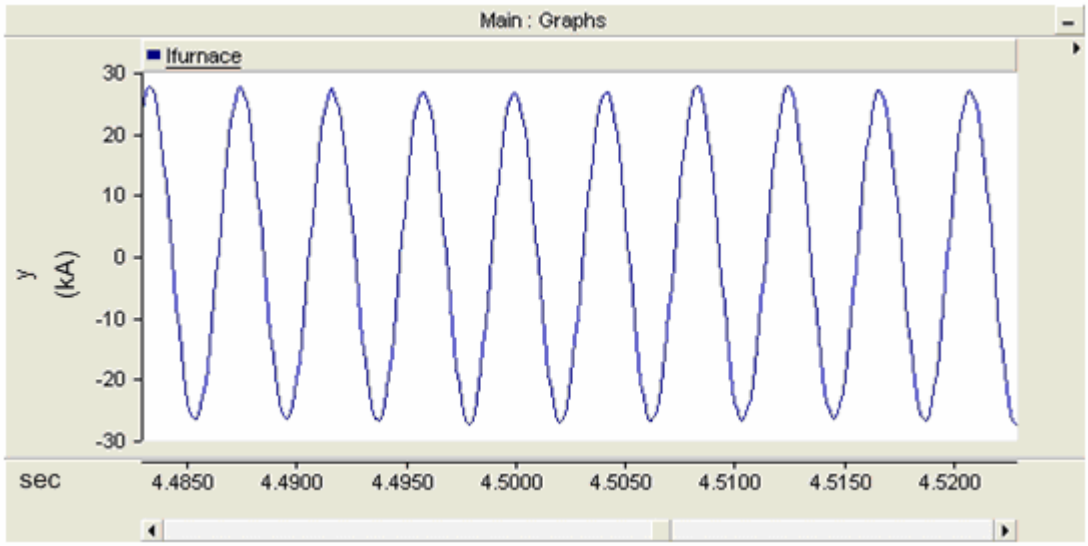

Figure 4.15 Induction furnace current

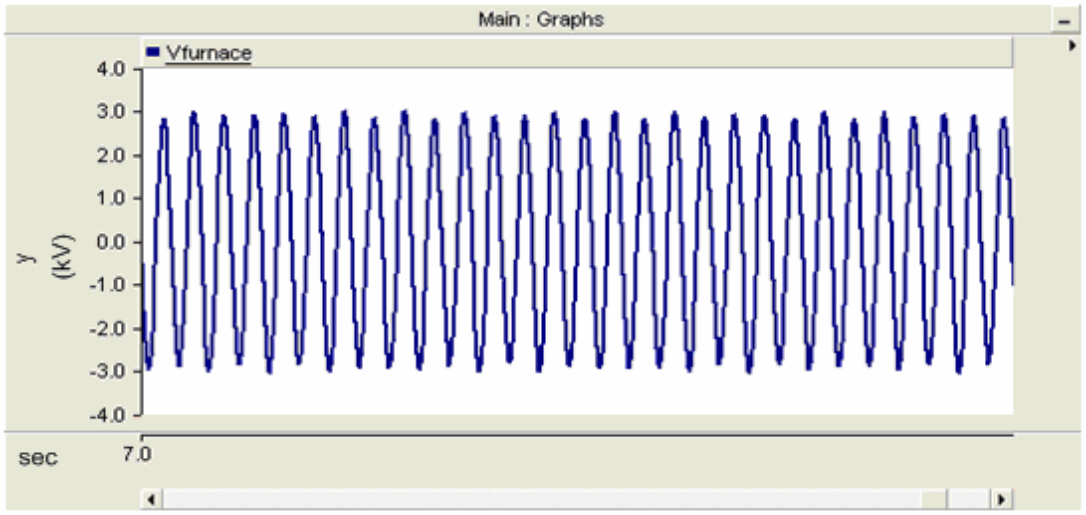

Figure 4.16 Induction furnace voltage

In the figure 4.17 the DC link current of furnace is shown. Figure 4.18 shows the operating frequency of furnace at this time interval. It is shown that there is 32 dc link ripple cycle between 0.1 second. At this time interval, furnace operating frequency is approximately 160 Hz is shown in figure 4.18. It is obviously seen that the period of one cycle ripple current is equal to 0.1/32 ≈ 3.125ms and the frequency of ripple current is equal to 1/3.125ms ≈ 320 Hz which is the two times operation frequency f_o.

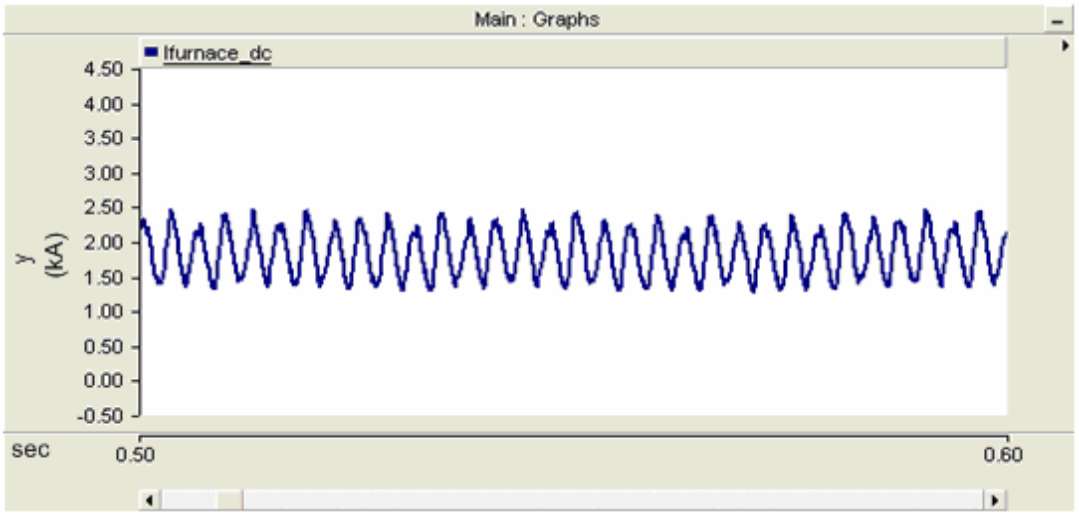

Figure 4.17 Induction furnace DC ripple current at t=0.5s

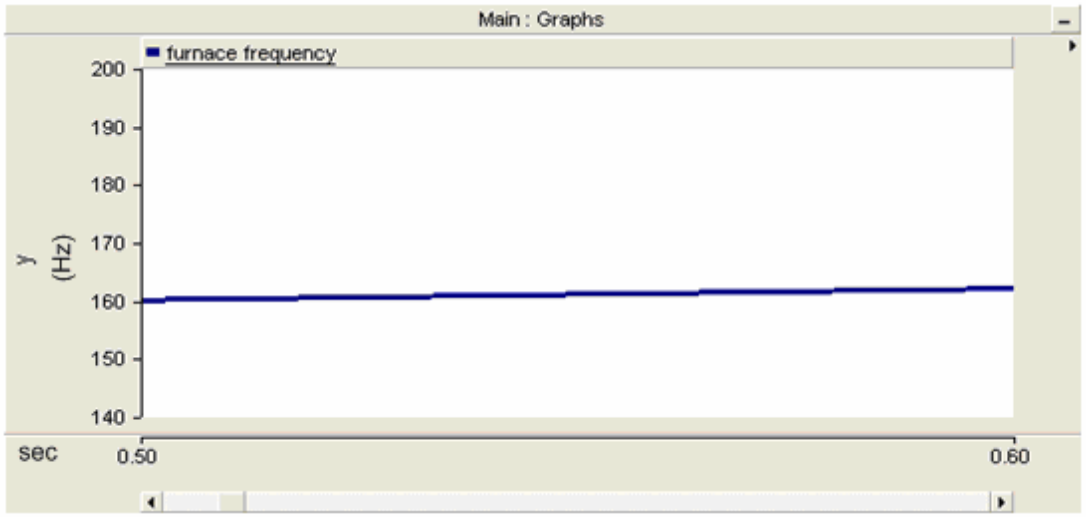

Figure 4.18 Induction furnace operating frequency at t=05s

Figure 4.19 shows the DC link current of furnace at another time period of simulation. In figure 4.20 the operating frequency of furnace at this time interval is shown. It is shown that there is 50 dc link ripple cycle between 0.1 second. At this time interval, furnace operating frequency is approximately 250 Hz is shown in figure 4.20. It is obviously seen that the period of one cycle ripple current is equal to 0.1/50 ≈ 2ms and the frequency of ripple current is equal to 1/2ms ≈ 500 Hz which is the two times operation frequency f_o.

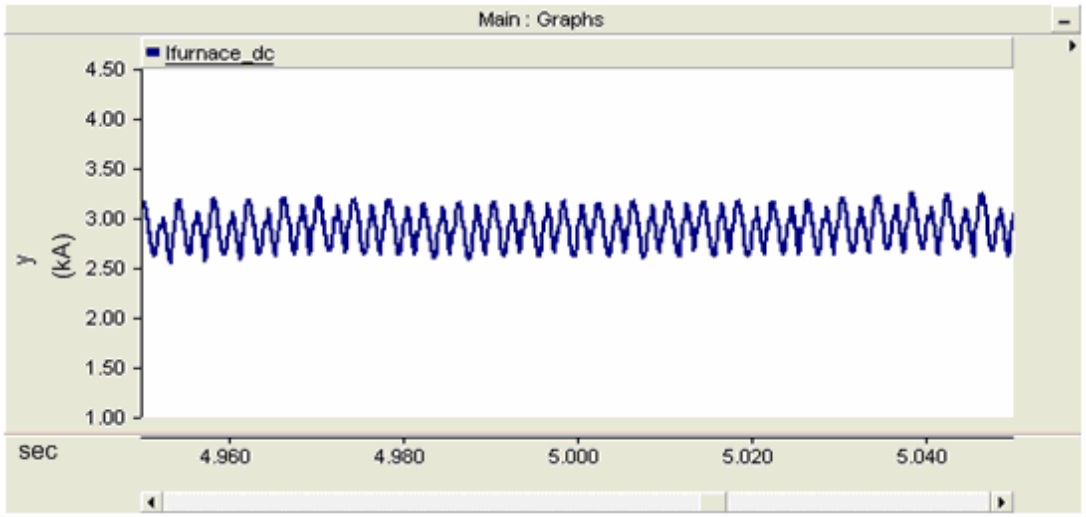

Figure 4.19 Induction furnace DC ripple current at=4.95s

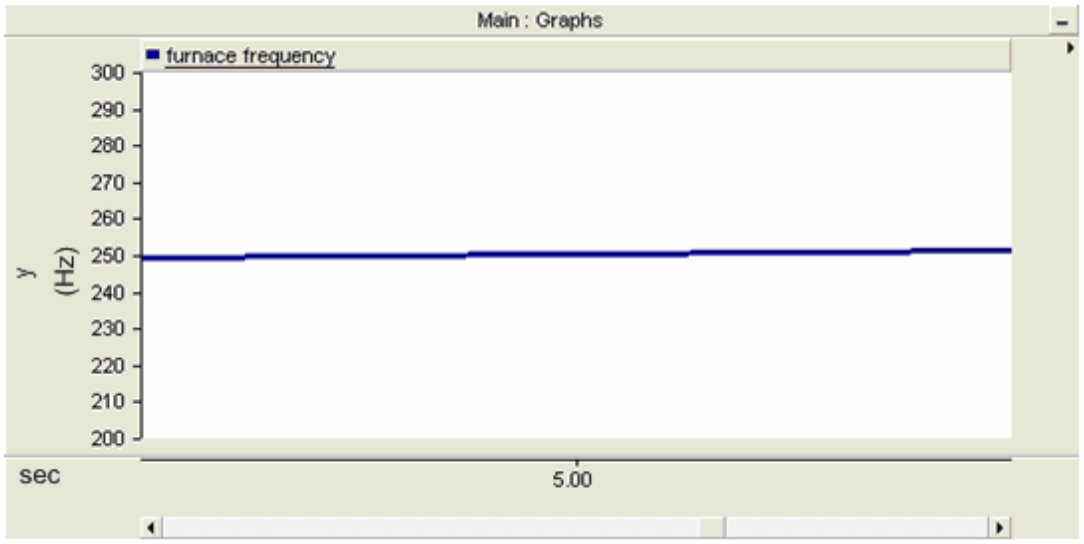

Figure 4.20 Induction furnace operating frequency at t=4.95s

It is obviously explained that the furnace creates varying harmonics and interharmonics.One part of harmonics is created by the rectifier. In proposed furnace, 12 pulse rectifier is used and 12 pulse rectifier produce 11^{th}, 13^{th}, 23^{rd}, 25^{th}; … harmonics. Other part of the harmonics is formed because of the DC link current ripple related to operating frequency and the harmonics of $2f_o \pm f_s$, $4f_o \pm f_s$… are seen in the supply current of furnace. In figure 4.21 harmonic spectrum of furnace current are shown. The harmonic spectrum shows the harmonics with the steps of 10

Hz to indicate the interharmonics Figure 4.22 shows the operating frequency of the furnace at this time interval. It is seen that the furnaces operates approximately 165Hz.From the equation $2f_o \pm f_s$, between the 280 Hz and 380 Hz components are created. These harmonic components are obviously seen in figure 4.21.

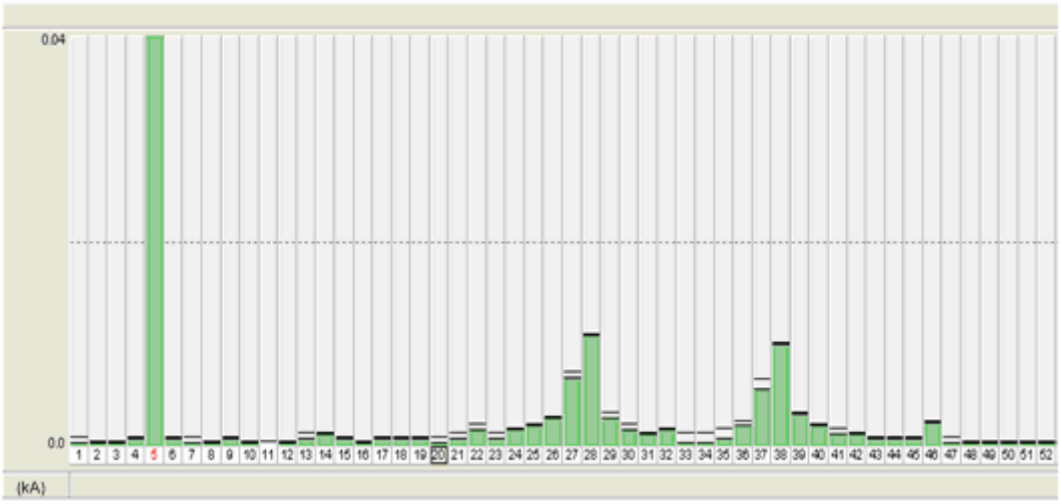

Figure 4.21 Harmonic spectrum of induction furnace at t=0.7s

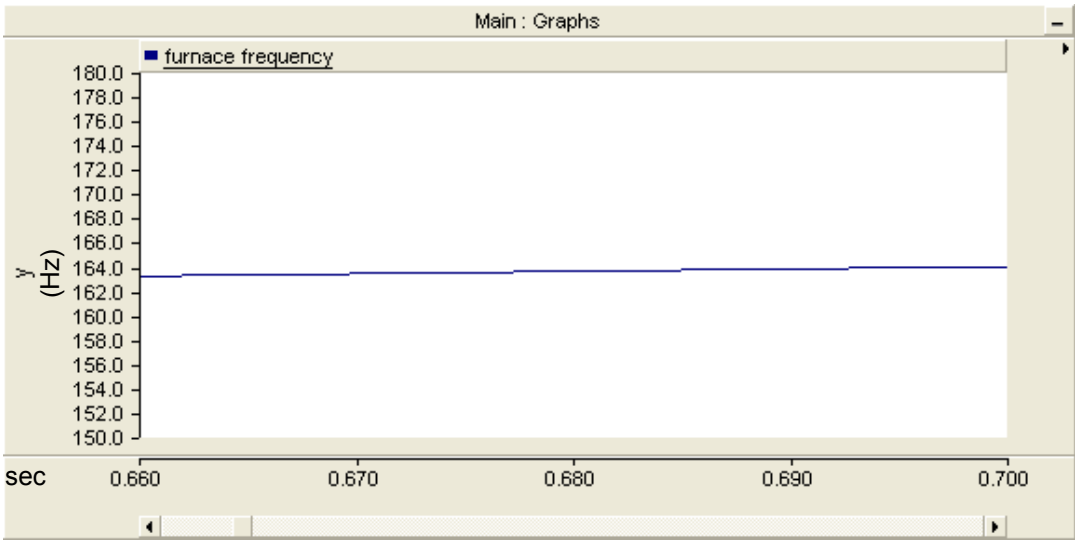

Figure 4.22 Operating frequency of induction furnace at t=0.7s

Figure 4.23 shows the harmonic spectrum of furnace at another time period. At this time interval, the operating frequency of the furnace is shown in figure 4.24.

It is clearly shown in figure 4.24; the furnace operates approximately 185Hz. From the equation between the 320 Hz and 420 Hz components are created. Figure 4.23 verifies the theoretical calculation.

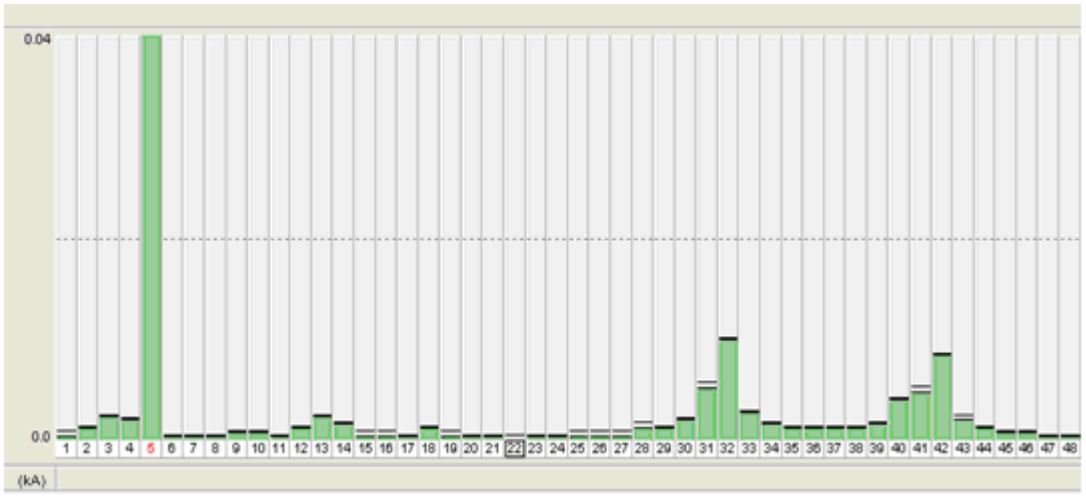

Figure 4.23 Harmonic spectrum of induction furnace at t=1.7s

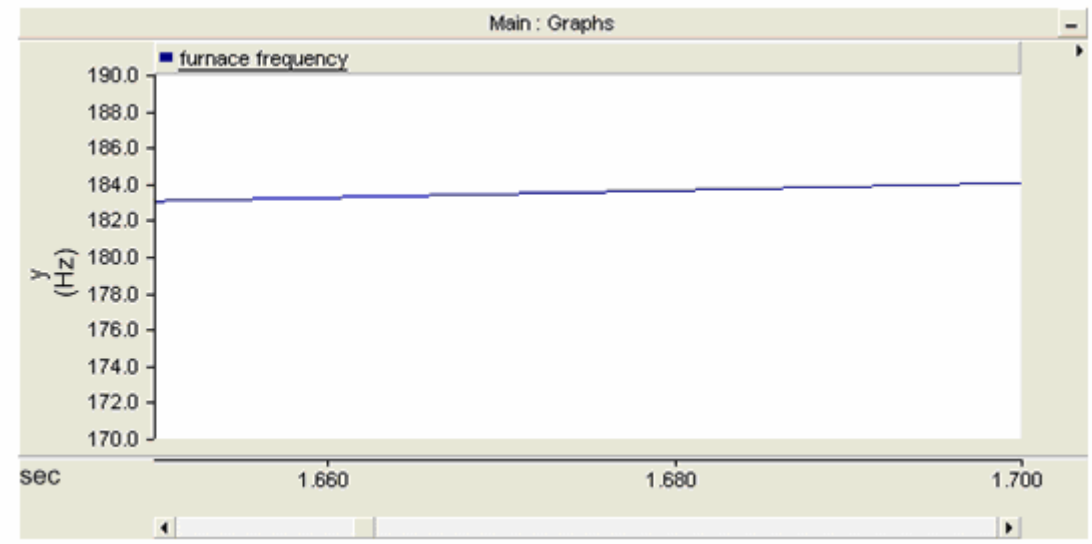

Figure 4.24 Operating frequency of induction furnace at t=1.7s

Figure 4.25 shows the harmonic spectrum of furnace at another time period. At this time interval furnace operates at 225 Hz. It is shown that the figure 4.26.

From the equation between the 400 Hz and 500 Hz components are created. Figure 4.25 verifies the theoretical calculation.

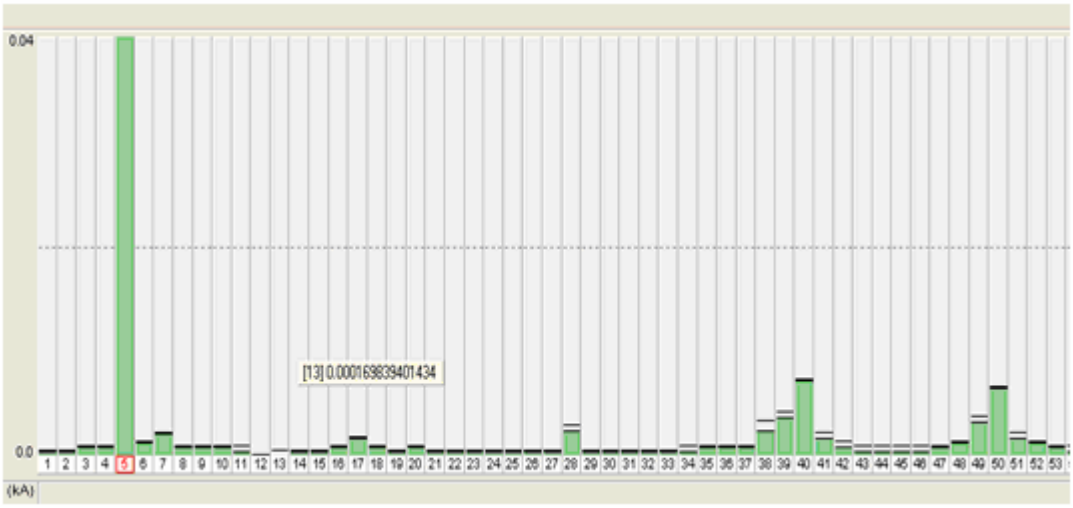

Figure 4.25 Harmonic spectrum of induction furnace at t=3.7s

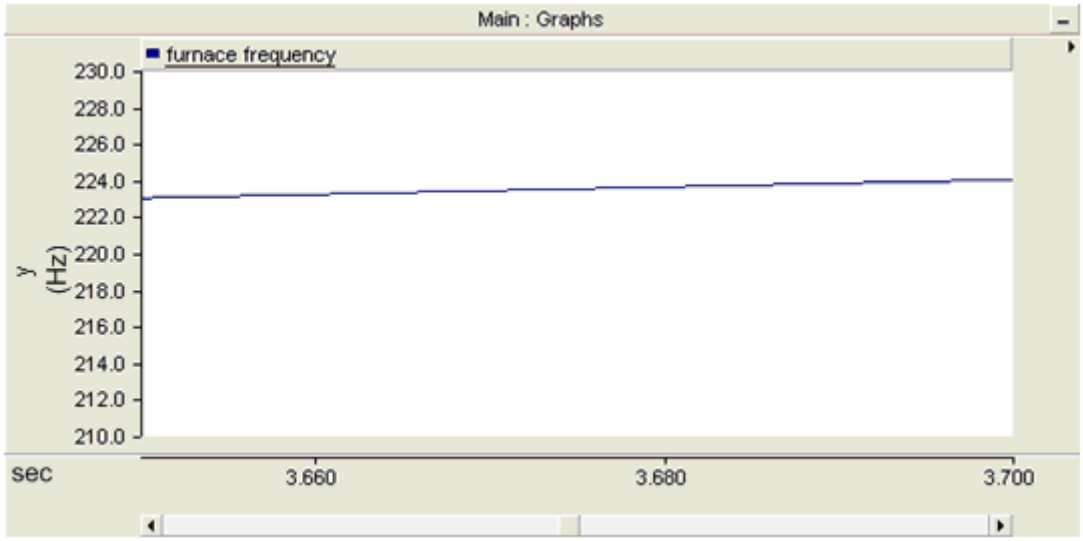

Figure 4.26 Operating frequency of induction furnace at t=3.7s

Figure 4.27 shows the harmonic spectrum of furnace at another time period. At this time interval furnace operates at 250 Hz. It is shown that the Figure 4.28.From the equation between the 450 Hz and 550 Hz components are created. Figure 4.27 verifies the theoretical calculation.

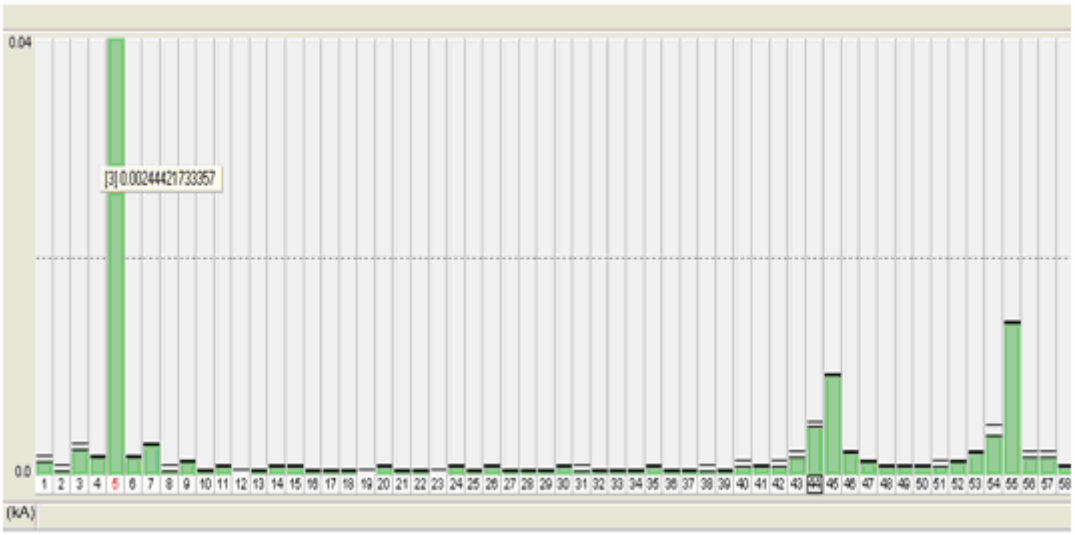

Figure 4.27 Harmonic spectrum of induction furnace at t=4.95s

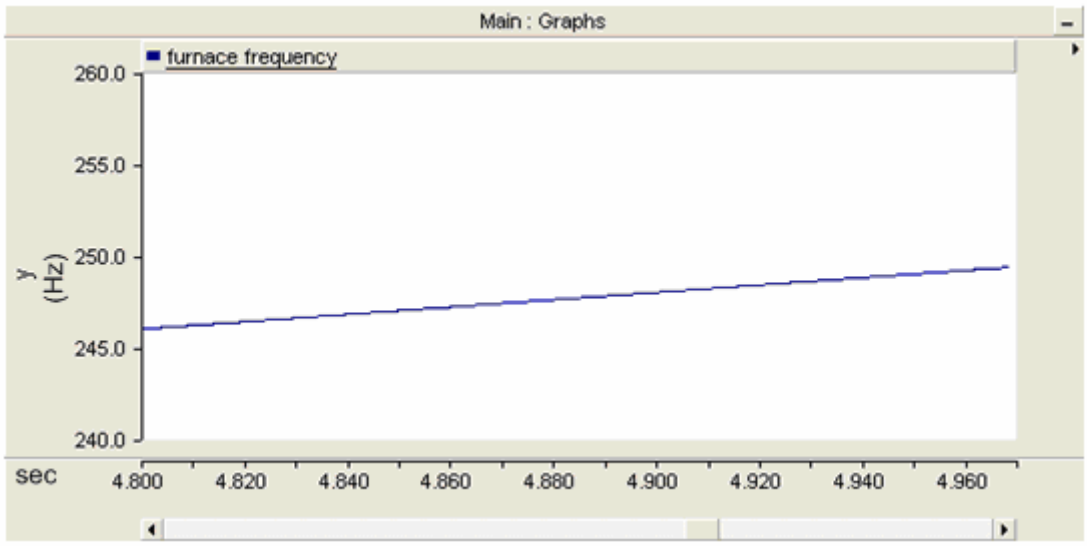

Figure 4.28 Operating frequency of induction furnace at t=4.95s

Figure 4.29 shows the harmonic spectrum of furnace at another time period. At this time interval furnace operates at 300 Hz. It is shown that the Figure 4.30.From the equation between the 550 Hz and 650 Hz components are become higher. Figure 4.29 verifies the theoretical calculation.

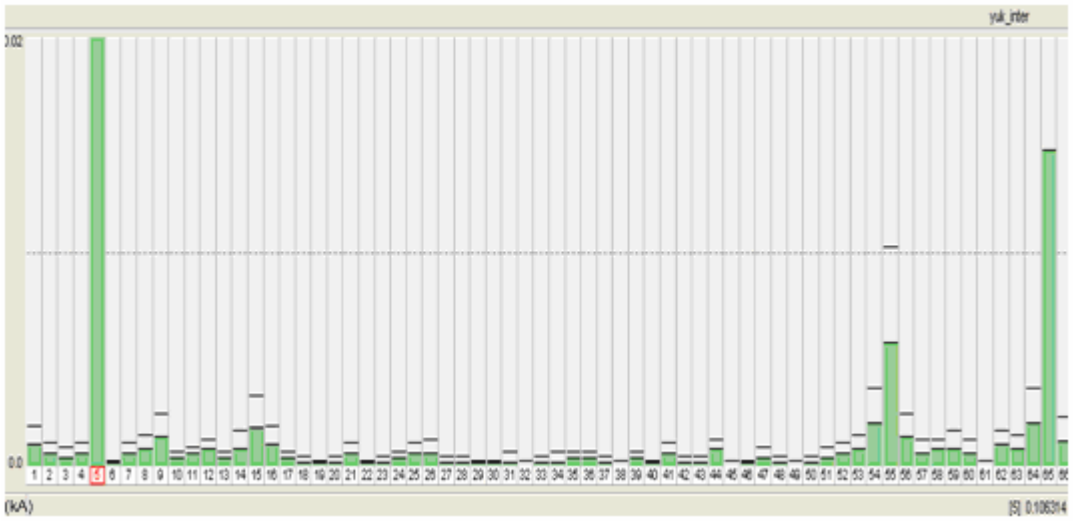

Figure 4.29 Harmonic spectrum of induction furnace at t=7.5s

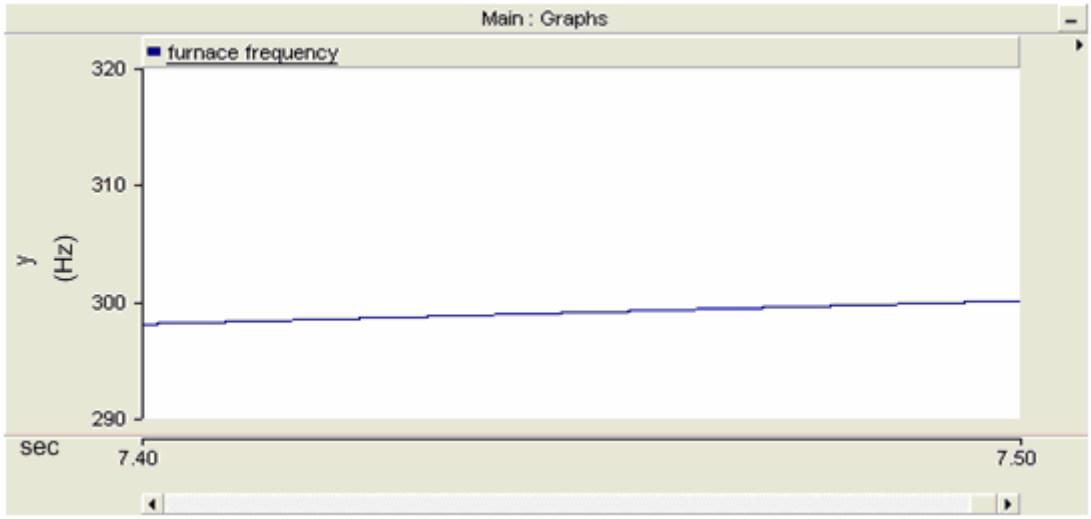

Figure 4.30 Operating frequency of induction furnace at t=7.5s

5. OPERATION PRINCIPLE AND MODELING OF PROPOSED SHUNT ACTIVE POWER FILTER

5.1 Operation Principle of Shunt Active Power Filter

Power Quality (PQ) is an important measure of an electrical power system. The term PQ means to maintain purely sinusoidal current wave form in phase with a purely sinusoidal voltage wave form. The power generated at the generating station is purely sinusoidal in nature. The deteriorating quality of electric power is mainly because of current and voltage harmonics due to wide spread application of static power electronics converters, zero and negative sequence components originated by the use of single phase and unbalanced loads, reactive power, voltage sag, voltage swell, flicker, voltage interruption etc.

To improve the power quality traditional compensation methods such as passive filters, synchronous capacitors, phase advancers, etc. were employed. However traditional controllers include many disadvantages such as fixed compensation, bulkiness, electromagnetic interference, possible resonance etc. These disadvantages urged power system and power electronic engineers to develop adjustable and dynamic solutions using custom power devices. Custom power devices are power conditioning equipments using static power electronic converters to improve the power quality of distribution system customers. These include Active Power Filter (APF), dynamic voltage restorer (DVR) and Unified Power Quality Conditioner (UPQC). DVR is a series compensator used to eliminate the disturbances in voltage. Recently UPQC, which consists of both shunt and series compensators, is proposed as a one shot solution for power quality problems.

Between the different technical options available to improve power quality, active power filters have proved to be an important alternative to compensate for current and voltage disturbances in power distribution systems (Moran et.al., 1999). There are many configurations of active filters, such as the series active filter, shunt active filter, and combination of shunt and series active filter. Shunt APF is considered to be the most basic configuration for active power filter. Shunt APF is a device that is connected in parallel with the AC line as shown in Figure 5.1. It needs

to be sized only for the harmonic current drawn by the non-linear loads and function as a current source to cancel the reactive and harmonic currents generated from a group of nonlinear loads, so that the resulting total current drawn from the AC main is sinusoidal (Rudnick et.al., 2003).

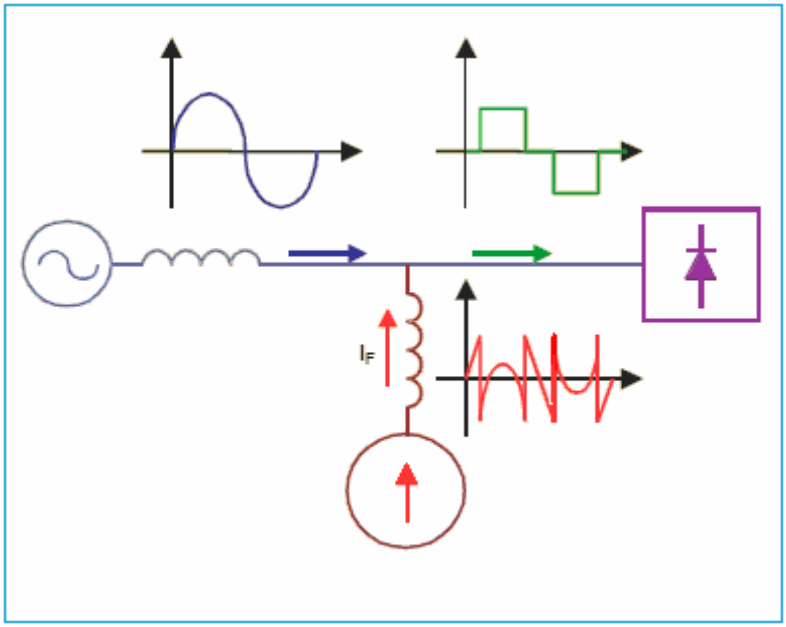

Figure 5.1 Shunt APF connected to the nonlinear load (Rudnick et.al., 2003).

In three-phase unbalanced loads it is also possible to redistribute and equalize the mains phase-currents, providing that the total amount of active power remains the same. In this form, the filter can solve three problems at once: a) elimination of unwanted harmonics b) power factor compensation c) redistribution of power to keep the system balanced.

In the practical implementation of this kind of filter, force commutated, current-controlled voltage-source inverters are widely used. The quality and performance of the active power filter depends mainly on three considerations a) the design of the power inverter (semiconductors, inductances, capacitors, dc voltage); b) the modulation method used to follow the current template (hysteresis, triangular carrier, periodical sampling); and c) the method implemented to generate the reference generator (Dixon et.al., 1995).

Figure 5.2 shows the basic compensation principle of the shunt active power filter. It is controlled to draw or supply a compensating current ic from or to the

utility, so that it cancels current harmonics on the ac side. Figure 5.2 shows the different waveforms. Curve A is the load current waveform, and curve B is the desired main current. Curve C shows the compensating current injected by the active filter containing all the harmonics, to make the mains current sinusoidal. In this manner a shunt active power filter can be used to eliminate current harmonics and reactive power compensation. (Jain et.al., 2007)(Usta et. al.2006).

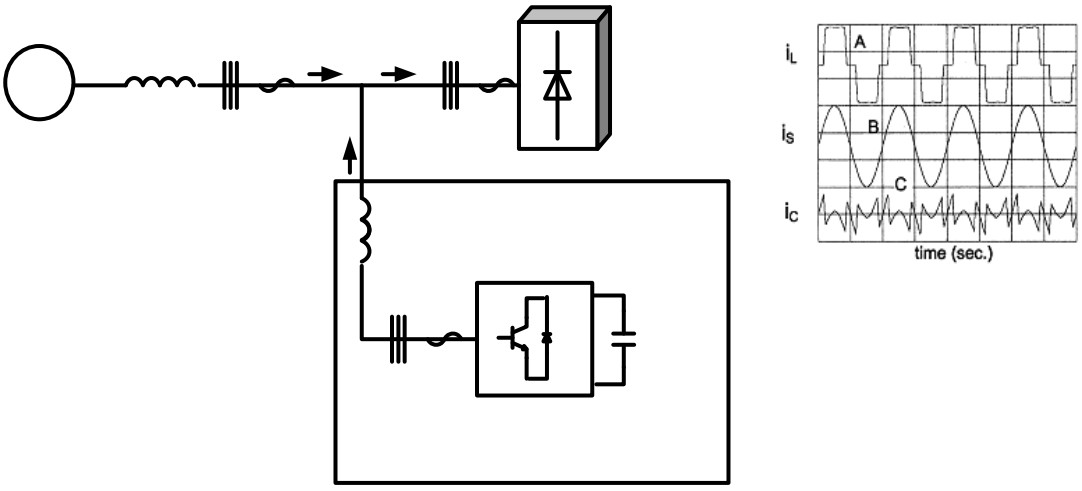

Figure 5.2 Basic compensation principle and shapes of the load, source, and filter current

Shunt active power filters are normally implemented with pulse-width modulated voltage source inverters (Moran et.al.,1999). There are two types of inverters used in the development of APF's. Figure 5.3 shows the current-fed pulse width modulation (PWM) inverter bridge structure. It behaves as a non-sinusoidal current source to meet the harmonic current requirement of the nonlinear load. A diode is used in series with the self commutating device (IGBT) for reverse voltage blocking. However, GTO-based configurations do not need the series diode, but they have restricted frequency of switching. They are considered sufficiently reliable but have higher losses and require higher values of parallel ac power capacitors. Moreover, they cannot be used in multilevel or multistep modes to improve performance in higher ratings.

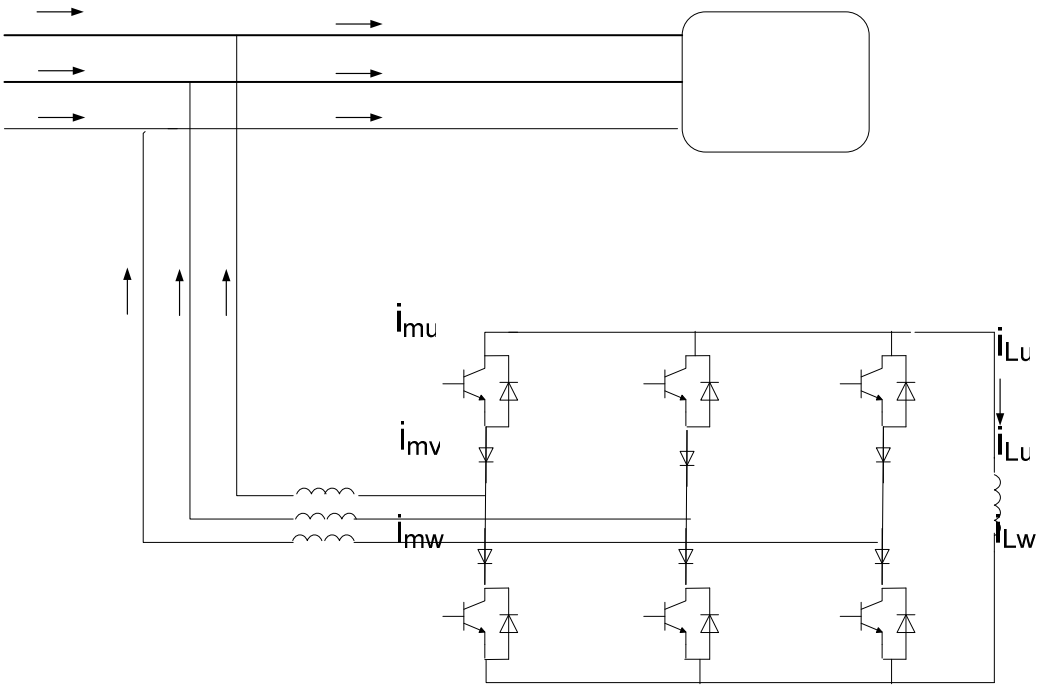

Figure 5.3 The power circuit of current fed Active Power Filter

The other converter used as an APF is a voltage-fed PWM inverter structure, as shown in Figure 5.4.The voltage-source-based power converter is used to generate the compensation current. This current can be injected into the power feeder such that both the harmonics and the reactive load current can be cancelled It has a self-supporting dc voltage bus with a large dc capacitor. It has become more dominant, since it is lighter, cheaper, and expandable to multilevel and multistep versions, to enhance the performance with lower switching frequencies. It is more popular in UPS based applications, because in the presence of mains, the same inverter bridge can be used as an APF to eliminate harmonics of critical nonlinear loads (Singh et.al., 1999). In this study we use voltage fed PWM inverter for power circuit of SAPF.

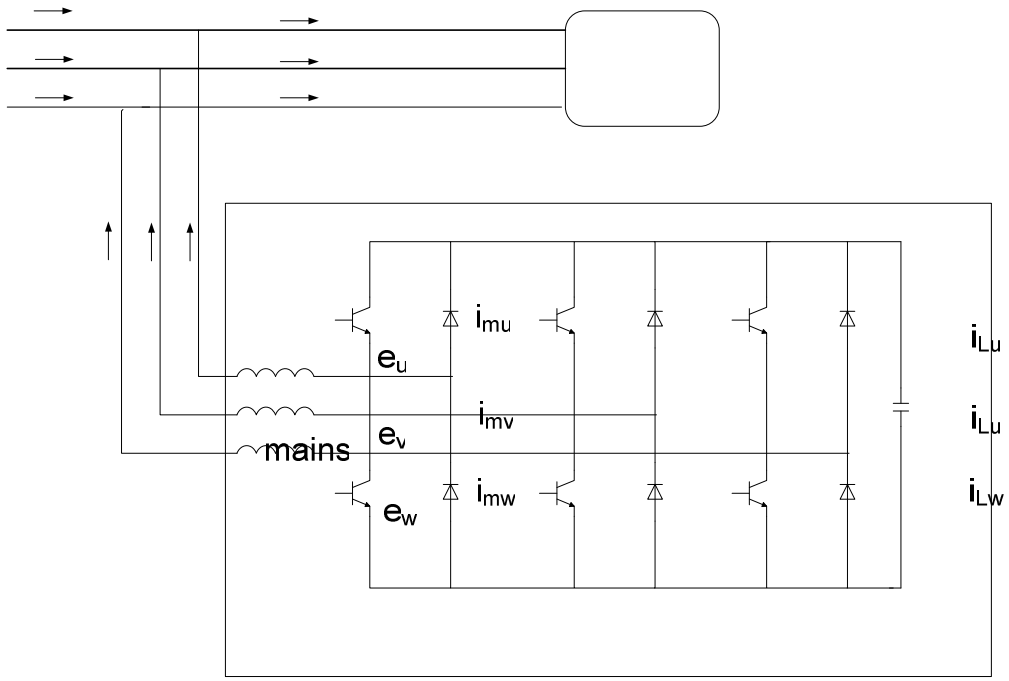

Figure 5.4 The power circuit of voltage fed Active Power Filter

In recent years, there has been an increasing interest in using multilevel inverters for high power energy conversion, especially for drives and reactive power compensation. Multilevel PWM inverters can be connected to high voltage source without a coupling transformer. The use of neutral-point-clamped (NPC) inverters allows equal voltage shearing of the series connected devices in each phase. However, the neutral point potential deviates, resulting in an excess voltage stress to either the upper or lower set of devices (Moran et.al.,1999).

Numerous types of shunt active power filters have been proposed in many papers. Most of these papers discuss the standard and function for controlling different topologies of APF's. This project is concerned on a PLL based control topology and voltage source inverter power circuit for a shunt active power filter.

5.2 Available Control Methods of Shunt Active Filters

Figure 5.5 shows the main components of a typical active power filter system and their interconnections. Active power filter consist of power circuit and control circuit. The operation of APF consists of two stages; detecting the harmonics current

and generating compensation current injecting to the line. The detected current is used as the input signal for reference current generator and the target is the harmonics current component without fundamental component. The output of reference current generator will be used as reference signal for PWM to controlled voltage source inverter (VSI). Finally the current generated by voltage source inverter will be injected to the line.

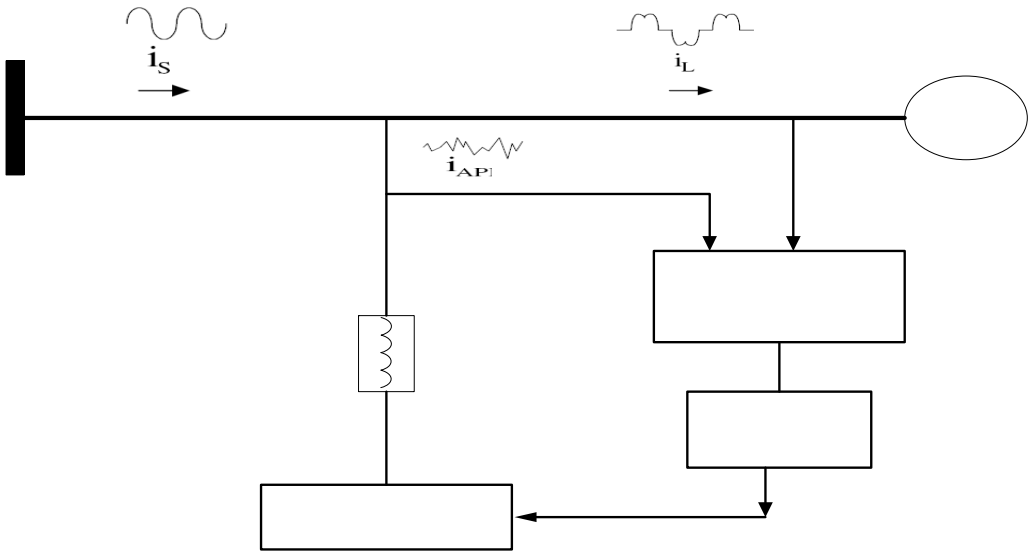

Figure 5.5 Diagram illustrating components of the shunt connected active power filter (Bayindir, 2006)

Before 90's the most popular control schemes are FFT (Fast Fourier Transform) in frequency-domain and IRP (Instantaneous Reactive Power Compensation) in time-domain.

Because the control signal is computed by the historic data, frequency domain correction depends on the periodic characteristics of the distortion. The disadvantage of frequency-domain technique lies in the increased computational requirements. With the increase of the order of highest harmonic to be eliminated, the number of calculations also increases, resulting in longer response times. IRP is based on the instantaneous reactive power theory. The greatest advantage of time-domain correction is the fast response to changes in the power system. It is easy to implement and has little computational burden.

In the last decade of the last century, power switching devices and high performance digital signal processors have been developed rapidly, which makes it possible to improve the control strategies applied to active power filters. At the same time, the industrial applications have required better performance of the APF. In 1990's, several new and innovative control strategies have been published continually. The development of the APF control techniques has reached the upsurge (Chen et.al.,2004).

At present, the research trends of the control strategies are mainly towards the optimizing and practical application of the control strategies.

5.2.1 Current Reference Generation Techniques

The performance of an active power filter depends on many factors, but mainly on the selected reference generation scheme. The current reference template must include the amplitude and phase information to produce the desired current component compensation, while keeping the voltage across the dc bus constant. The reference generation scheme must operate adequately under steady state and transient condition.

5.2.1.1 p-q Method

In 1984, the instantaneous reactive power theory has been published. Based on this theory, the so-called "p-q method" can be successfully applied in the control of APF.

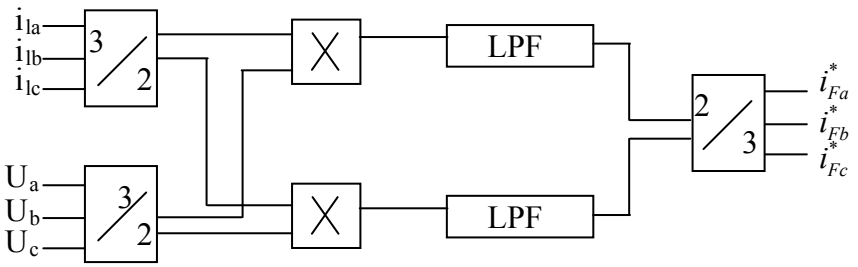

Figure 5.6 Calculation block diagram of p-q method

The calculation block diagram is shown in figure 5.6. At first, the three-phase voltage and the three-phase load currents are transformed into the static *α-β* frame by the following:

$$\begin{bmatrix} u_\alpha \\ u_\beta \end{bmatrix} = \sqrt{\frac{2}{3}} \cdot \begin{bmatrix} 1 & -1/2 & -1/2 \\ 0 & \sqrt{3}/2 & -\sqrt{3}/2 \end{bmatrix} \cdot \begin{bmatrix} u_1 \\ u_2 \\ u_3 \end{bmatrix} \tag{5.1}$$

$$\begin{bmatrix} i_{l\alpha} \\ i_{l\beta} \end{bmatrix} = \sqrt{\frac{2}{3}} \cdot \begin{bmatrix} 1 & -1/2 & -1/2 \\ 0 & \sqrt{3}/2 & -\sqrt{3}/2 \end{bmatrix} \cdot \begin{bmatrix} i_{l1} \\ i_{l2} \\ i_{l3} \end{bmatrix} \tag{5.2}$$

The instantaneous real power p_1 and the instantaneous imaginary power q_1 are given by:

$$\begin{bmatrix} p_l \\ q_l \end{bmatrix} = \begin{bmatrix} u_\alpha & u_\beta \\ u_\beta & -u_\alpha \end{bmatrix} \cdot \begin{bmatrix} i_{l\alpha} \\ i_{l\beta} \end{bmatrix} \tag{5.3}$$

According to the instantaneous reactive power theory, p_1 and q_1 are decomposed into instantaneous real and imaginary powers, respectively

$$p_l = \bar{p}_l + \tilde{p}_l, q_l = \bar{q}_l + \tilde{q}_l \tag{5.4}$$

where $\bar{p}$ and $\bar{q}$ are the dc components corresponding to the fundamental current, and $\tilde{p}$ and $\tilde{q}$ are the ac component corresponding to the harmonic current.

So the current reference signal can be achieved:

$$\begin{bmatrix} i_{F1} \\ i_{F2} \\ i_{F3} \end{bmatrix} = \sqrt{\frac{2}{3}} \begin{bmatrix} 1 & 0 \\ -1/2 & \sqrt{3}/2 \\ -1/2 & -\sqrt{3}/2 \end{bmatrix} \cdot \begin{bmatrix} u_\alpha & u_\beta \\ u_\beta & -u_\alpha \end{bmatrix}^{-1} \cdot \begin{bmatrix} \tilde{p}_l \\ \tilde{q}_l \end{bmatrix} \tag{5.5}$$

Because the zero-sequence component is neglected in the system, the p-q method is not accurate when the three-phase system is unbalanced or distorted.

The instantaneous reactive power theory allows the possibility of different compensation strategies:

- Compensate the instantaneous imaginary power q only. In this case the main supplies the whole instantaneous real power p.

-Compensate the instantaneous imaginary power q plus the AC term of the instantaneous real power p (Gonzalez et.al,1998).

5.2.1.2 Discrete Fourier Transform (DFT) Control

Discrete Fourier Transform (DFT) is a mathematical transformation for discrete signals which gives the both the amplitude and phase information of the desired harmonic by calculating (5.6).

$$\overline{X}_h = \sum_{n=0}^{N-1} x(n).\cos\left(\frac{2\pi hn}{N}\right) - j.\sum_{n=0}^{N-1} x(n).\sin\left(\frac{2\pi hn}{N}\right) \tag{5.6}$$

$$\overline{X}_h = X_{hr} + j.X_{hi} \tag{5.7}$$

$$\left|\overline{X}_h\right| = \sqrt{(X_{hr})^2 + (X_{hi})^2} \;\; ; \;\; \phi_h = \arctan\left(\frac{X_h}{X_{hr}}\right) \tag{5.8}$$

where N is the number of samples per fundamental period; x(n) is the input signal(voltage or current) at point n; X_h is the complex Fourier vector of the h^{th} harmonic of the input signal; X_{hr} is the real part of X_h ; X_{hi} is the imaginary part of X_h . $|X_h|$ is the amplitude of the vector; ϕ_h is the phase of the vector.

Once the harmonics are detected and isolated with (5.6) it is just a matter of reconstruction back in time-domain to create the compensation signal for the controller (Asiminoaei et. al.,2005).

This method is affected voltage distortions is sensitive to parameter variations and operating conditions characteristic. The classical DFT is a widely spread algorithm. However, it disposes by a relatively high computational burden, and thus, it is not basically eligible for real-time applications.

5.2.1.3 Synchronous Reference Frame Method (SRF)

In this method, the real currents are transformed into a synchronous reference frame. The reference frame is synchronized with the ac mains voltage, and is rotating at the same frequency. As for the instantaneous reactive power theory, the current in *d-q* frame can be composed by the instantaneous active current $i_{ld} = \tilde{i}_{ld} + \bar{i}_{ld}$. The division of the dc and ac can be obtained across a low-pass filter. The reference current signal can be achieved by the ac component in d-q frame through a counter-transformation.

One of the most important characteristics of this method is that the reference currents are derived directly from the real load currents without considering the source voltages. The generation of the reference signals is not affected by voltage unbalance or voltage distortion, therefore increasing the compensation robustness and performance.

The fundamental current of the dq components is now a dc value. The harmonics appear like ripple. Harmonic isolation of the dq transformed signal is achieved by removing the dc offset. This is accomplished using a high pass filter (HPF). The reference currents are obtained with an inverse transformation. Figure 5.7 illustrates a block diagram of the dq synchronous reference frame method (Marques,1998).

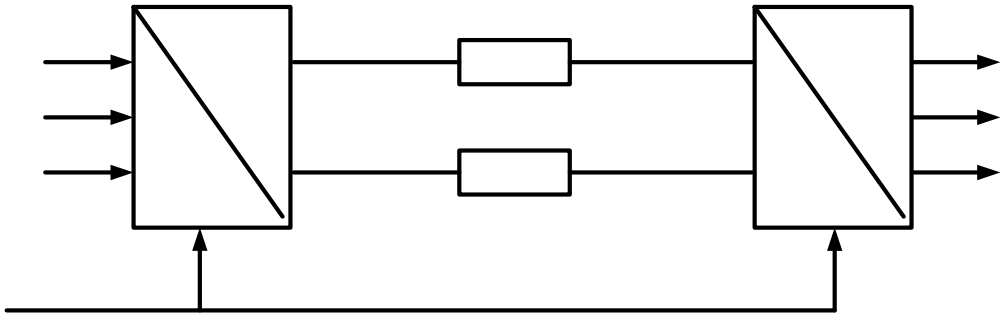

Figure 5.7 Principle of the synchronous reference frame method

5.2.2 Current Control Techniques

The performance of an active power filter is affected significantly by the selection of current control techniques. To compensate for the distorted current drawn by the rectifiers from the utility grid, the active filter and its current control must have the capability to track sudden slope variations in the current reference, corresponding to very high di/dt value, which makes the design of the control and the practical implementation of the filter particularly critical. Therefore, in the active power filter application, the choice and implementation of the current regulator is more important for the achievement of a satisfactory performance level.

5.2.2.1 Hysteresis Current Control

The basic principle of hysteresis current control technique is that the switching signals are derived from the comparison of the current error signal with a fixed width hysteresis band. With simple, extreme robustness, good stability, fast dynamic and automatic current limited characteristic, this current control technique exhibits some unsatisfactory features. The main one is that it produces a varying modulation frequency for the active power filter. And it is difficult to design the input filters to the possible generation of unwanted resonance on the utility grid. That the performance of active power filter affected by the phase current interaction is also a negative feature and the current coupling restrict the current control technique applied in the system with insulated neutral. In order to overcome the intrinsic shortcomings, many improvements have been suggested.

This technique is simple and robust but has many drawbacks as a phase current interaction and a varying modulation frequency that causes acoustic noise and difficulty in designing input filters (Meo et.al.,2002).

5.2.2.2 Triangle-Comparison PWM control

This current control technique is also called linear current control. The principle of the conventional triangle comparison PWM control is that the

modulation signal achieved by a current regulator from the current error signal is intersected with the triangle wave and the pulse signals obtained are to control the switches of the converter. With analog PWM circuit, this current control technique is with fast speed of response and simple implementation. Because the modulation frequency equals the triangle frequency, the current loop gain crossover frequency must be kept below the modulation frequency (Chen et.al.,2004).

5.2.2.3 Space vector modulation (SVM)

The goal of the space vector modulation is to find the appropriate switching combinations and their duty ratios according to certain modulation scheme. The space vector modulation operates in a complex plane divided in the six sectors separated by a combination of conducting or non conducting switches in the power circuit. The reference vector is used to locate two adjacent switching-state vectors and compute the time for which each one is active. Although with the good reliability and strong anti jamming of digital control technique, SVM is of low speed of response caused by the inherent calculation delay (Chen et.al.,2004).

5.3 Proposed Control Strategy for Shunt Active Power Filter

5.3.1 Reference Generation Method

Extraction of signals representing harmonics, reactive current and symmetrical components is a requirement for status evaluation, control and power-quality monitoring/enhancement in power systems (Karimi et.al.,2004). An integral part of an active compensation device is the detection unit which generates the reference signals. Various methods, e.g. Discrete Fourier Transform (DFT), notch filtering and theory of instantaneous reactive power have been presented in the literature for this purpose (Mokhtari et.al, 2004).

In this study we use EPLL based control method for shunt active power filter and voltage source inverter for power circuit. A paper which is written by Karimi

(2004) proposes this control algorithm for shunt active power filter. Figure 5.8 shows the overall block diagram of the detection system for a three phase system. Both voltage and current signals are first passed through one stage of EPLL (enhanced phase locked loop) units to extract harmonic contents and amplitude, phase angle and frequency of the fundamental components. The SC (symmetrical components) blocks are to estimate the symmetrical positive and negative sequence components of both voltage and current signals. The second stage of EPLL units, after the SC blocks, estimates the amplitudes and phase angles of the voltage and current positive-sequence components, for calculation of reactive currents. The last block, shown by R(reactive), calculates the reactive currents (Karimi et.al,2004).

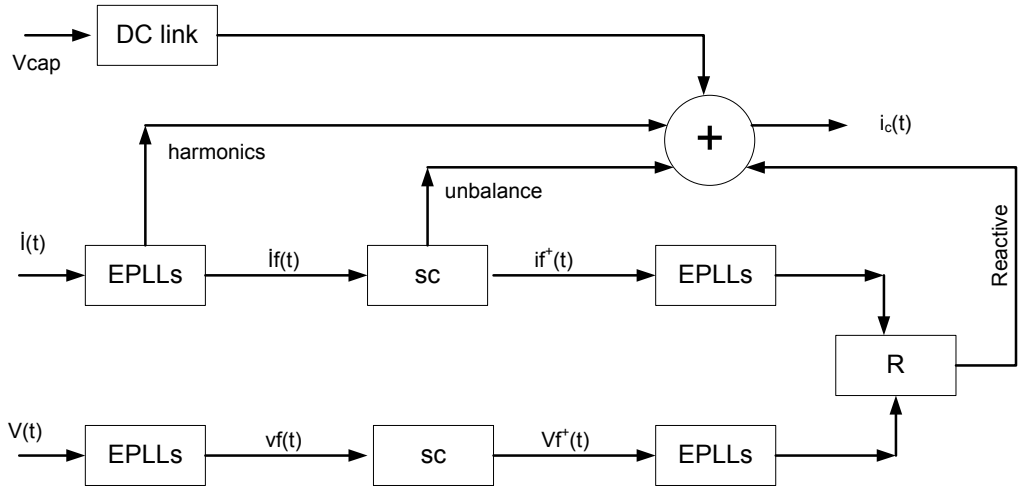

Figure 5 8 Block diagram of control circuit

In this thesis voltage source inverter circuit topology is used. The PWM Bridge consists of six controllable switches (IGBTs) with anti parallel diodes. The current stresses of the semiconductor devices are limited to the peak value of the compensating current if and the devices have to withstand the unipolar dc link voltage vdc as the switching voltage. The voltage-source topology requires the filter to be placed between the supply and the PWM Bridge. The filter has usually either first order (L) or third-order (LCL) structure. Moreover, the filter makes it possible to control the currents. In the dc link there is an electrolytic capacitor with a dc voltage as energy storage. Figure 5.9 shows the power circuit of Shunt Active Power filter of PSCAD model.

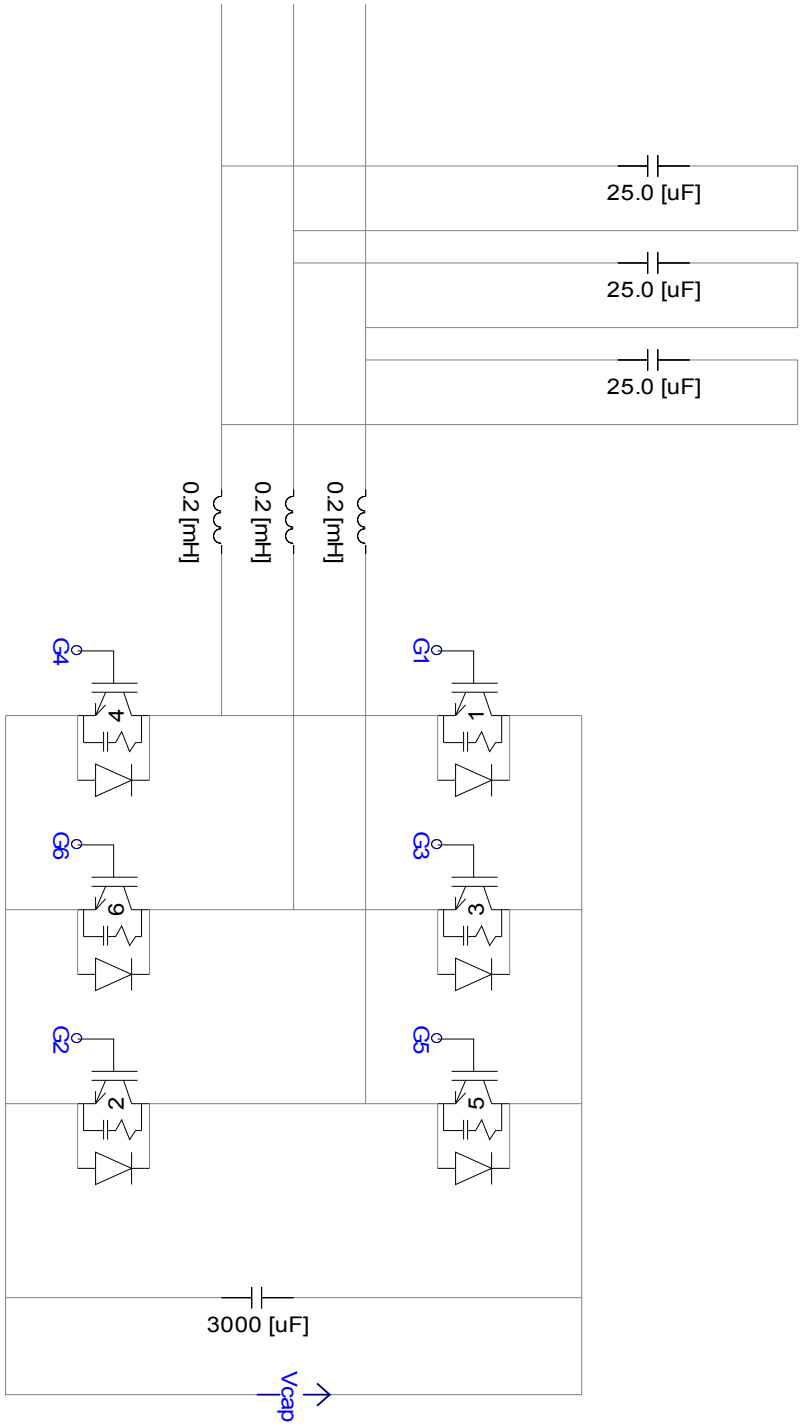

Figure 5.9 Power circuit of PSCAD Model

Figure 5.10 shows the overall control block diagram of PSCAD Model of this topology.

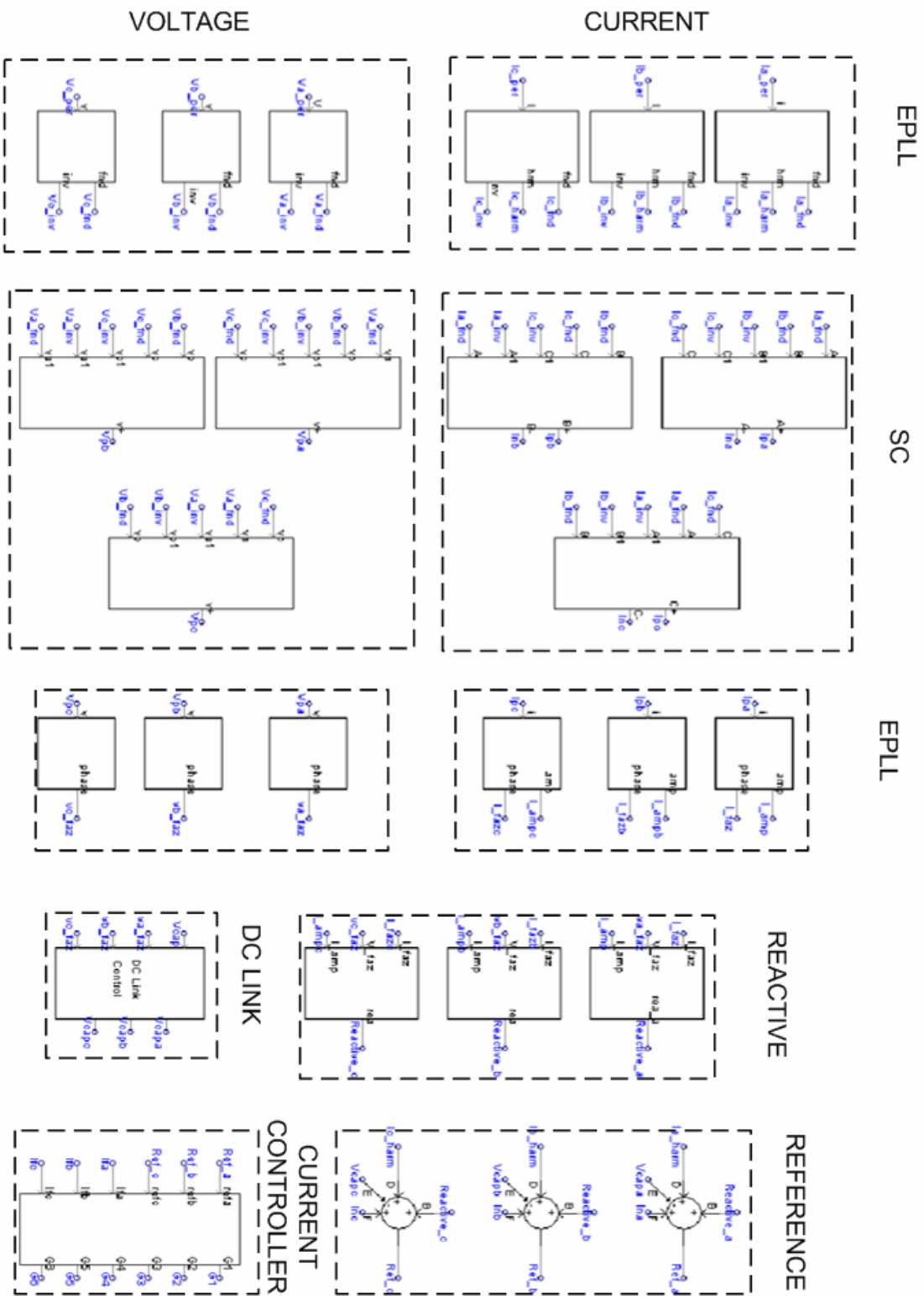

Figure 5.10 Overall block diagram of control in PSCAD Model

5.3.1.1 Enhanced Phase Lock Loop(EPLL) Block

Both voltage and current signals are first passed through the EPLL units. A block diagram of the EPLL is shown in Figure 5.11. The EPLL receives the input signal u(t) and provides an online estimate of the following signals (Fellow et.al,2004).

_ synchronized fundamental component y(t)

_ Amplitude A (t) of y(t)

_ Phase angle

_ time-derivatives of amplitude, phase and frequency

_ 90^0 phase-shifted version of the fundamental component y(t)

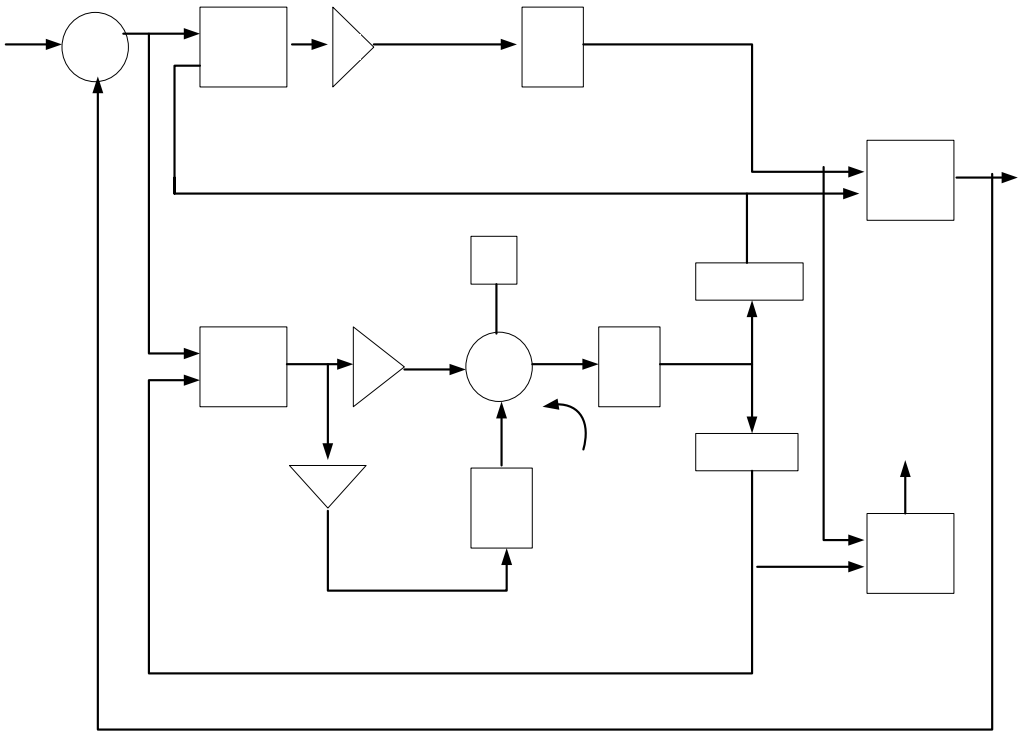

Figure 5.11 Block diagram of enhanced phase locked loop

Figure 5.12 and figure 5.13 shows the EPLL block of PSCAD model for current calculation.

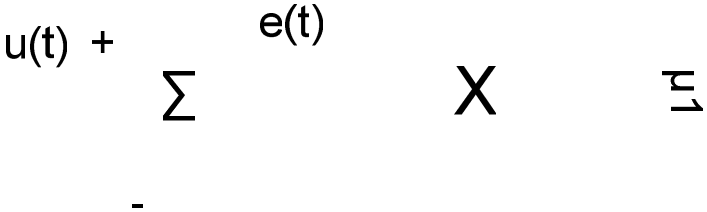

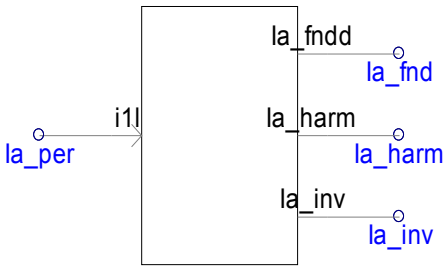

Figure 5.12 EPLL block of PSCAD model for current signal

This block receive current signal and provide fundamental component of current signal, harmonic content of current signal and 90^0 phase-shifted version of the fundamental component. Figure 5.13 shows inside of this block. We use this block separately for each phase current.

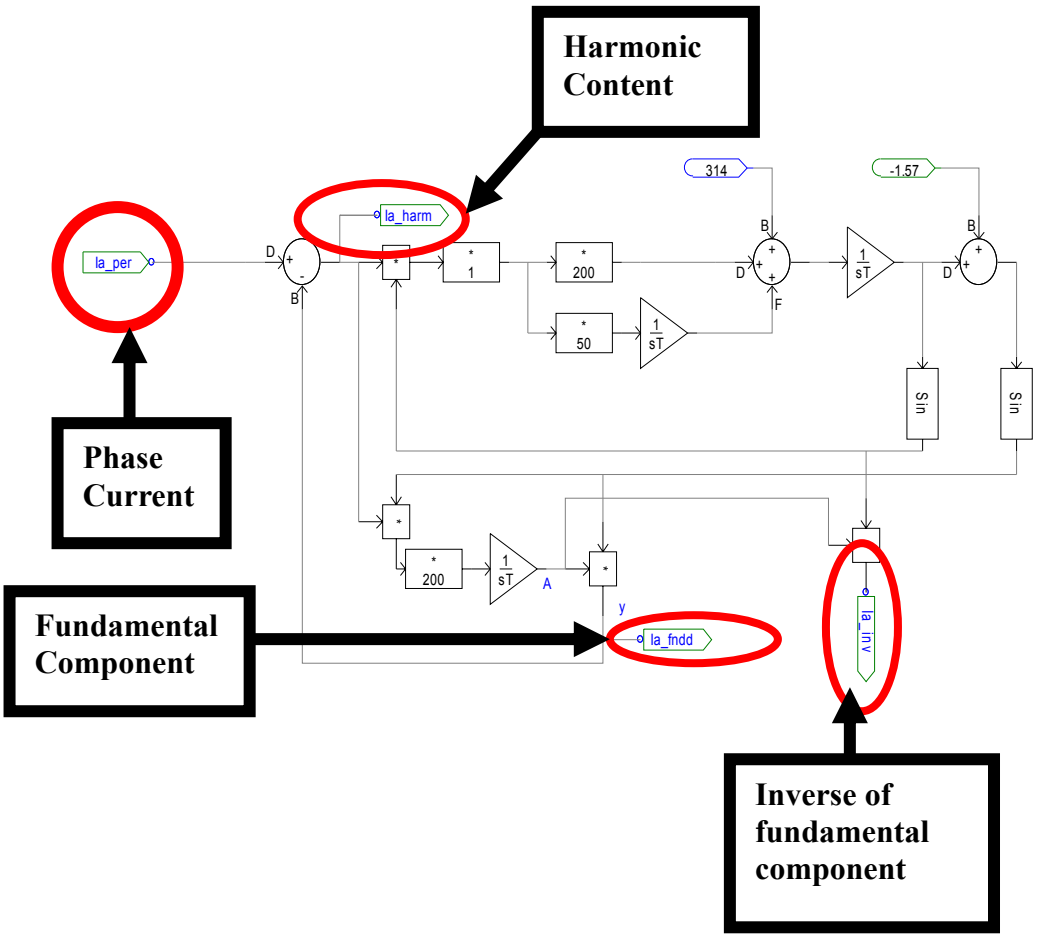

Figure 5.13 Inside of EPLL block of PSCAD model

For the voltage signal we use EPLL block only to extract the fundamental component. Figure 5.14 and figure 5.15 shows the EPLL block for voltage signal.

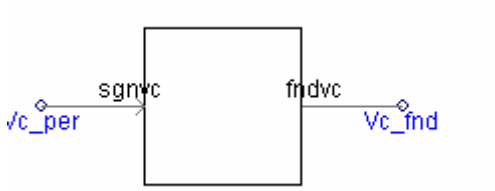

Figure 5.14 EPLL block for voltage signal

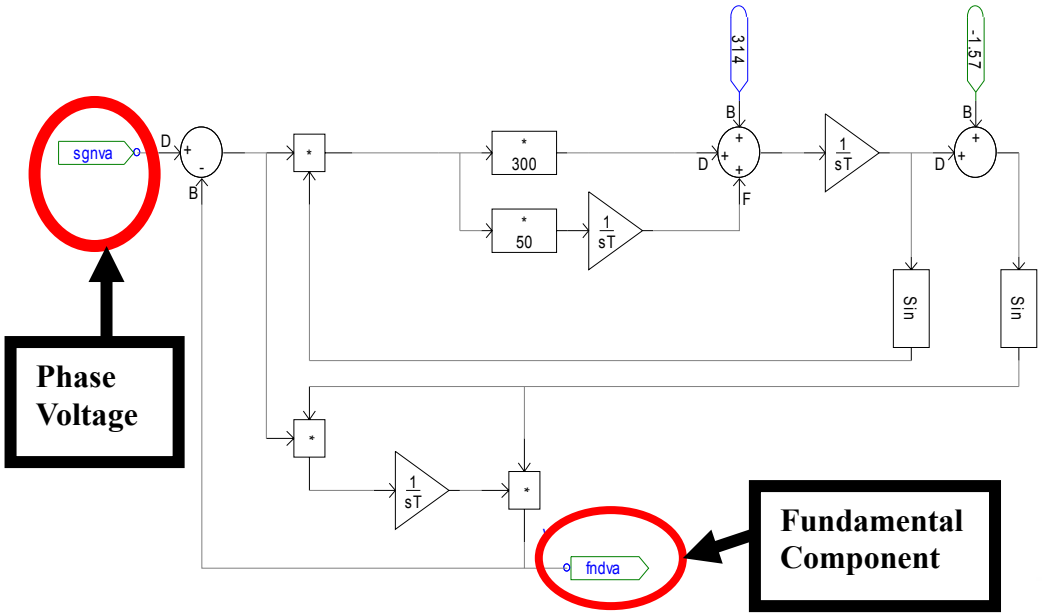

Figure 5.15 Inside of EPLL block for voltage signal

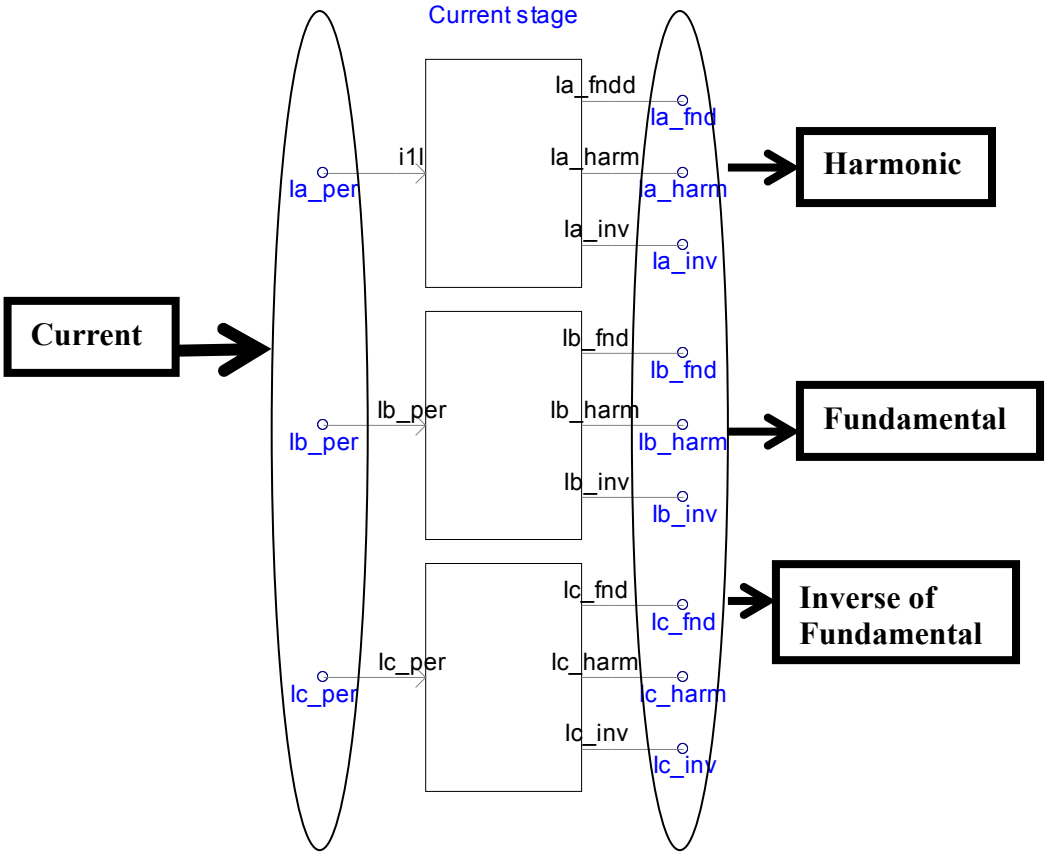

Figure 5.16 EPLL Blocks for three phase current

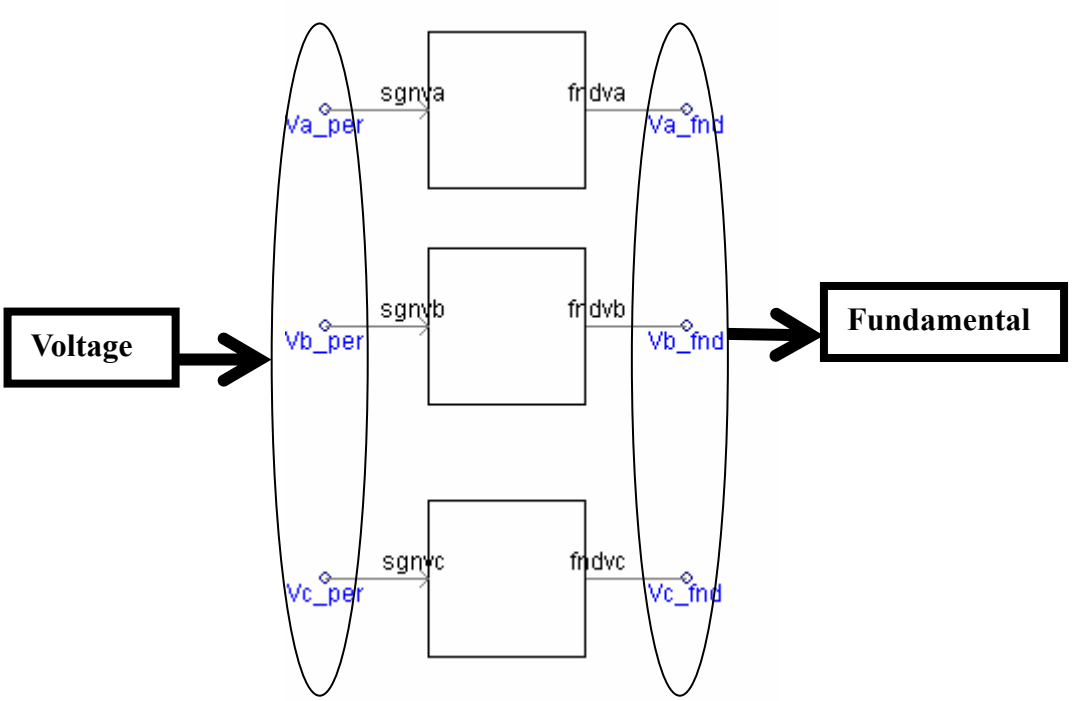

Figure 5.17 EPLL Blocks for three phase voltage

Figure 5.16 and Figure 5.17 shows the three phase voltage and current EPLL blocks of PSCAD. Figure 5.16 shows the current branch of first step EPLL blocks. Figure 5.17 shows the voltage branch of first step EPLL blocks.

5.3.1.2 Symmetrical Component(SC) Block

After the EPLL block, the SC blocks are to estimate the symmetrical positive and negative sequence components of both voltage and current signals.

The instantaneous positive-sequence system of a set of three-phase voltages is defined as

$$\begin{pmatrix} v_a^+(t) \\ v_b^+(t) \\ v_c^+(t) \end{pmatrix} = \frac{1}{3}\begin{pmatrix} 1 & \beta & \beta^2 \\ \beta^2 & 1 & \beta \\ \beta & \beta^2 & 1 \end{pmatrix}\begin{pmatrix} v_a^f(t) \\ v_b^f(t) \\ v_c^f(t) \end{pmatrix} \tag{5.9}$$

Where $\beta = e^{j120}$ is a 120 degree phase shift in the time domain.

It is also possible to extend the EPLL-based system to separately obtain negative- and zero-sequence components and provide more functionally within the control system. The instantaneous negative-sequence system is defined as

$$\begin{pmatrix} v_a^-(t) \\ v_b^-(t) \\ v_c^-(t) \end{pmatrix} = \frac{1}{3}\begin{pmatrix} 1 & \beta^2 & \beta \\ \beta & 1 & \beta^2 \\ \beta^2 & \beta & 1 \end{pmatrix}\begin{pmatrix} v_a^f(t) \\ v_b^f(t) \\ v_c^f(t) \end{pmatrix} \tag{5.10}$$

Assume that v(t) and i(t) denote the load phase-voltage and current signals for which the fundamental components and harmonics are extracted by EPLL units as:

$$v(t) = \begin{pmatrix} v_a(t) \\ v_b(t) \\ v_c(t) \end{pmatrix} = \begin{pmatrix} V_a \sin(\phi_a^v) + v_a^h(t) \\ V_b \sin(\phi_b^v) + v_b^h(t) \\ V_c \sin(\phi_c^v) + v_c^h(t) \end{pmatrix} \tag{5.11}$$

Figure 5.18 shows the symmetrical components blocks in PSCAD model. These blocks receive fundamental three phase current signal and inverse of the two phase current signal and provide positive sequence signal, negative sequence signal and zero sequence signal.

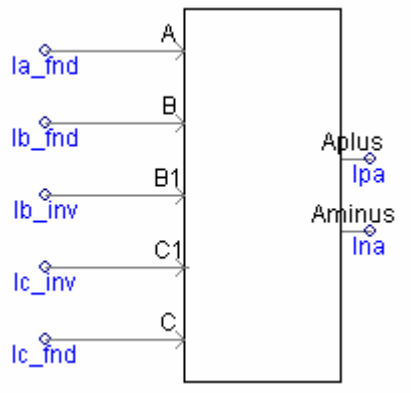

Figure 5.18 SC blocks in PSCAD model.

The symmetrical components present a mathematical approach for the analysis of an asymmetrical polyphase system (under steady-state conditions) by transforming it into a set of symmetrical sequence networks called positive-, negative and zero-sequence networks. The sequence networks are used for the analysis of faults and relay protection of power systems.

If F_a, F_b and F_c denote the corresponding original phasors of phases a, b and c of a three-phase system, then

$$\begin{pmatrix} F_a \\ F_b \\ F_c \end{pmatrix} = \begin{pmatrix} F_a^+ \\ F_b^+ \\ F_c^+ \end{pmatrix} + \begin{pmatrix} F_a^- \\ F_b^- \\ F_c^- \end{pmatrix} + \begin{pmatrix} F_a^0 \\ F_b^0 \\ F_c^0 \end{pmatrix} \tag{5.12}$$

Where +, _, and 0 denote positive-, negative- and zero sequence components, respectively. Since each set of sequence components are balanced, one can deduce.

$$\begin{pmatrix} F_a^0 \\ F_a^+ \\ F_a^- \end{pmatrix} = \frac{1}{3}\begin{pmatrix} 1 & 1 & 1 \\ 1 & \beta & \beta^2 \\ 1 & \beta^2 & \beta \end{pmatrix}\begin{pmatrix} F_a \\ F_b \\ F_c \end{pmatrix} \tag{5.13}$$

where $\beta = \exp(j2\pi/3)$.

The concept of symmetrical components described in above deals with the phasors and hence is a steady state concept. It is extended to accommodate dynamic and transient conditions as follows:

$$\begin{pmatrix} f_a^0(t) \\ f_a^+(t) \\ f_a^-(t) \end{pmatrix} = \frac{1}{\sqrt{3}}\begin{pmatrix} 1 & 1 & 1 \\ 1 & \beta & \beta^2 \\ 1 & \beta^2 & \beta \end{pmatrix}\begin{pmatrix} f_a(t) \\ f_b(t) \\ f_c(t) \end{pmatrix} \tag{5.14}$$

where f_a (t), f_b (t) and f_c(t) are the corresponding instantaneous signals of the three phases.

The instantaneous positive- and negative-sequence components defined by (5.14) are in general complex signals. There is yet another definition which yields real signals. The idea is to replace the complex phasor b with a 120^o phase-shift operator in the time domain. Thus

$$\begin{pmatrix} f_a^0 \\ f_a^+ \\ f_a^- \end{pmatrix} = \frac{1}{3}\begin{pmatrix} f_a + f_b + f_c \\ f_b + S_{120}f_b + S_{240}f_c \\ f_b + S_{240}f_b + S_{120}f_c \end{pmatrix} \tag{5.15}$$

where Sx stands for a x-degree phase-angle operator in the time domain. Another formulation can be derived based on a 90^o phase-shift operator which is easier to implement. The idea is to write:

$$e^{\pm j120} = -\frac{1}{2} \pm \frac{\sqrt{3}}{2} e^{j90}$$

and the result is:

$$\begin{pmatrix} f_a^0 \\ f_a^+ \\ f_a^- \end{pmatrix} = \frac{1}{3} \begin{pmatrix} f_a + f_b + f_c \\ f_b + \frac{1}{2}(f_b + f_c) + \frac{\sqrt{3}}{2} S_{90}(f_b - f_c) \\ f_b + \frac{1}{2}(f_b + f_c) - \frac{\sqrt{3}}{2} S_{90}(f_b - f_c) \end{pmatrix} \tag{5.16}$$

The instantaneous symmetrical components are used for dynamic compensation, balancing and control of power systems by means of static compensators. This concept can be defined both on a total signal (such as above) or on a single frequency component of it (for example its fundamental component). It can be shown that (5.15) and (5.16) are equivalent with respect to the fundamental components.

The instantaneous symmetrical components of a three phase system {fa(t), fb(t), fc(t)} are defined by (5.14) which yields complex quantities. Two alternative definitions which yield real instantaneous symmetrical components are (5.20) and (5.16). Although these definitions are valid for the total signals, they are usually applied to a specific component, e.g. the fundamental components. Among the constituting components of a signal, the fundamental component carries the most significant pieces of information and is used for load balancing, power factor correction and other purposes in the context of power systems. Hence, the derivations in this section, without lose of generality, are applied to the fundamental components.

Rewriting (5.14) for the fundamental components results in.

$$\begin{pmatrix} v_a^0(t) \\ v_a^+(t) \\ v_a^-(t) \end{pmatrix} = \frac{1}{\sqrt{3}} \begin{pmatrix} 1 & 1 & 1 \\ 1 & \beta & \beta^2 \\ 1 & \beta^2 & \beta \end{pmatrix} \begin{pmatrix} \hat{v}_a \sin(\phi_a) \\ \hat{v}_b \sin(\phi_b) \\ \hat{v}_c \sin(\phi_c) \end{pmatrix} \tag{5.17}$$

where caret identifies the peak value and ϕ denotes the total phase angle. Note that the zero components are real and the positive and negative components are the complex conjugate of each other.

The EPLL's directly provide the fundamental components. Therefore, the instantaneous symmetrical components can be computed by adding a simple set of calculation units, i.e. addition, subtraction and gain. Figure 5.19 shows a block diagram of the estimator.

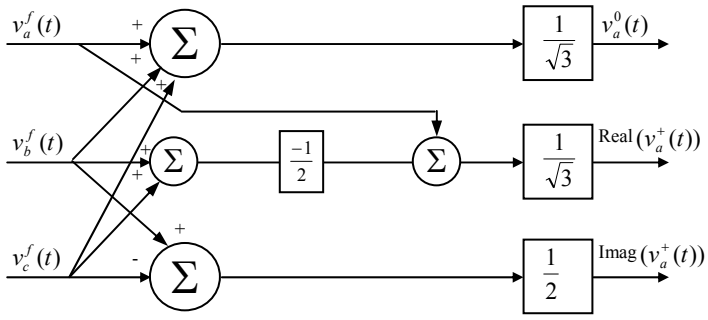

Figure 5.19 Block diagram of the structure to estimate the instantaneous symmetrical components defined by (5.14)

The instantaneous symmetrical components defined by (5.15) can also be deduced by the EPLL. Phase-shift operations are realized using the estimated amplitude and phase angle. A block diagram of the symmetrical components estimator, based on (5.15), is shown in Figure 5.20. The inputs are the three fundamental components, the amplitudes and phase angles of the two phases b and c. This set of information is provided by three EPLL's. Sine trigonometric operation is involved in this unit in addition to the arithmetic operations.

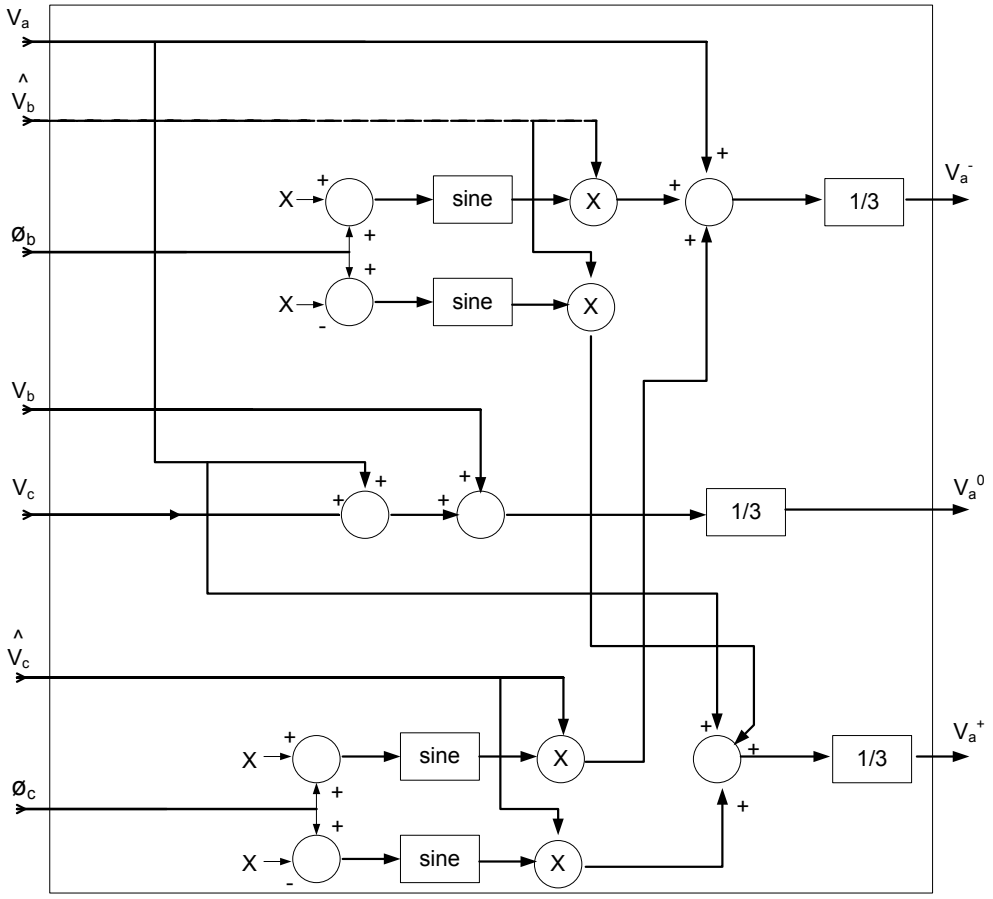

Figure 5.20 Block diagram of the structure to estimate the instantaneous symmetrical components defined by (5.15)

The instantaneous symmetrical components defined by (5.16) can be obtained using EPLL's in a simpler manner than that of (5.15). This is due to the fact that the EPLL automatically provides the 90^o phase shifted version of the fundamental component. A block diagram of the corresponding estimator is shown in Figure 5.21. This structure is simpler than that of Figure 5.20 since it does not involve trigonometric functions.

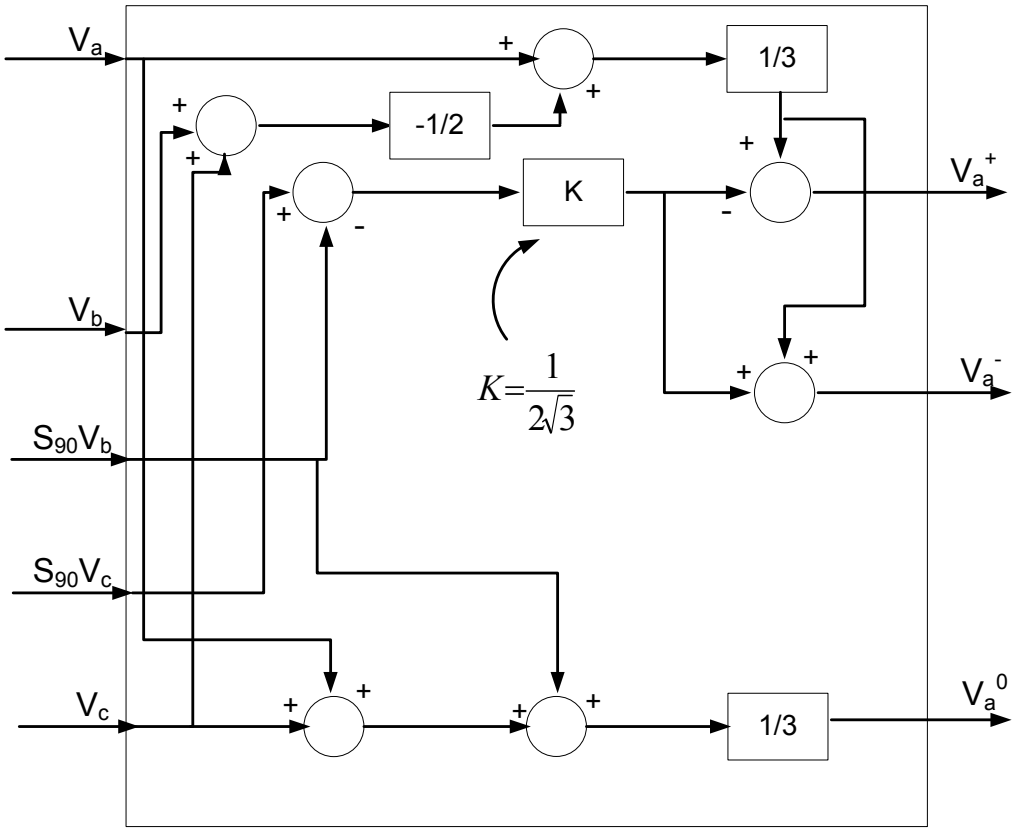

Figure 5.21 Block diagram of the structure to estimate the instantaneous symmetrical components defined by (5.16)

The EPLL furnishes the proposed method of estimation of the symmetrical components with a flexible structure (Iravani et.al.,2003). For example, the time-domain positive components, which are used in various applications, can be extracted readily. The time-domain positive sequence system is defined as:

$$\begin{pmatrix} v_a^+(t) \\ v_b^+(t) \\ v_c^+(t) \end{pmatrix} = \frac{1}{3}\begin{pmatrix} 1 & \beta & \beta^2 \\ \beta^2 & 1 & \beta \\ \beta & \beta^2 & 1 \end{pmatrix}\begin{pmatrix} v_a^f(t) \\ v_b^f(t) \\ v_c^f(t) \end{pmatrix} \tag{5.18}$$

Rewriting (5.18) in terms of the 90^o phase-shift operator yields:

$$\begin{pmatrix} \frac{1}{3}u_a(t)-\frac{1}{6}\left(u_b(t)+u_c(t)\right)-\frac{1}{2\sqrt{3}}S_{90}(u_b(t)-u_c(t)) \\ -u_a^+(t)-c_c^+(t) \\ \frac{1}{3}u_c(t)-\frac{1}{6}\left(u_a(t)+u_b(t)\right)-\frac{1}{2\sqrt{3}}S_{90}(u_a(t)-u_b(t)) \end{pmatrix} \quad (5.19)$$

A realization of (5.19) is shown in Figure 5.22.

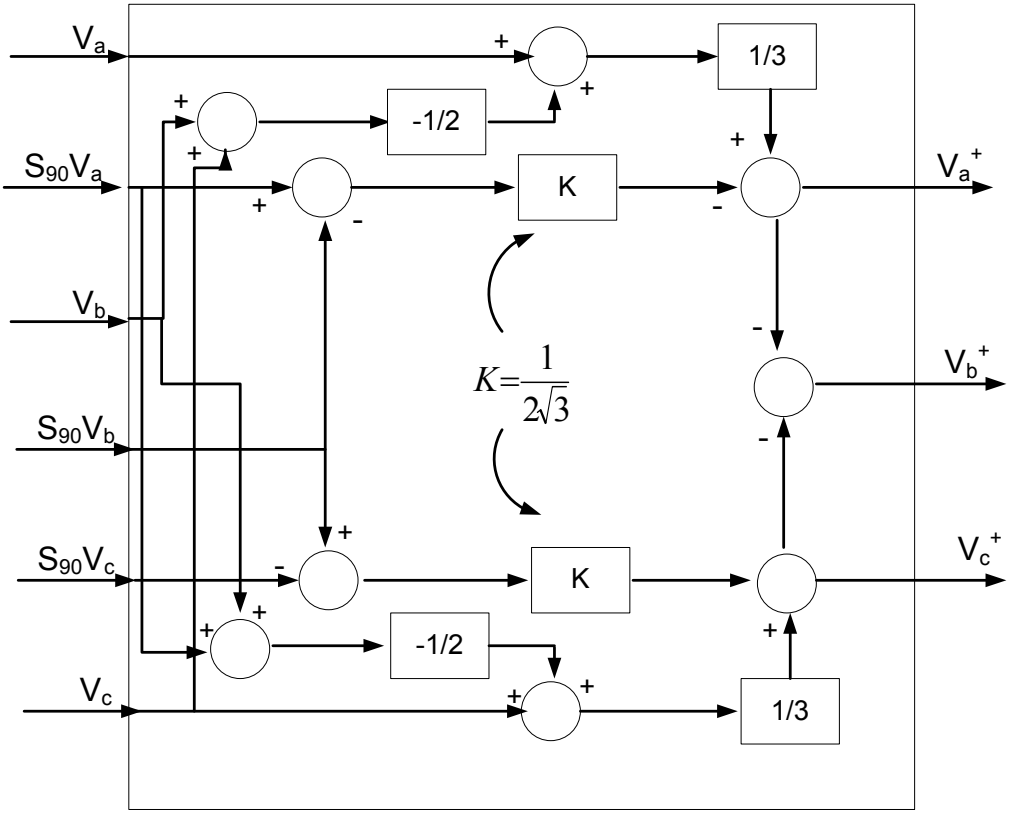

Figure 5.22 Block diagram of the structure to estimate instantaneous positive sequence components defined by (5.19)

Figure 5.23 shows the inside of symmetrical components block of the PSCAD model. We use that blocks separately each phase current and voltage signal.

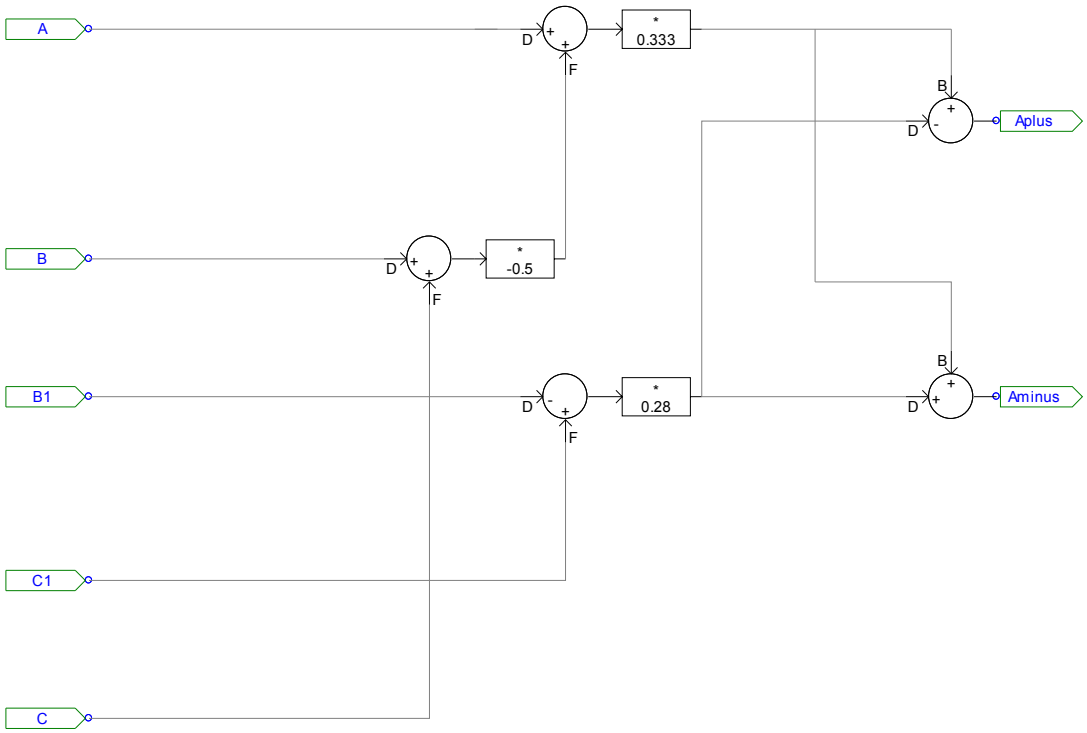

. Figure 5.23 Symmetrical Components Block of PSCAD model

5.3.1.3 Reactive Current Calculation Block

The instantaneous positive-sequence components of the voltage and current signals are also extracted by the EPLL based system, described previously and denoted by

$$v^{+}(t)=\begin{pmatrix} V^{+}\sin\omega t \\ V^{+}\sin(\omega t-120) \\ V^{+}\sin(\omega t+120) \end{pmatrix} \tag{5.20}$$

$$i^{+}(t)=\begin{pmatrix} I^{+}\sin(\omega t+\theta) \\ I^{+}\sin(\omega t-120+\theta) \\ I^{+}\sin(\omega t+120+\theta) \end{pmatrix} \tag{5.21}$$

Where θ denotes the phase displacement between the corresponding voltage and current positive-sequence components. The current fundamental component can be decomposed into active and reactive fundamental components as

$$i_a^+(t) = \begin{pmatrix} I^+ \cos\theta \sin \omega t \\ I^+ \cos\theta \sin(\omega t - 120) \\ I^+ \cos\theta \sin(\omega t + 120) \end{pmatrix} \tag{5.22}$$

$$i_r^+(t) = \begin{pmatrix} I^+ \sin\theta \cos \omega t \\ I^+ \sin\theta \cos(\omega t - 120) \\ I^+ \sin\theta \cos(\omega t + 120) \end{pmatrix} \tag{5.23}$$

The second stage of EPLL units, after symmetrical components block estimates the amplitudes and phase angles of the voltage and current positive sequence components for calculation of reactive currents. Figure 5.24 shows the second stage of the EPLL (Karimi et.al.,2004).The second stages EPLL for voltage side we use only obtain the phase angle of the signal.

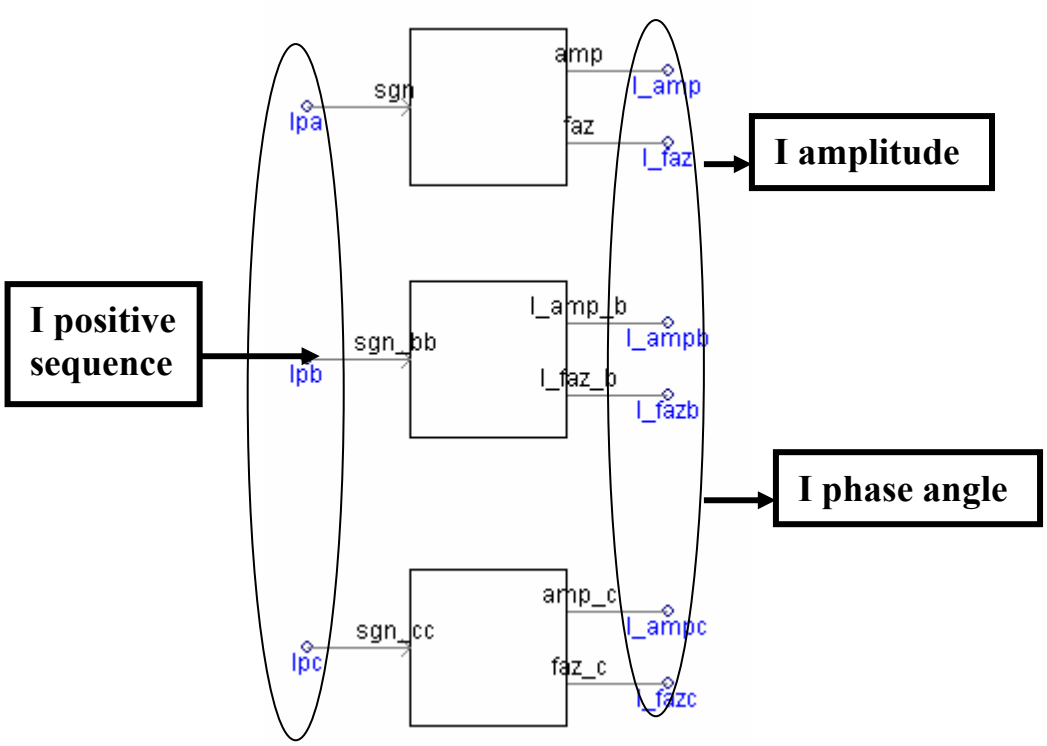

Figure 5.24 Second Stage EPLL block

Figure 5.25 shows a block diagram of the reactive current extractor. For each phase two identical EPLL units are used for voltage and current signals. The top

portion of the unit is used for voltage and the bottom portion is used for current signal processing. The link between the two parts is to calculate the fundamental reactive current component.

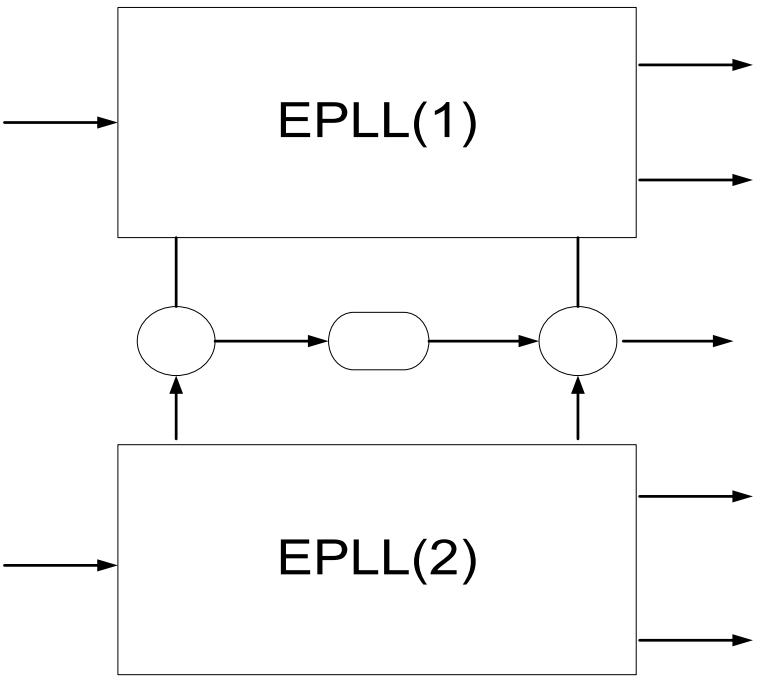

Figure 5.25 Block diagram of the reactive current extraction unit

Let $i(t)=i^f(t)+ i^h(t)$ denote the distorted load current where represents its fundamental component which is extracted by another EPLL unit. Signal $i^h(t)$ represents the total distortions of the current signal. The amplitude and phase angle of the fundamental component of the current signal are also made available at the outputs of the unit.

The fundamental component $i^f(t)$of the current signal i(t) can be written as

$$i^f(t) = I_1 \sin(\phi_i) = i_a^f(t) + i_r^f(t) \quad (5.24)$$

Where $i^{fa}(t)$ and $i^{fr}(t)$ represent active and reactive components of and expressed as

$$i_a^f(t) = I_1 \cos(\phi_i - \phi_v)\sin(\phi_v) \quad (5.25)$$

$$i_r^f(t) = I_1 \sin(\phi_i - \phi_v)\cos\phi_v) \quad (5.26)$$

Figure 5.26 and figure 5.27 shows the reactive current calculation block of PSCAD model.

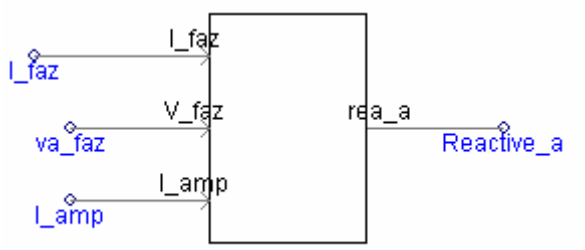

Figure 5.26 Block diagram of the reactive current extraction of PSCAD Model

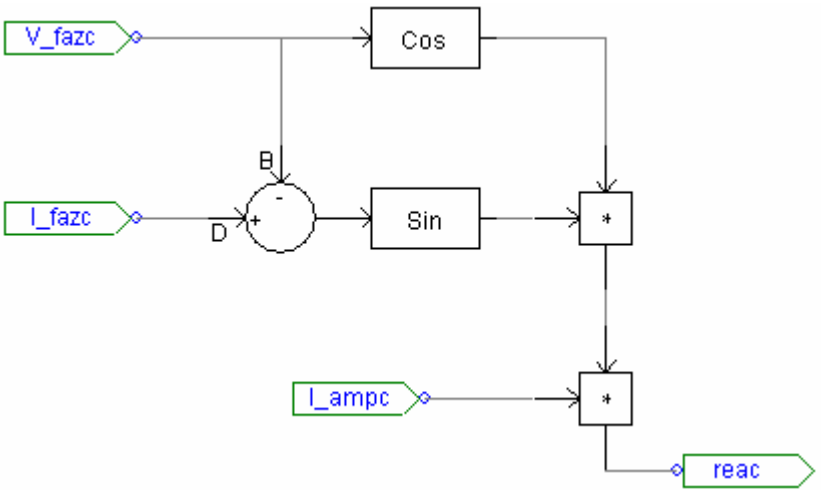

Figure 5.27 Inside of the reactive current extraction block

5.3.1.4 DC Link Control Block

In this thesis we have appended the dc link control reference to control circuit for control the dc link voltage of the active power filter. The DC link control of Shunt APF can be achieved by control of active power. In ideal conditions APF do not consume any active power but because of the switching losses and conduction losses of switching devices and resistance of inverter output filter, APF must consume active power to control the DC link voltage. In the proposed control scheme of APF, active power control is obtained by PI controller that control of active component of current. Figure 5.28 shows the block diagram of dc link control

scheme. The D.C voltage across the capacitor is measured compared with reference and the error is processed in a PI controller. This error multiplies fixed amplitude which is pure and is in 180^{o} phase with the source. The product forms one component of the current reference signal. The second stage EPLL block is used for extract voltage phase angle for each phase. Figure 5.29 shows the PSCAD block of dc link control scheme. Figure 5.30 shows the inside of this block. Finally after we generate dc link control signal, we add this signal to reference signal.

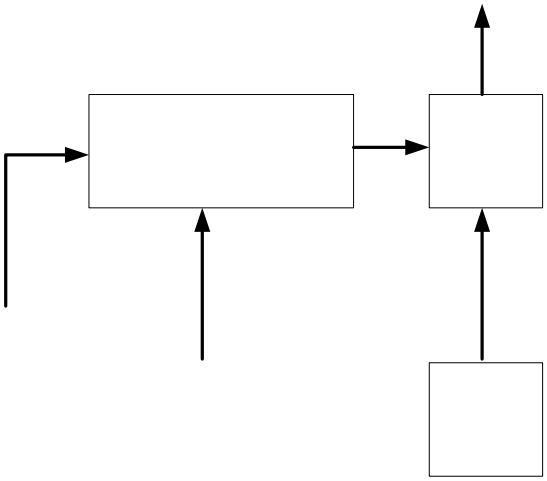

Figure 5.28 Block diagram of the DC link control

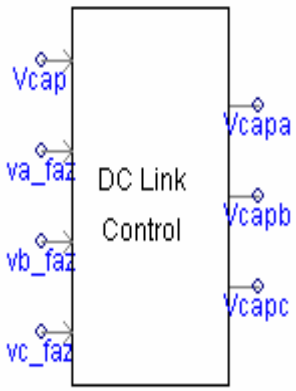

Figure 5.29 DC link control block of PSCAD Model

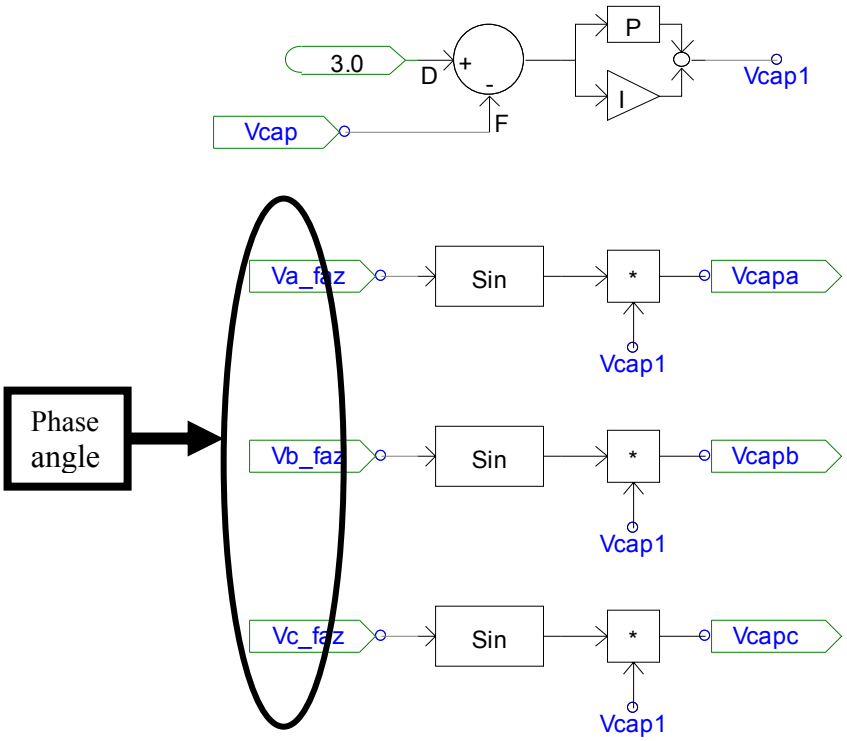

Figure 5.30 Inside of DC link control block of PSCAD Model

Finally we sum the reactive current, harmonic signal, unbalance signals and DC link control signal for reference signals. Figure 5.31 shows the sum block of PSCAD.

$$I_c(t)=i_r^{+}+i^{-}+i^{h}+i^{DC} \tag{5.27}$$

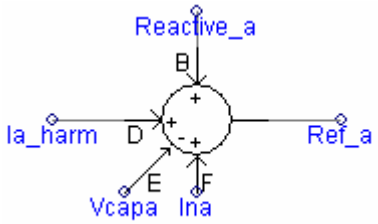

Figure 5.31 Reference signal

5.3.2 Current Controller

After generated reference signal we use classical PWM method for trigger IGBT of inverter. Figure 5.32 shows the PWM pulse generator block of PSCAD model and figure 5.33 shows the inside of this block.

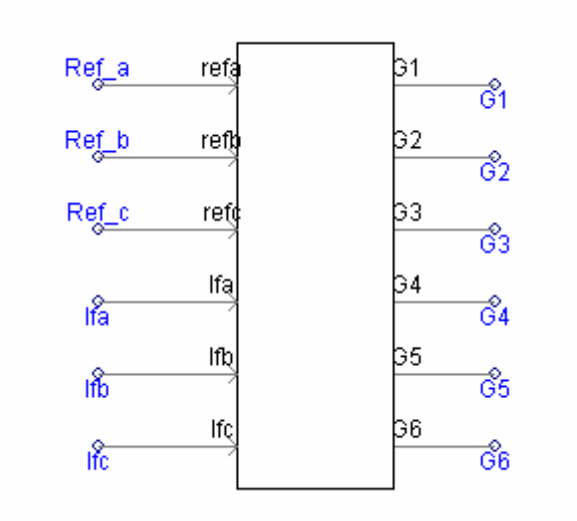

Figure 5.32 PWM block for PSCAD Model

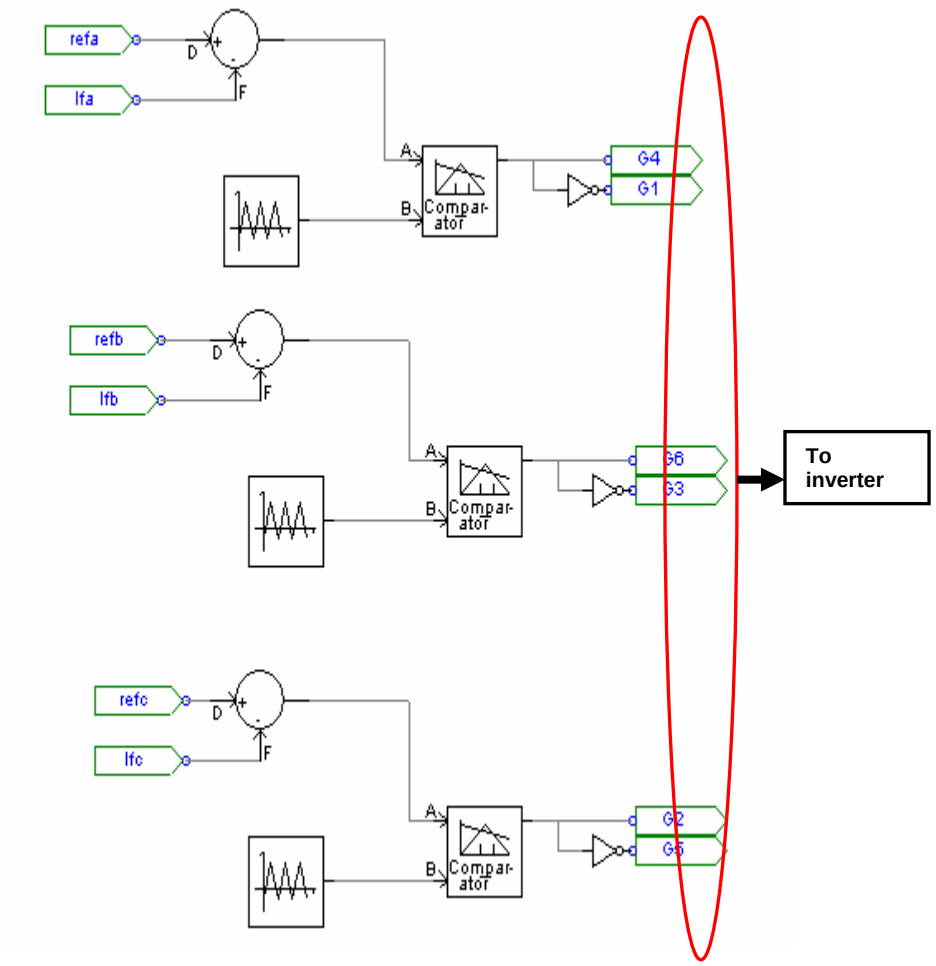

Figure 5.33 Inside of the PSCAD Block

5.4 Passive Filter

In this thesis the passive filter is used in addition to the shunt active power filter. The passive filter is not suitable solution to compensate varying harmonics and interharmonics of current source induction furnace. Its drawbacks are discussed at chapter3.However the main purpose of using passive filters in proposed compensation system is reactive power compensation to decrease the ratings of shunt active power filter. Figure 5.34 shows the simplified circuit configurations of filter topology. The main purpose of this configuration is to reduce initial costs and to improve efficiency.

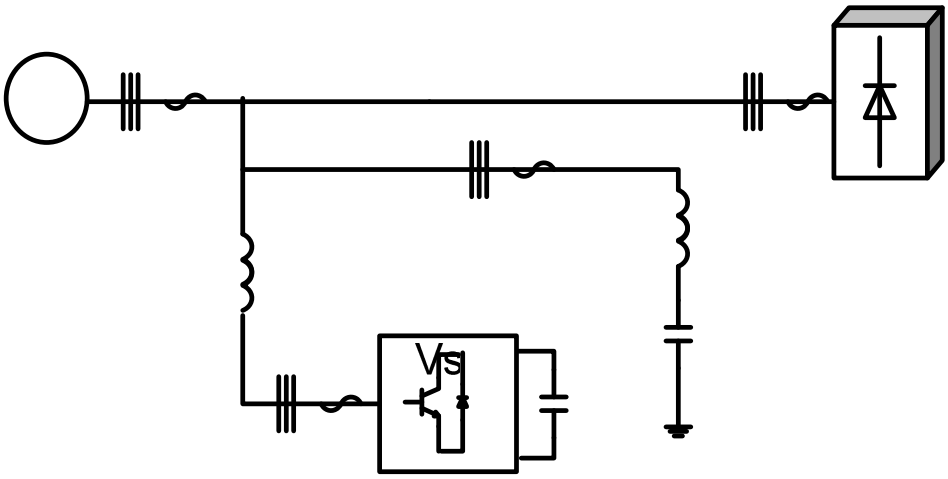

Figure 5.34 Combination of shunt active filter and passive filter

Our passive filter is only designed to compensate the reactive power. Because of induction furnace operation principle, the current harmonics is not taken into account If only one filter is used; it is usually tuned at the lowest characteristic harmonic. In this case, this would be the 5th harmonic. Thus, 4 - step reactive power compensation system is designed with detuned passive filters. Detuned passive filters are set to 215 Hz to shift the resonance point of system below the furnace operating spectrum because the proposed current source induction furnace is operating between 150 and 300 Hz and produces harmonics and interharmonics between 250 and 600 Hz.. Figure 5.35 shows the passive filter models of PSCAD.

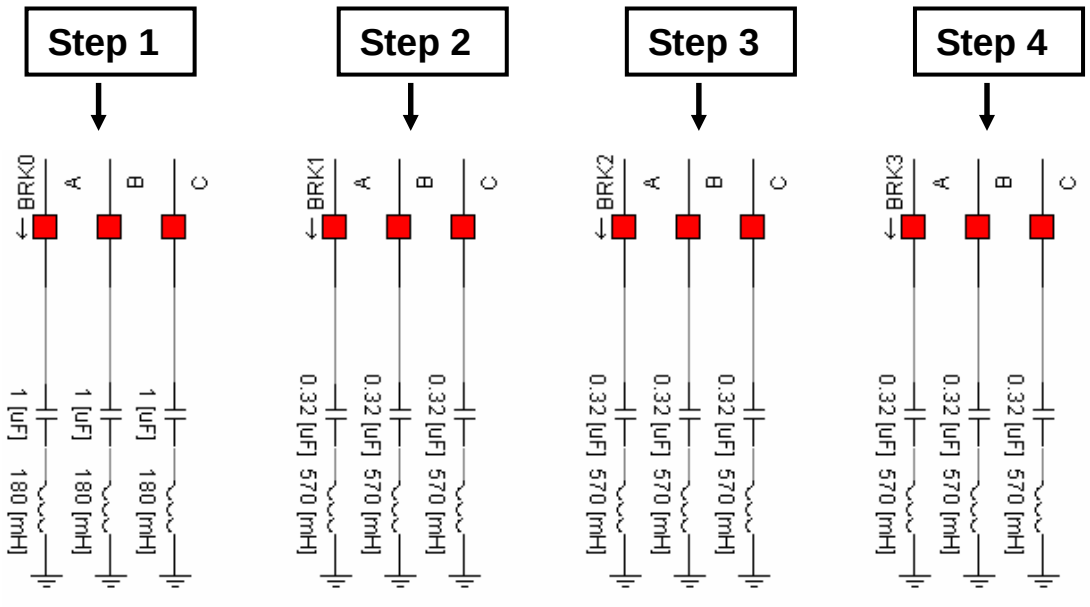

Figure 5.35 Passive filter models of the PSCAD

Passive filter ratings must be coordinated with reactive power requirements of the loads. The hysteresis on-off control is used for switching on/off passive filters The first step is always in use. When the reactive power is increase and exceeds permissible high level, step 2 is come in by our control circuit. After that step 3 is come in when the reactive power exceeds the permissible level. According to the changing reactive power of induction furnace passive filter steps is adjusted by our control circuit. Figure 5.36 shows the control circuit of passive filter in PSCAD model. BRK1, BRK2, BRK3 outputs control the passive filter. And low and up inputs of PSCAD blocks determine the permissible minimum and maximum reactive power level. Passive filter control block is constituted writing FORTRAN commands in PSCAD.

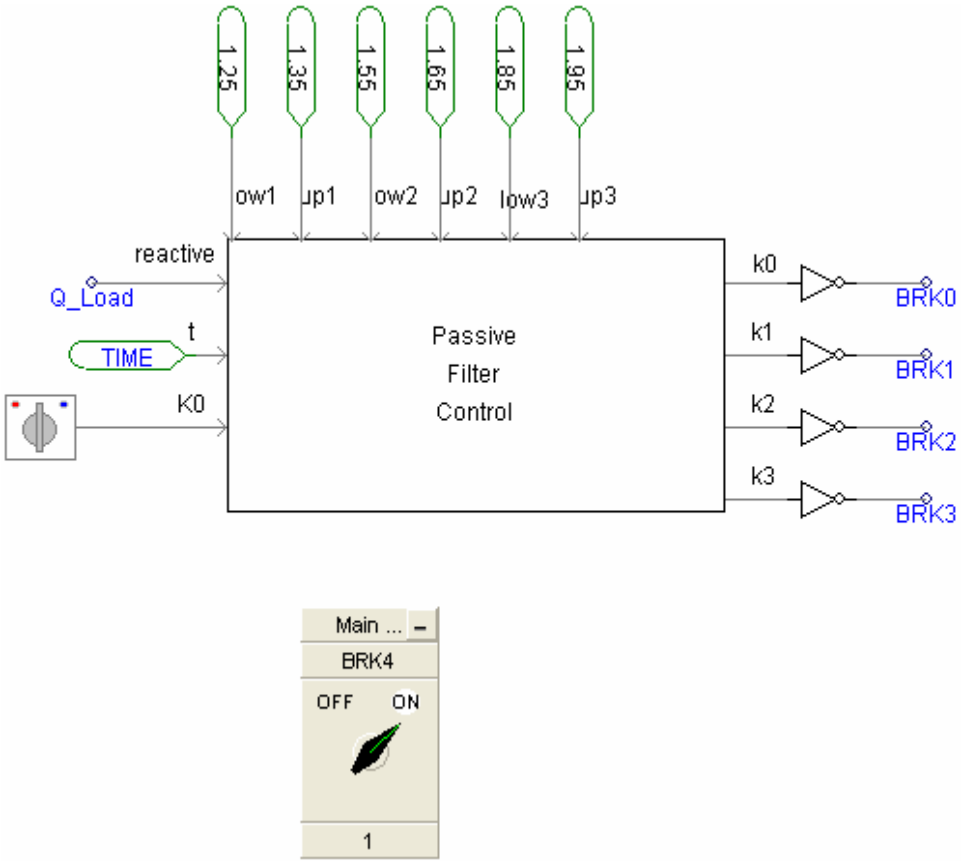

Figure 5.36 Passive filter control block of the PSCAD

While we determine the passive filter reactor impedance and capacitive impedance value we can use those formulas;

$$Q_C = \frac{V^2}{X_C} \tag{5.28}$$

$$Xc = \frac{1}{j2\pi fL.C} \tag{5.29}$$

$$F_R = \frac{1}{2\pi\sqrt{LC}} \tag{5.30}$$

Where;

Qc = Capacitive power which gives to line

V = Nominal line voltage

Xc = Capacitive impedance which connects to line

F_L= Line frequency

C= filter capacitor

F_R= Resonance frequency

L= filter inductance

The power circuit specifications of passive filter are shown in table5.1

Table 5.1 The Power Circuit Specifications of Passive Filters

	1 Step	***2,3,4 Steps***
Reactive Power	950 kVAR	300 kVAR
Tuned Frequency	215 Hz	215 Hz
L	180 mH	570 mH
C	1 μF	0.32 μF

6. CASE STUDIES AND DISCUSSIONS

In chapter 4 of thesis the simulation results of furnace which indicates the operating and power quality problems of furnace are presented. In this section of the thesis, simulation results of proposed compensation system which solves the power quality problems of current source induction furnace are introduced and the performance of the system is investigated with three different case studies. In the case studies, the current source induction furnace operates as the same scenario in the Chapter 4.

In first case, power quality problems of current source induction furnace is compensated with shunt APF and passive filter.In the second case power quality problems of current source induction furnace is compensated only with shunt APF.In the third case the power quality problems of induction furnace is compansated only with shunt APF. In the third case the control system of the shunt APF extracts only harmonics content.There is no reactive power compensation in the third case. The power circuit of proposed power quality compensation system and current source induction furnace is shown in figure 6.1.

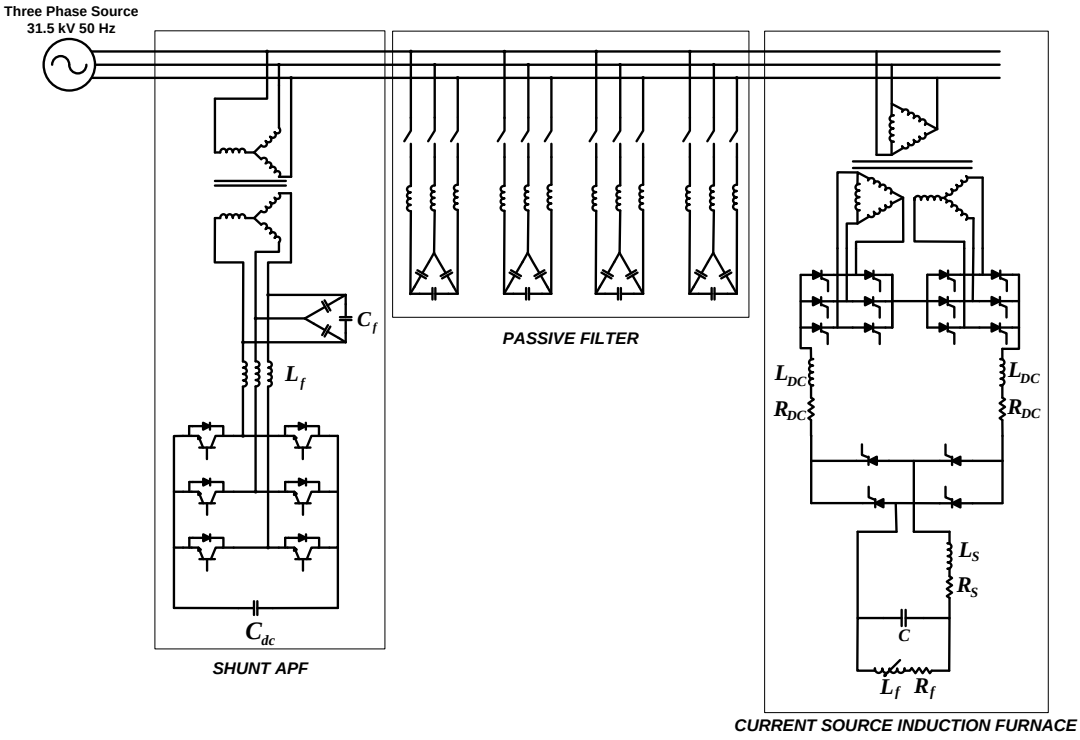

Figure 6.1 Power Circuit of Modeled System

In this simulation study 31.5kV utility power supply feeds the induction furnace. Our furnace is fed from a 12MVA three winding transformer. The voltage is reduced from 31.5 kV to 1.2 kV. The secondary winding feeds a thyristor controlled rectifier and the tertiary feeds another identical rectifier. The rectification has a 12-pulse configuration. Both rectifiers are connected in parallel including filtering coils that improve the direct current obtained. When current is flowing in the DC link, the two series connected inductors provide energy storage and filtering. Our inductor value is 1mH. The inverter is responsible for converting high voltage DC to AC to feed it to the load circuit. It is a single phase bridge connection of four current carrying arms. Configuration used is called H-bridge inverter, as load induction melting coil and capacitors are parallel to each other The induction furnaces work in the resonant frequency with the capacitor banks connected in parallel. Capacitor bank value is 5.28mF. Furnace coil changes according to melting to scrap. And inverter control system keeps the circuit in always resonance changing the inverter frequency.

To show the performance of the furnace and control algorithm, the system is tested for the following case studies:

6.1 Case 1

The induction furnace work with combination of shunt active power filter and shunt passive filter. The passive filter has four steps. . First step is 950kVAR and other steps are 300kVAR and all steps of passive filters are tuned to 215 Hz. Remaining reactive power is compensated by the active power filter.

The three phase compensated source current waveforms and distorted furnace current waveforms are shown in figure 6.2 and figure 6.3 respectively.

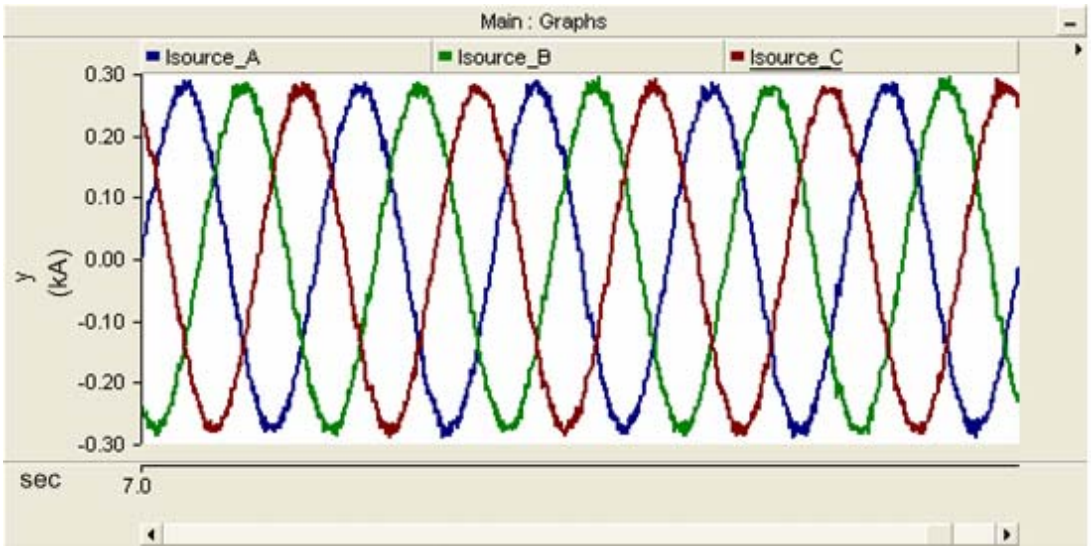

Figure 6.2 Three phase source current of the network

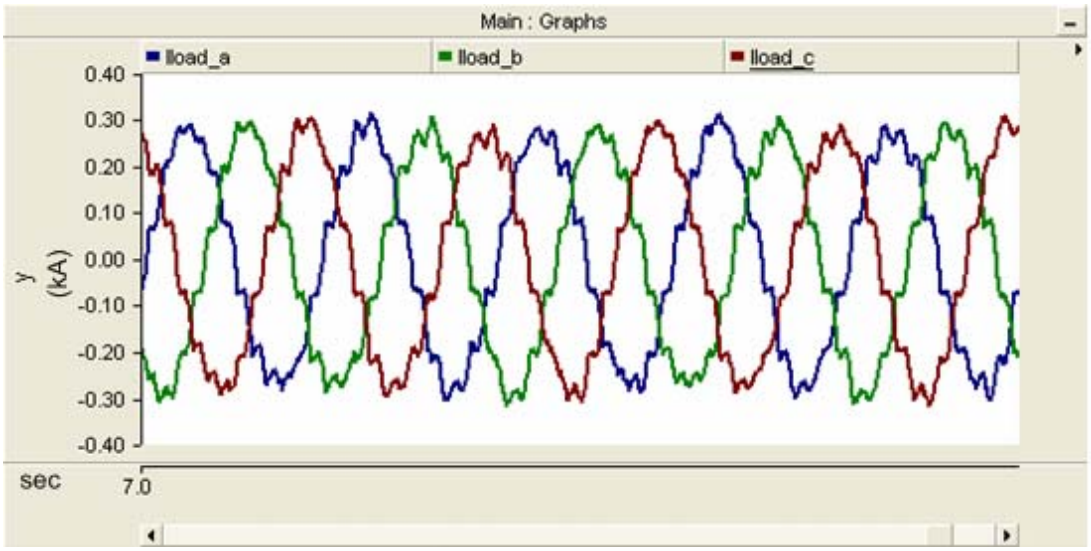

Figure 6.3 Three phase load current of the network

Figure 6.4 shows the compensated phase A source current. Phase A distorted furnace current is shown in figure 6.5. In figure 6.6, the compensated phase A current and the distorted furnace current is shown at the same graphic.

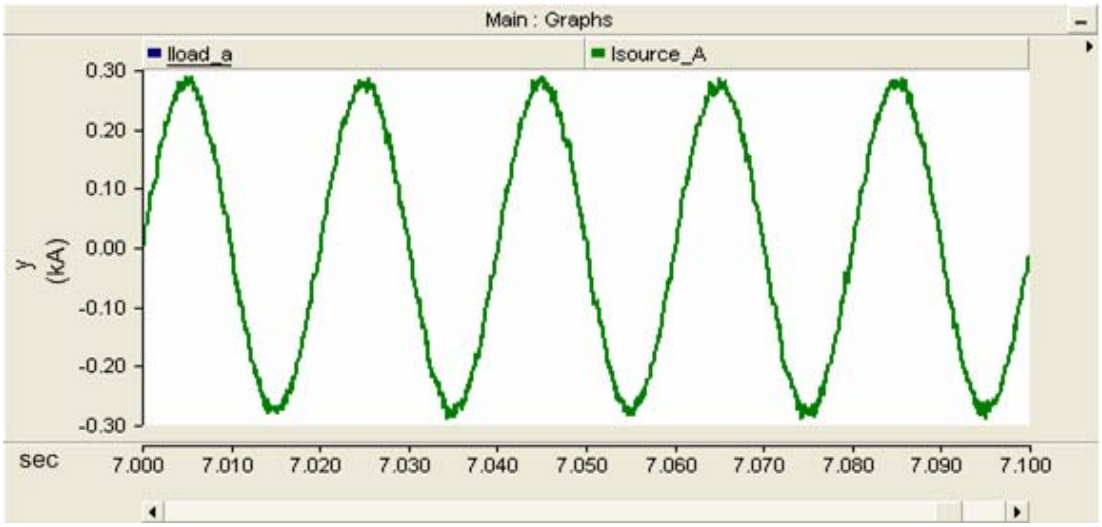

Figure 6. 4 Phase A source current of the network

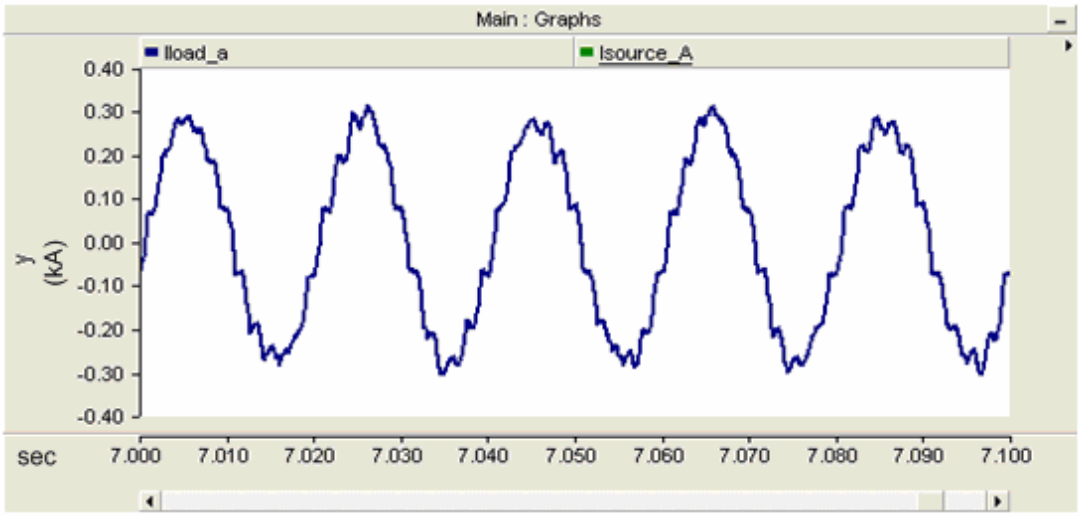

Figure 6.5 Phase A load current of the network

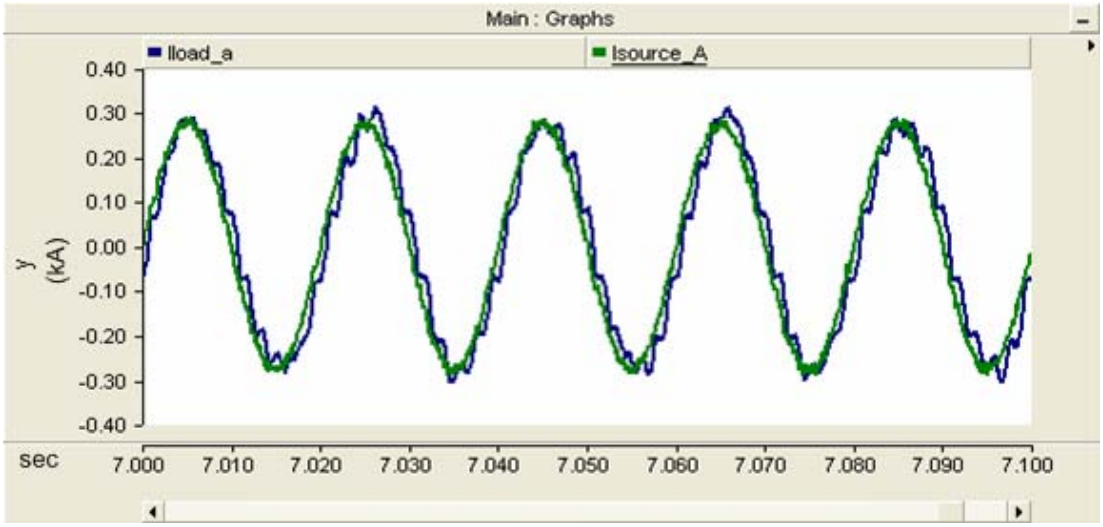

Figure 6.6 Phase A load and source current of the network

Three phase source voltage is shown in figure 6.7 and phase A source voltage is shown in figure 6.8.It is clearly seen that there is no distortion in the voltage waveforms.

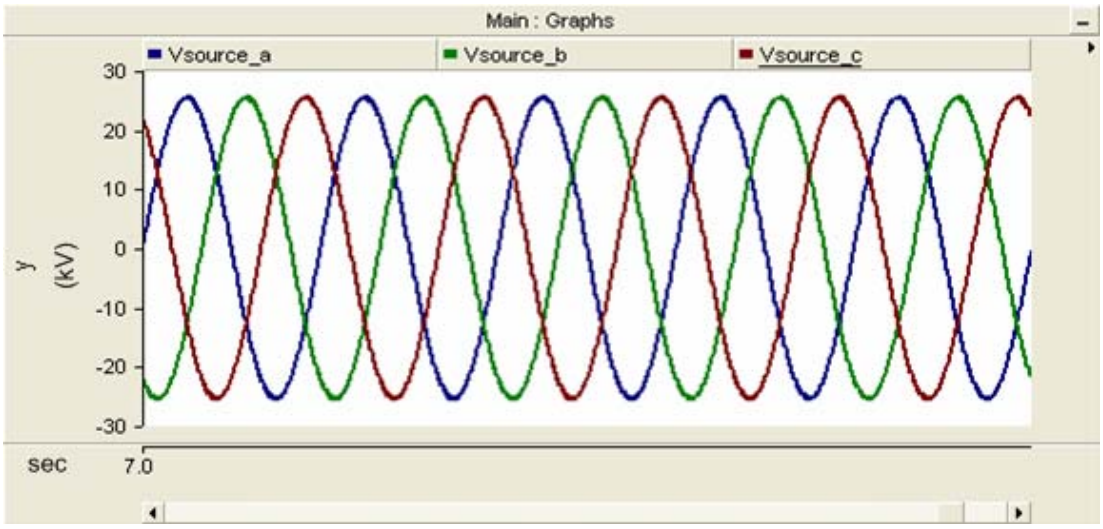

Figure 6.7 Three phase source voltage of the network

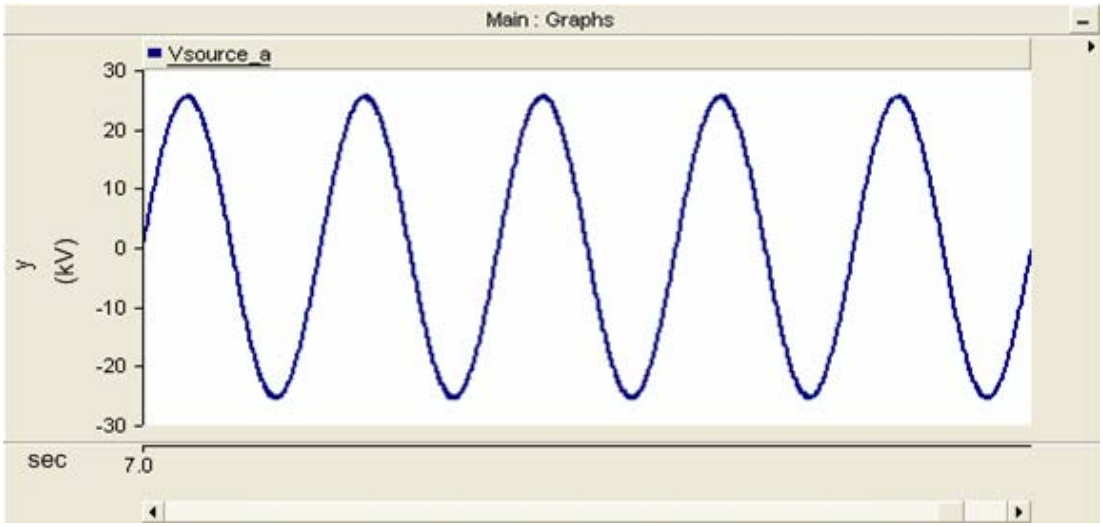

Figure 6.8 Phase A source voltage of the network

The trend of load current THD is changed between 10% and 15% as shown in Figure 6.9 and shunt APF decreases the source current THD below 4% as shown in Figure 6.10.

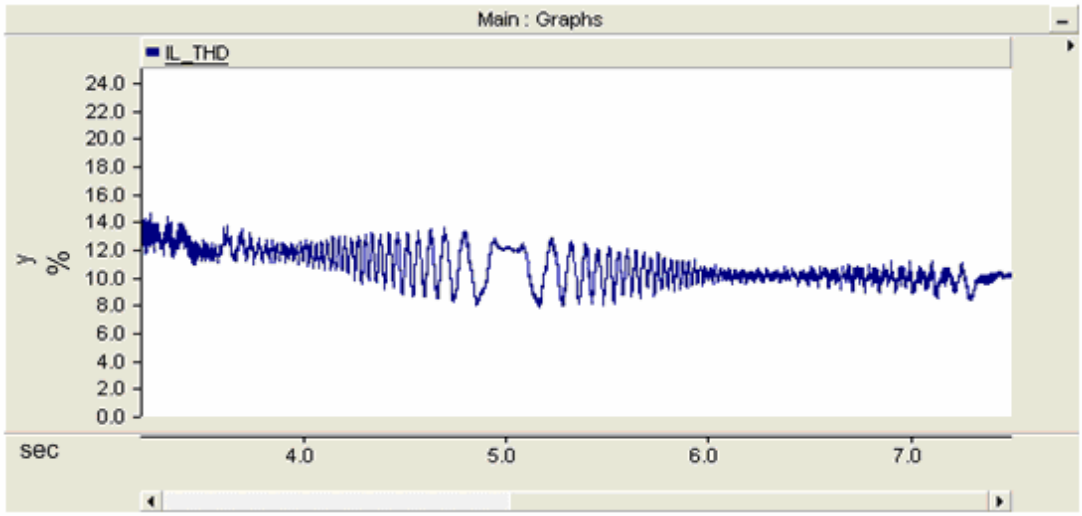

Figure 6.9 Total Harmonic Distortion of load current of the network

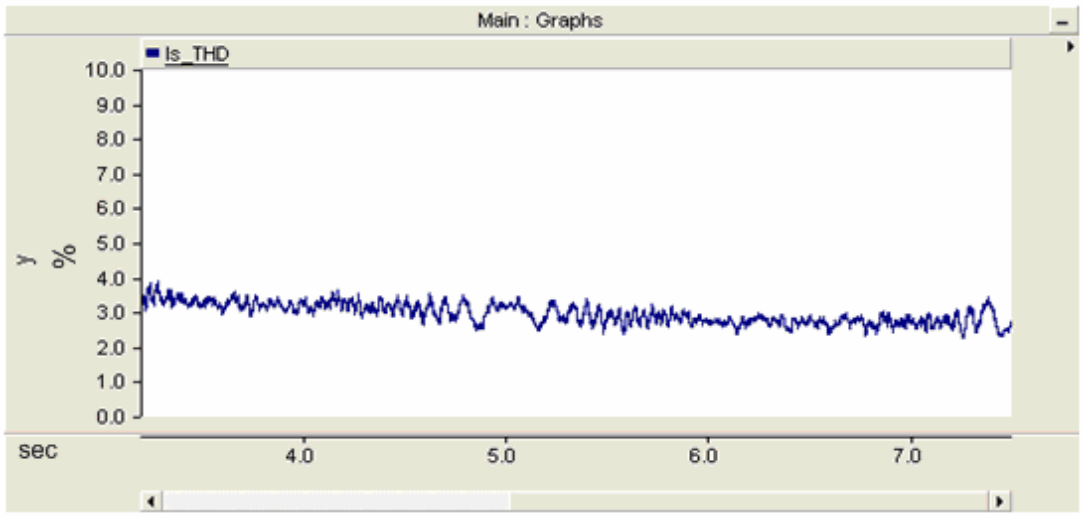

Figure 6.10 Total Harmonic Distortion of source current of the network

The DC link capacitor voltage is set to 3000V and its trend is shown in Figure 6.11.

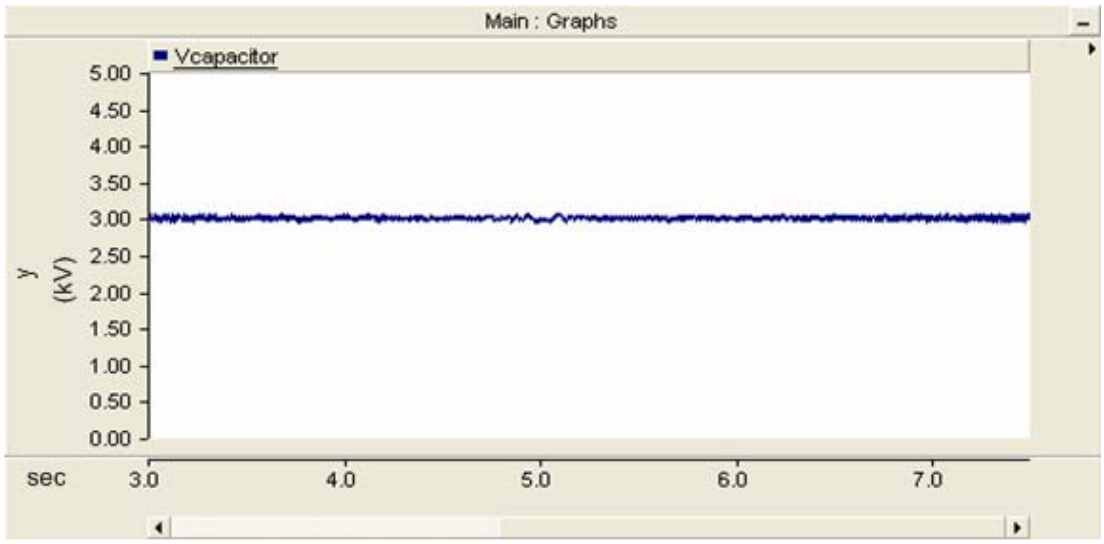

Figure 6.11 The DC Link voltage of the Active power filter

The trend of reactive power consumed by load, the connection point of passive filter point and the connection point of shunt APF is shown in Figure 6.12 As shown in figure 6.12, the reactive power of furnace increases up to 2.25MVAR with the increase of operating frequency of furnace. It is shown that passive filters compensate the one part of the reactive power and the other part of the reactive power is compensated by shunt APF.

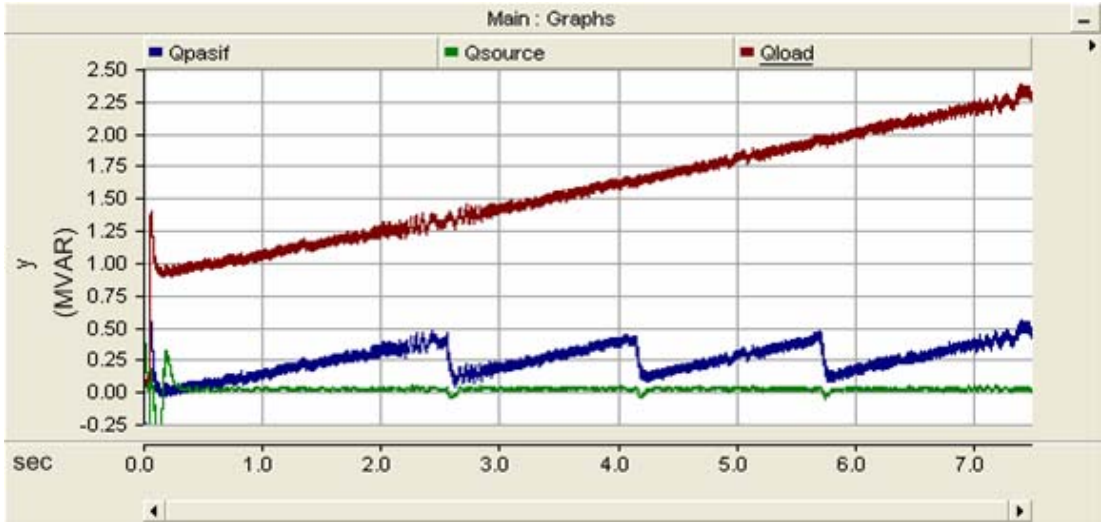

Figure 6.12 The reactive power of the source and load waveform

The rms trend of injected current of APF is shown in figure 6.13 and figure 6.14. The Shunt APF injects approximately between 20A and 25A from 31.5kV side of transformer. The 1 kV side of the transformer approximately 600A is injected by the shunt active power filter.

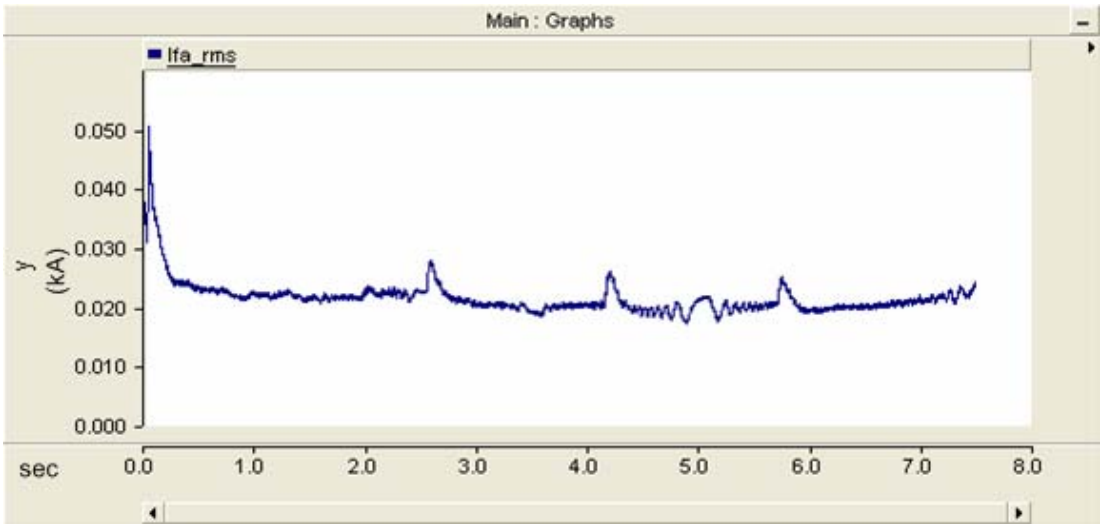

Figure 6.13 The Secondary side injected current RMS value of APF

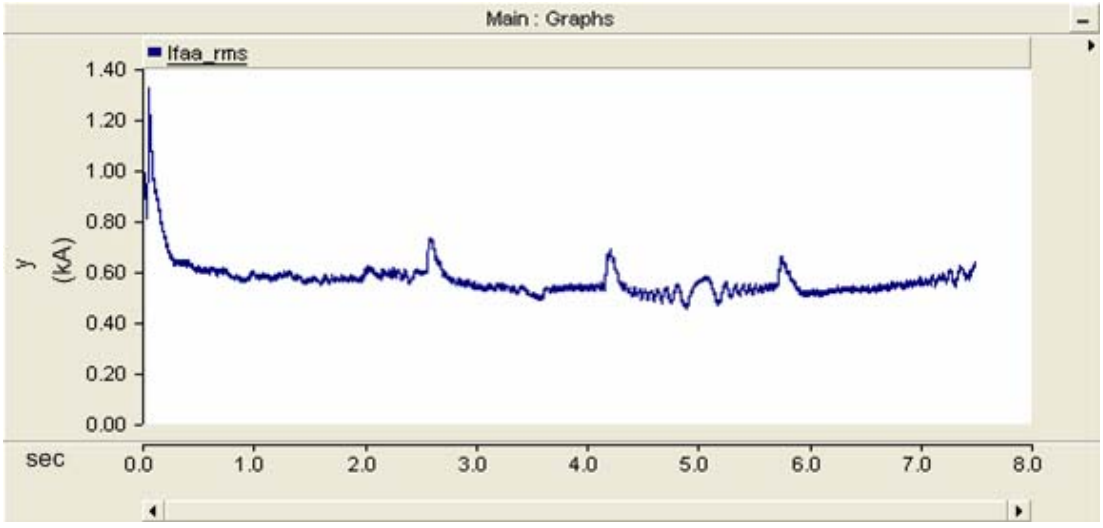

Figure 6.14 The Primary side injected current RMS value of APF

The figure 6.15, figure 6.16 and figure 6.17 shows the simulation results of EPLL used in Shunt APF. The load current measurement in figure 6.15 is applied to the input of EPLL and EPLL creates the fundamental components of input signal in figure 6.17 and harmonic components of input signal in figure 6.16.

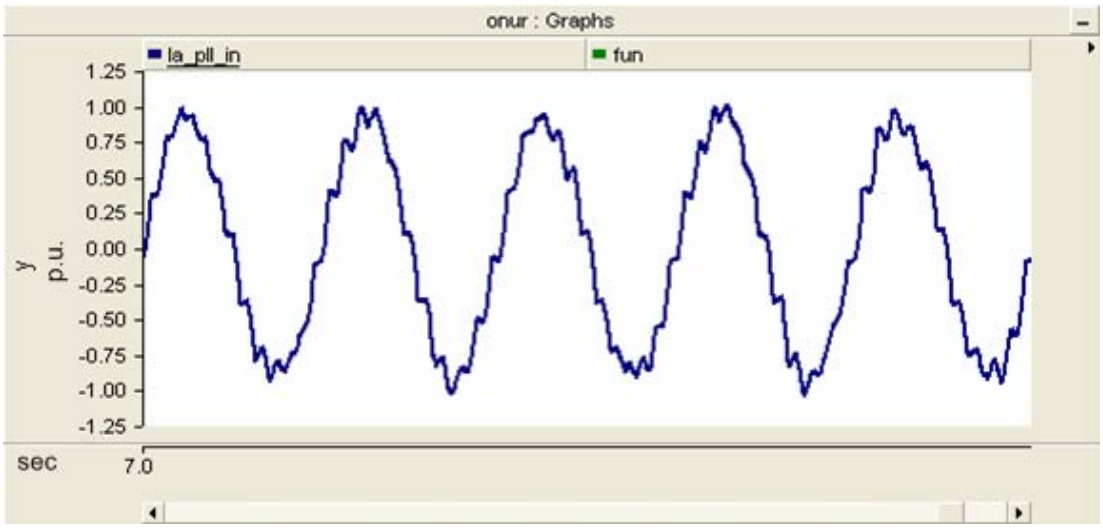

Figure 6.15 Input signal of EPLL circuit

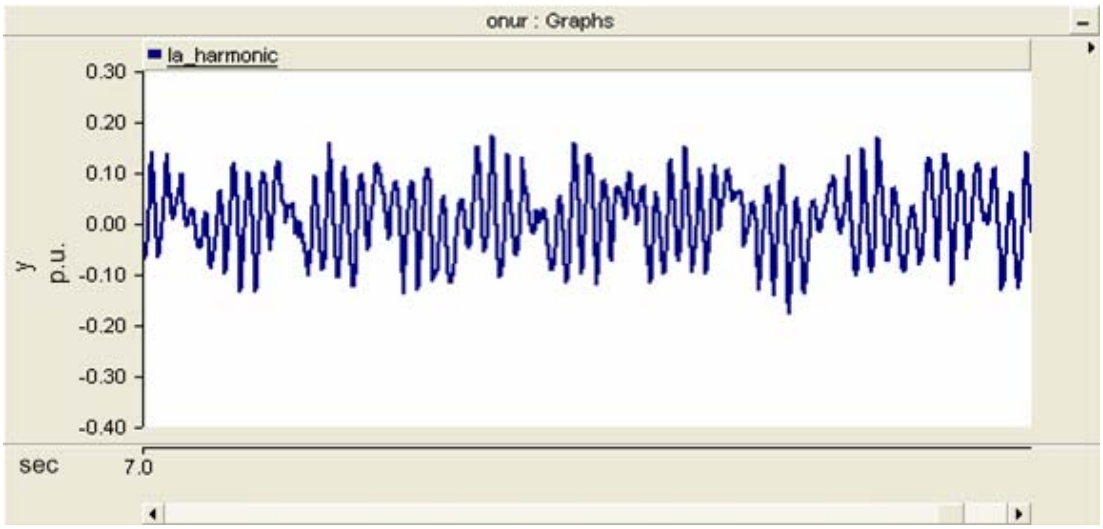

Figure 6.16 Error signal calculated by EPLL

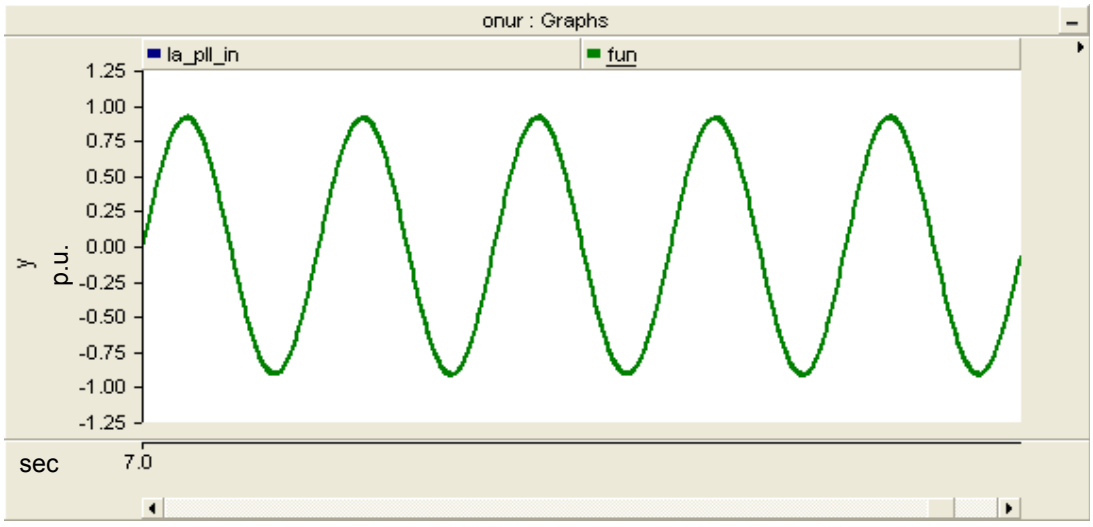

Figure 6.17 Output signal of signal of EPLL circuit

The reference signal created by the controller is shown at figure 6.18.For a perfect compensation; active filter must follow the reference current generated by the controller without delay and error. The injected currents of APF and reference signal created by controller of APF are shown in figure 6.19.

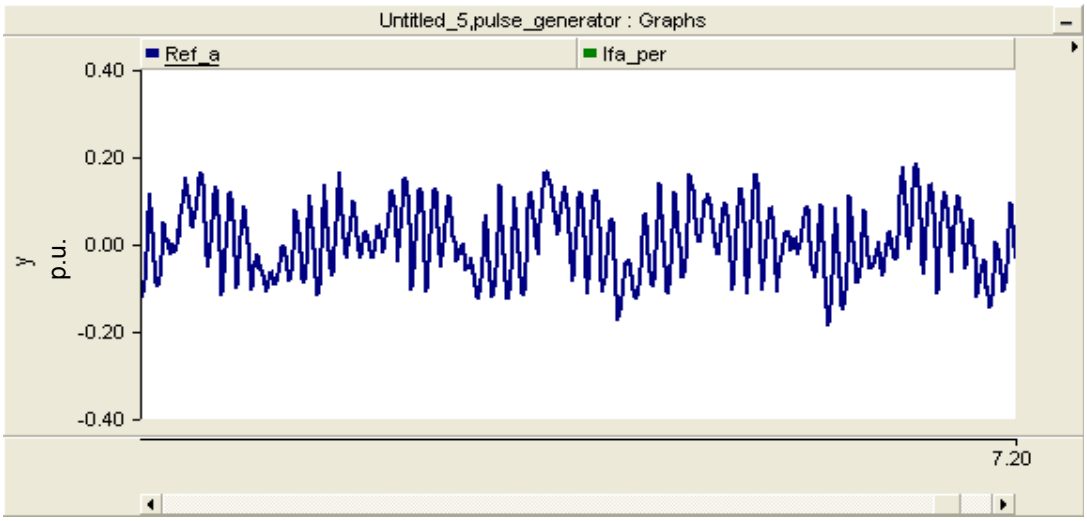

Figure 6.18 Reference signal generated by control circuit

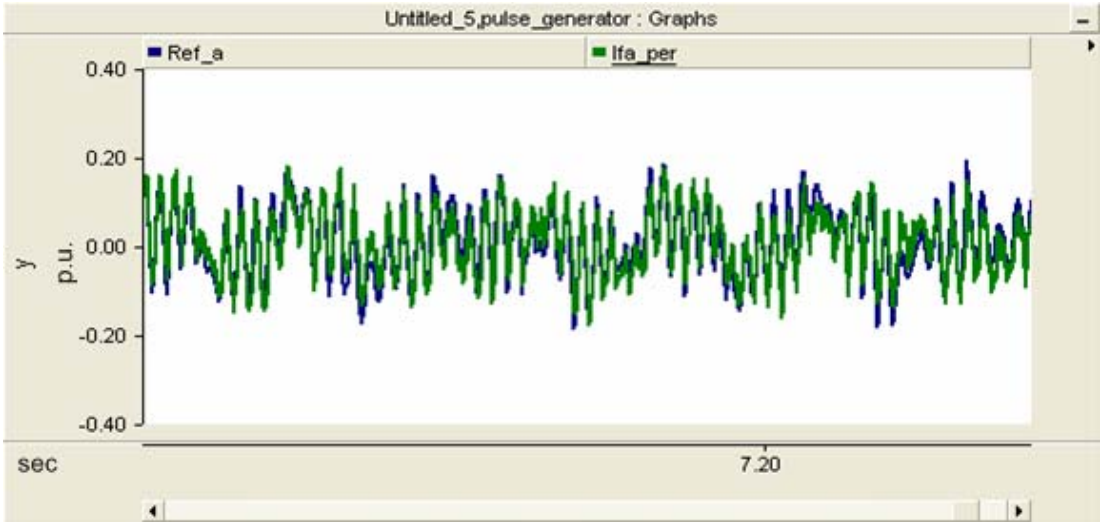

Figure 6.19 Reference signal and APF current signal

6.2 Case 2

The induction furnace works with only shunt active power filter. There is no passive filter in the network. In contrast to previous case, the reactive power compensation of induction furnace is achieved by only shunt active power filter.

The three phase compensated source current waveforms and distorted furnace current waveforms are shown in figure 6.20 and figure 6.21 respectively.

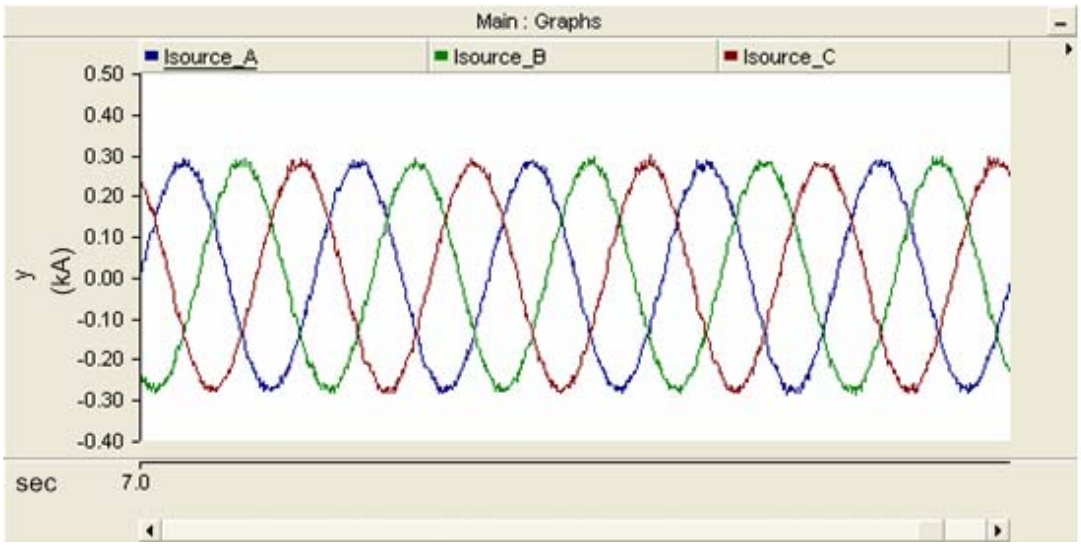

Figure 6.20 Three phase source current of the network

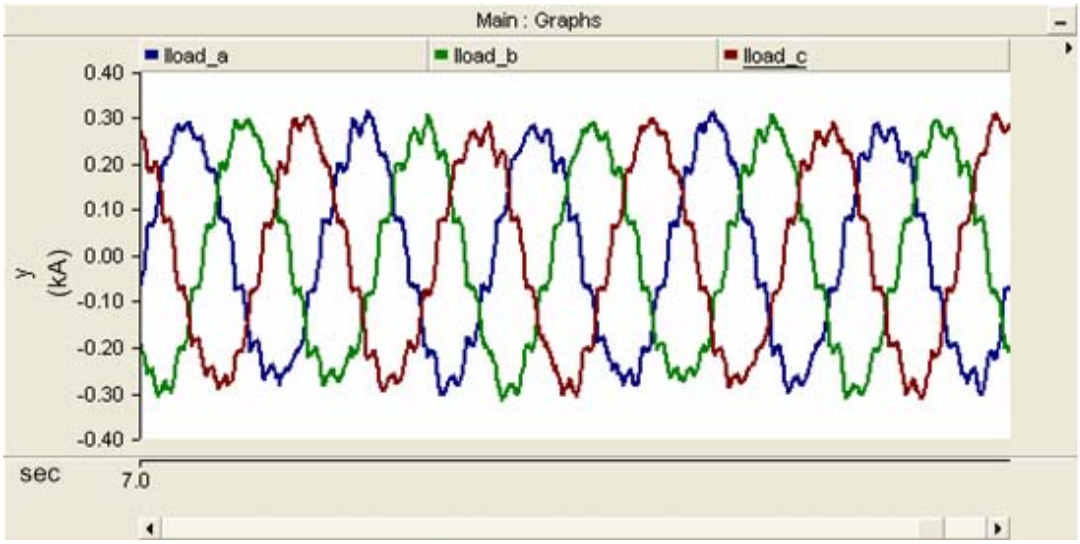

Figure 6.21 Three phase load current of the network

Figure 6.22 shows the compensated phase A source current. Phase A distorted furnace current is shown in figure 6.23. In figure 6.24, the compensated phase A current and the distorted furnace current is shown at the same graphic.

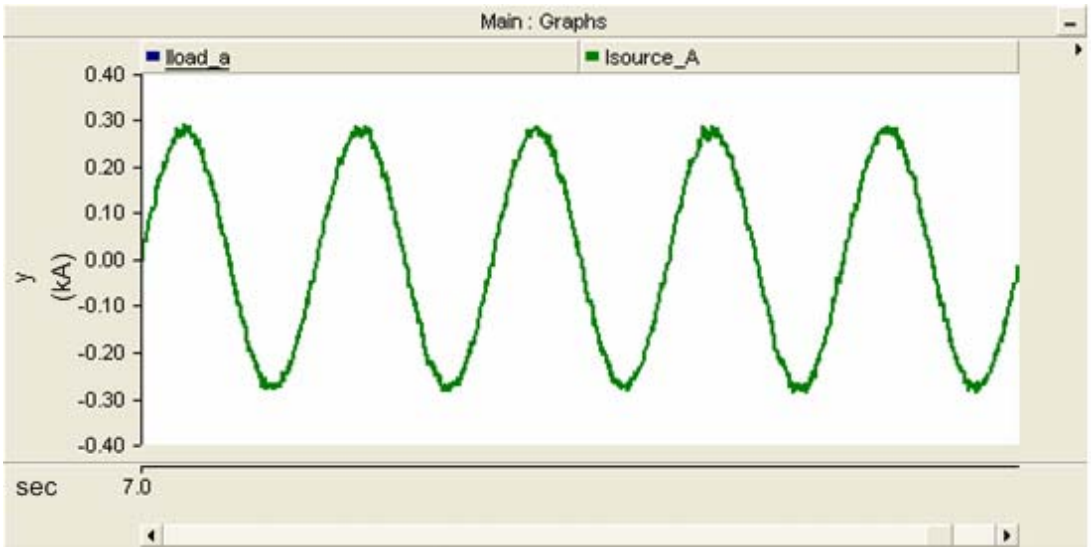

Figure 6.22 Phase A source current of the network

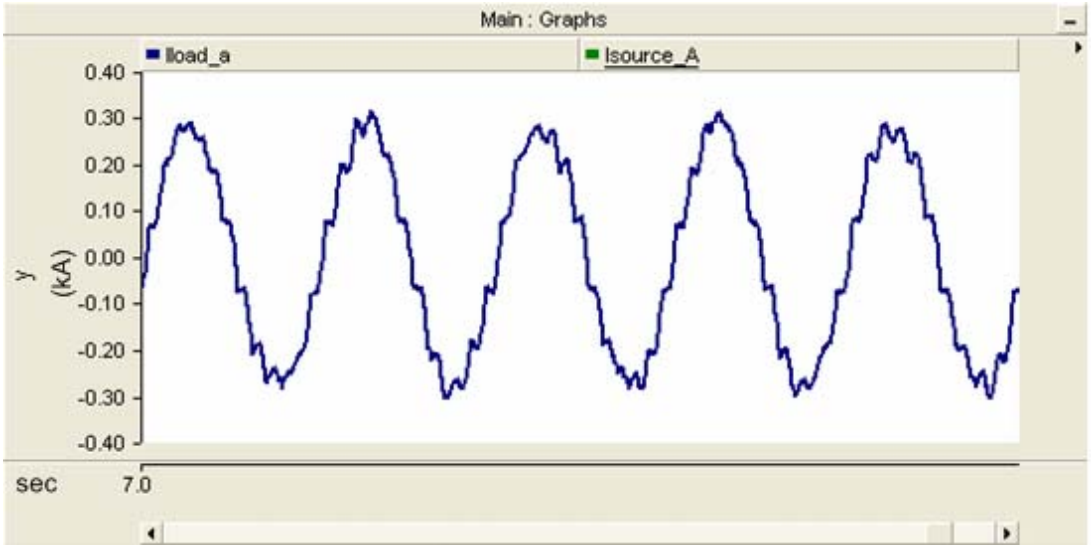

Figure 6.23 Phase A load current of the network

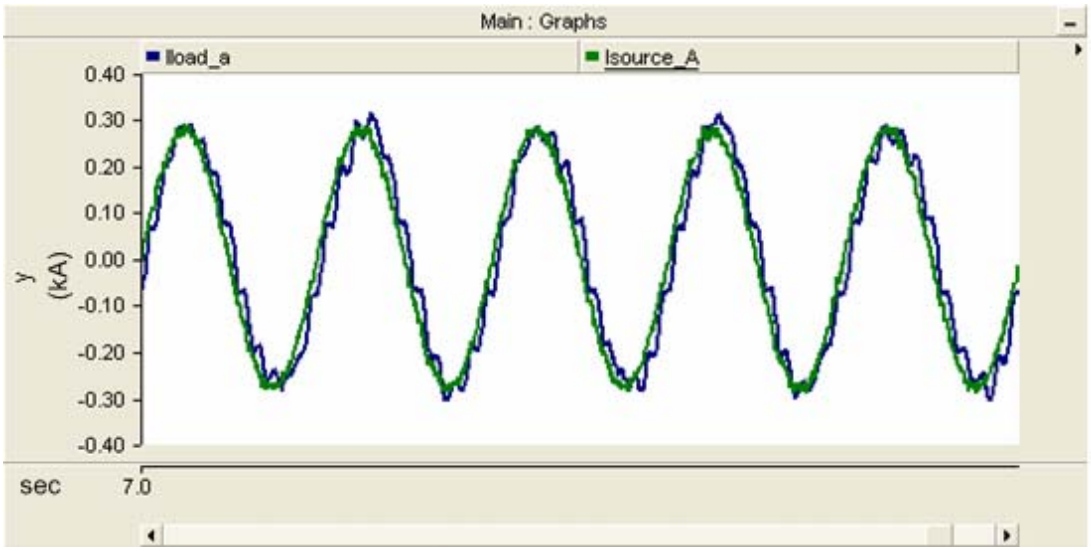

Figure 6.24 Phase A load and source current of the network

Three phase source voltage is shown in figure 6.25 and phase A source voltage is shown in figure 6.26. It is clearly seen that there is no distortion in the voltage waveforms.

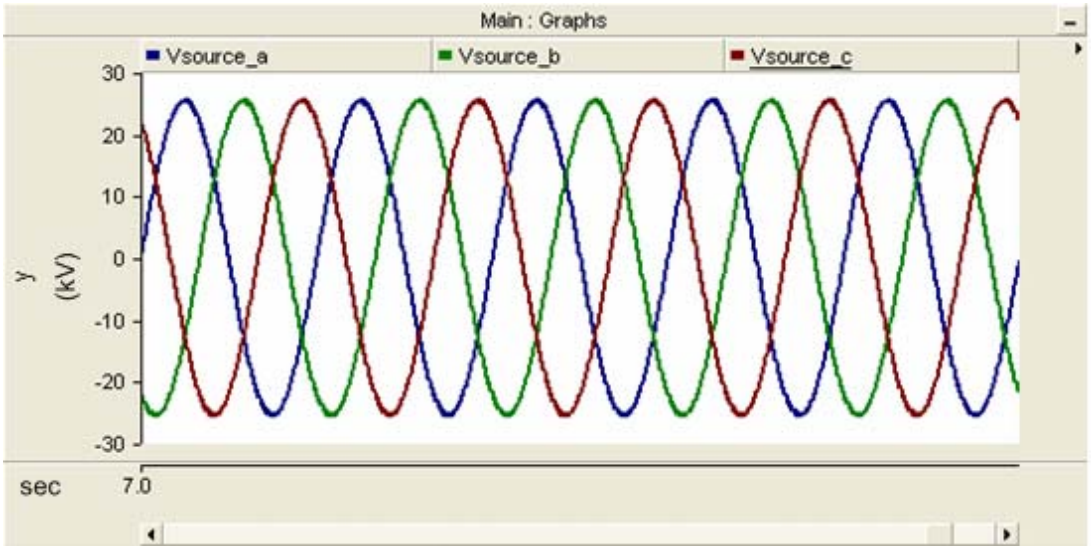

Figure 6.25 Three phase source current of the network

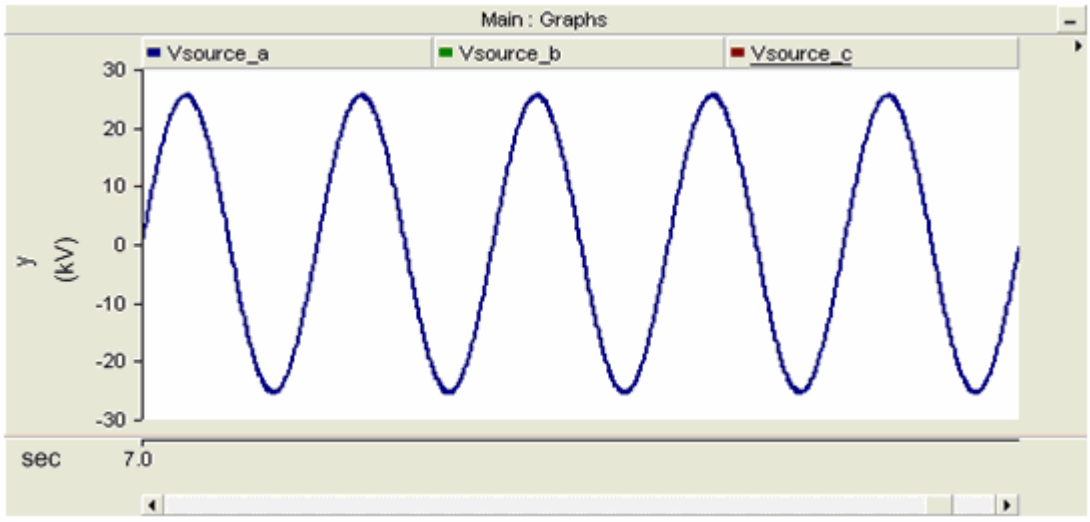

Figure 6.26 Phase A source voltage of the network

Again as the previous case, the trend of load current THD is changed between 10% and 20% as shown in figure 6.27 and Shunt APF decreases the source current THD below 4% as shown in figure 6.28.

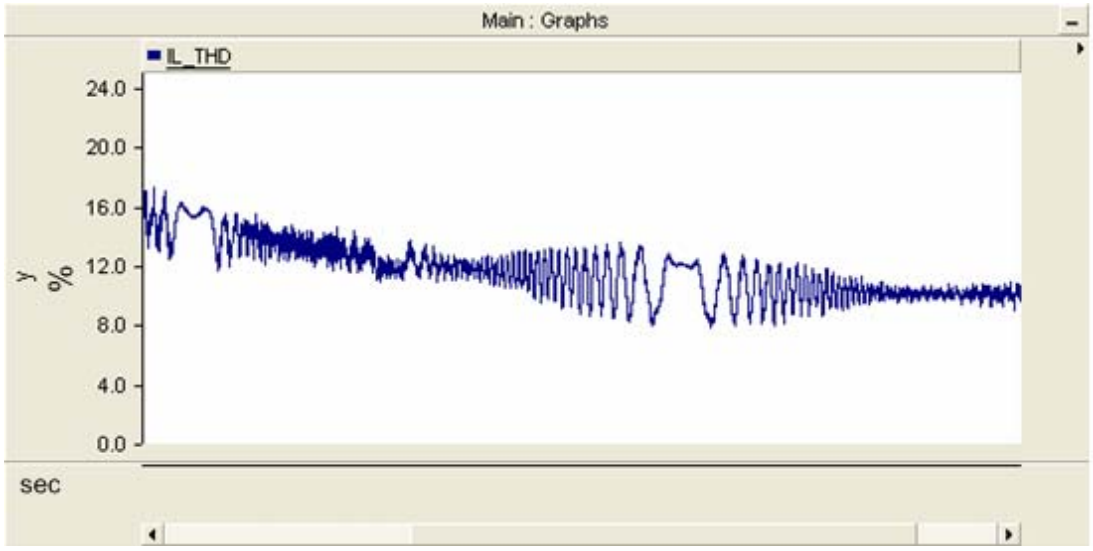

Figure 6.27 Total Harmonic Distortion of load current of the network

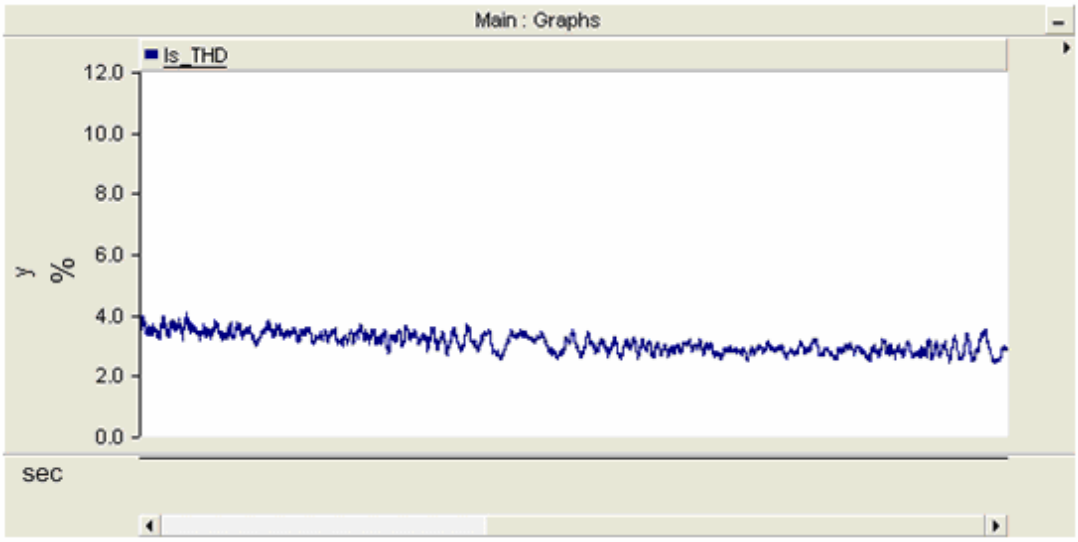

Figure 6.28 Total Harmonic Distortion of source current of the network

Like the previous case the DC link capacitor voltage is set to 3000V and its trend is shown in figure 6.29.

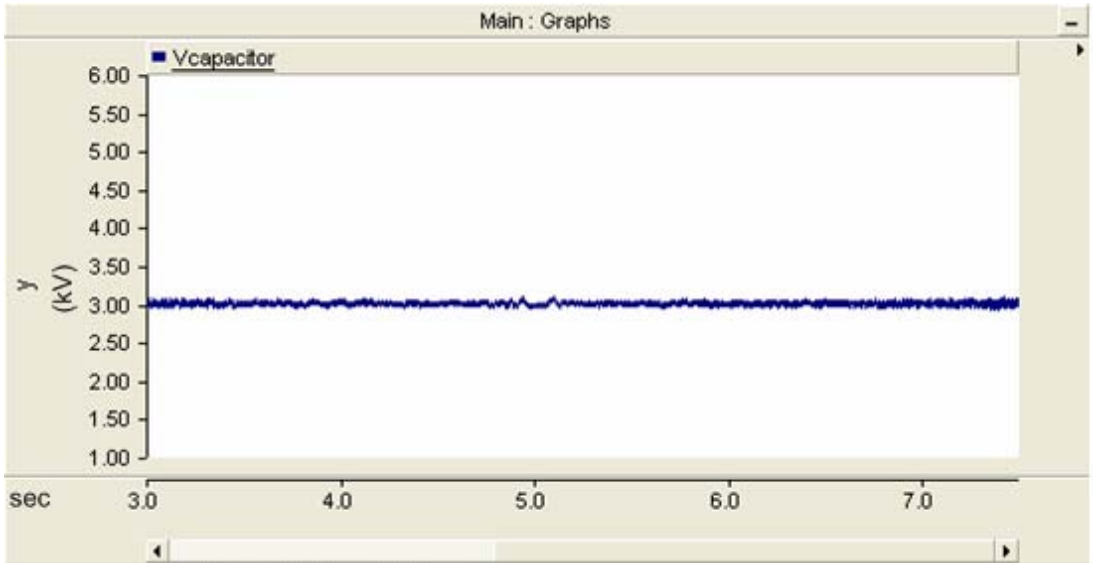

Figure 6.29 The DC Link voltage of the active power filter

As shown in figure 6.30, the reactive power of furnace increases up to 2.25 MVAR with the increase of operating frequency of furnace and the Shunt APF compensates the reactive power of furnace and nearly no reactive power is consumed from utility as shown in figure 6.30.

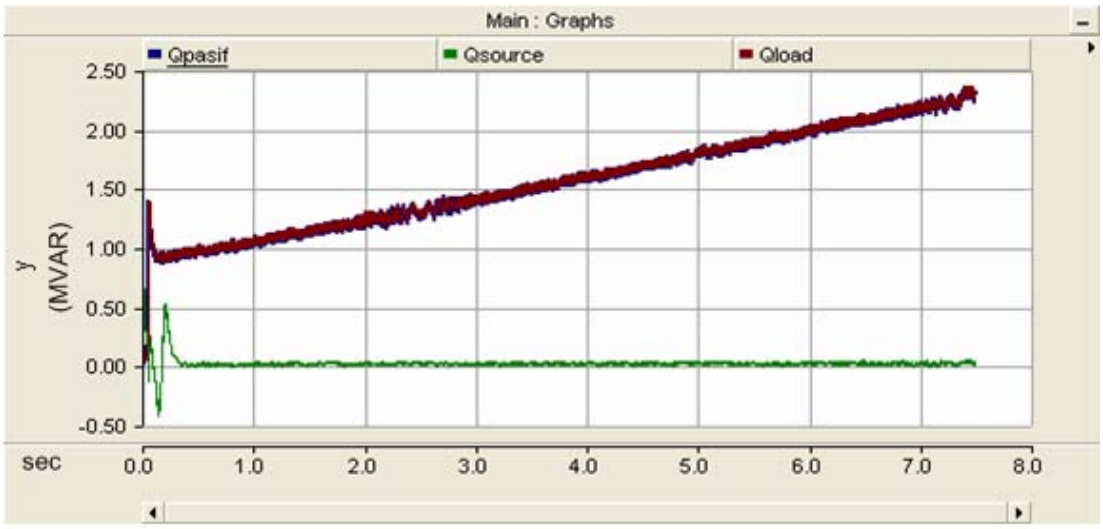

Figure 6.30 The reactive power of the source and load waveform

The rms trend of injected current of APF is shown in figure 6.31 and figure 6.32. The Shunt APF injects approximately between 30A and 45A from 31.5kV side of transformer. The 1 kV side of the transformer approximately between 900A and 1200A is injected by the shunt active power filter. It is obviously seen that the injected current of APF is higher than the previous case. Because reactive power compensation is achieved by shunt active power filter.

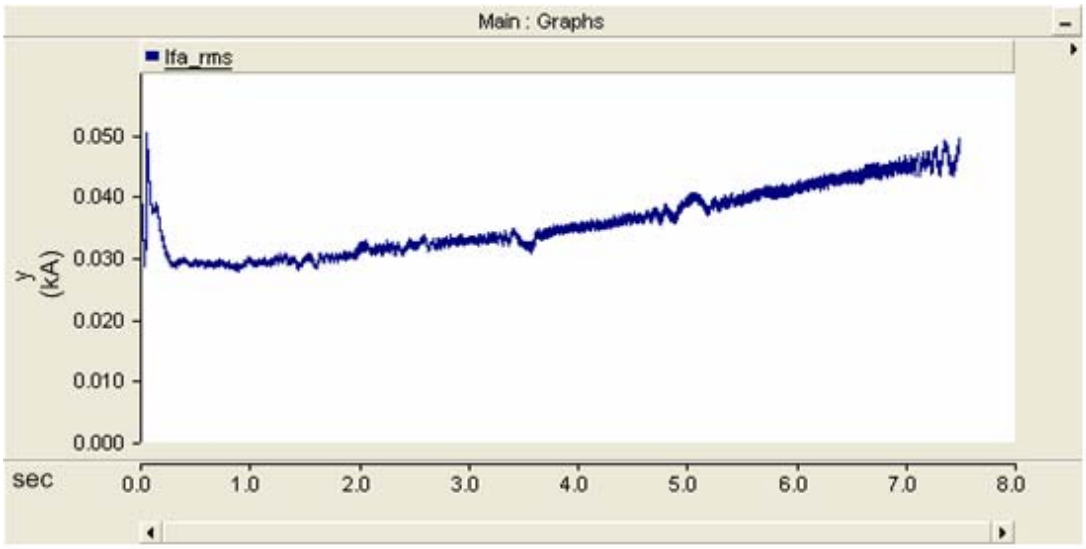

Figure 6.31 The Secondary side injected current RMS value of APF

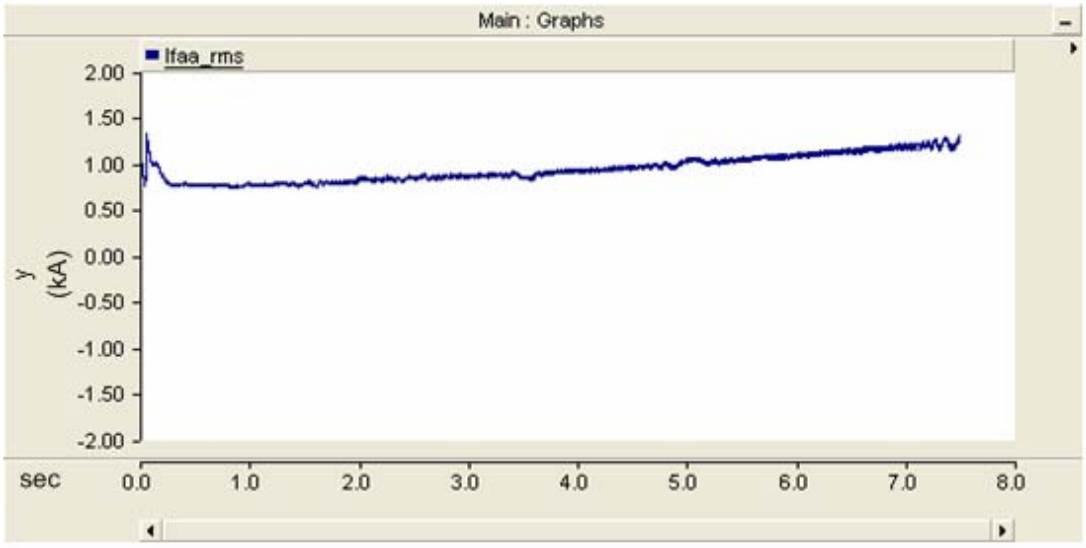

Figure 6.32 The Primary side injected current RMS value of APF

The figure 6.33, figure 6.34 and figure 6.35 shows the simulation results of EPLL used in Shunt APF. The load current measurement in figure 6.33 is applied to the input of EPLL and EPLL creates the fundamental components of input signal in figure 6.35 and harmonic components of input signal in figure 6.34.

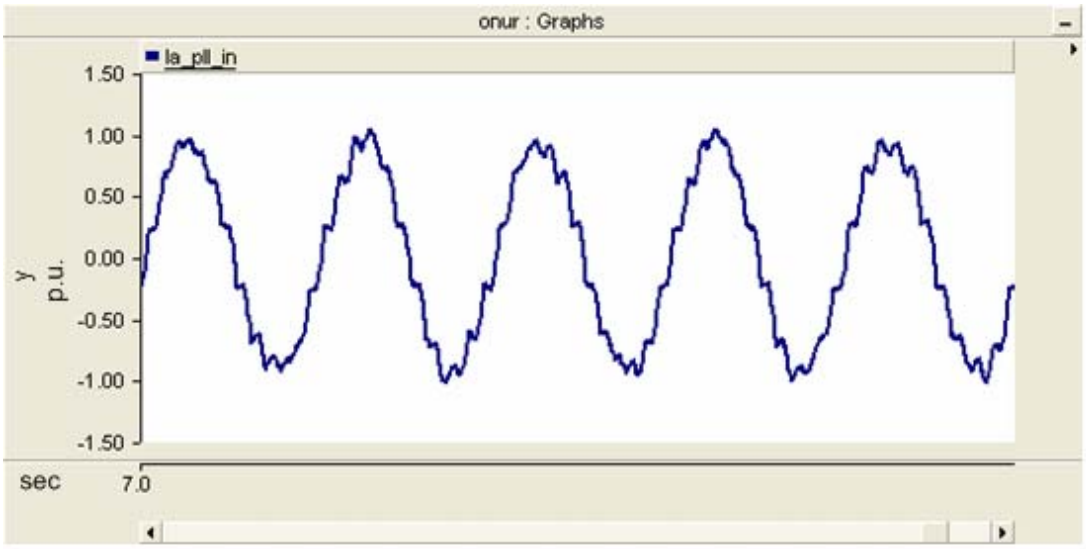

Figure 6.33 Input signal of EPLL circuit

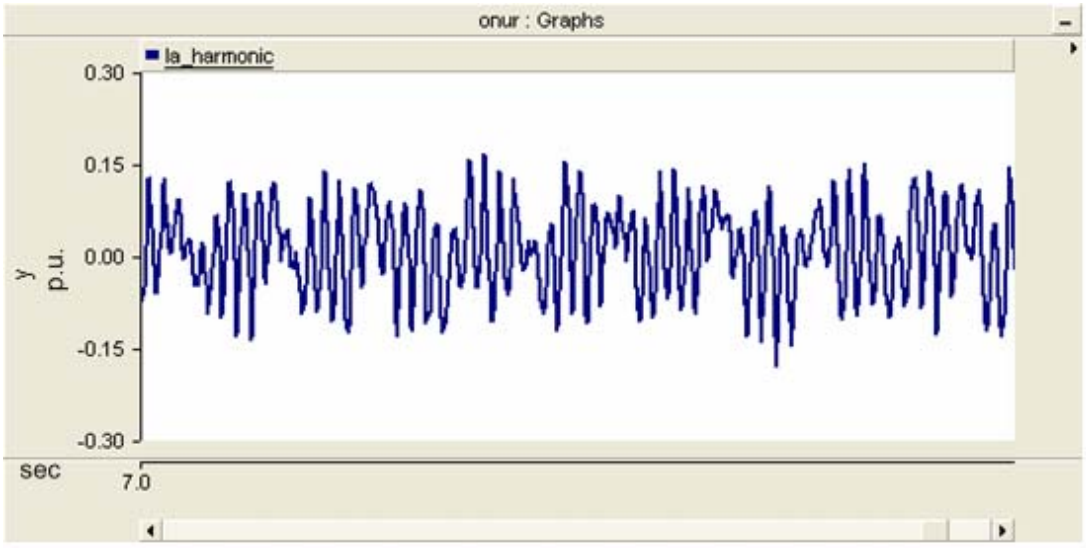

Figure 6.34 Error signal calculated by EPLL

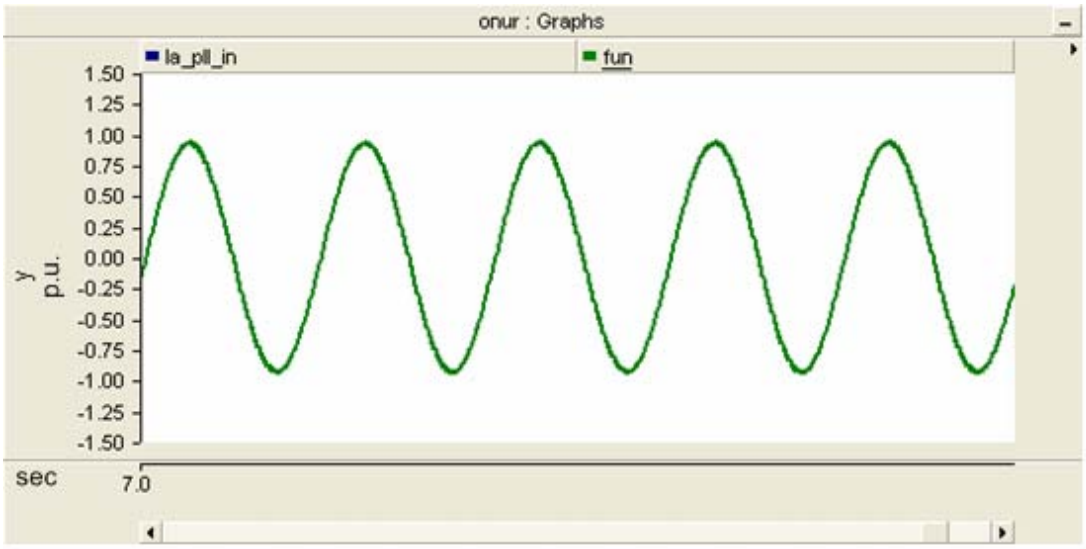

Figure 6.35 Output signal of EPLL circuit

The reference signal created by the controller is shown in figure 6.36. The injected currents of APF and reference signal created by controller of APF are shown in figure 6.37.

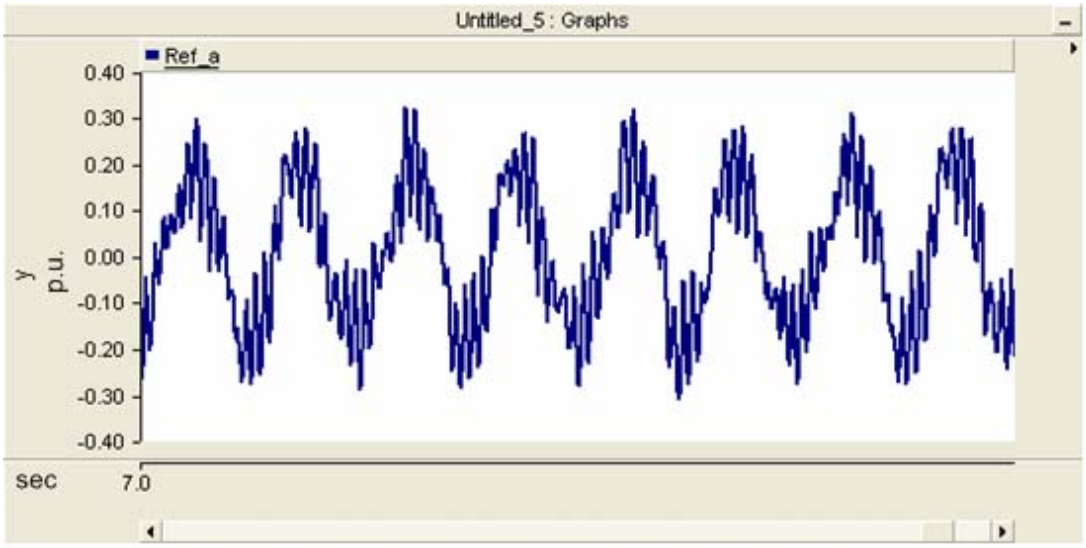

Figure 6.36 Reference signal generated by the control circuit

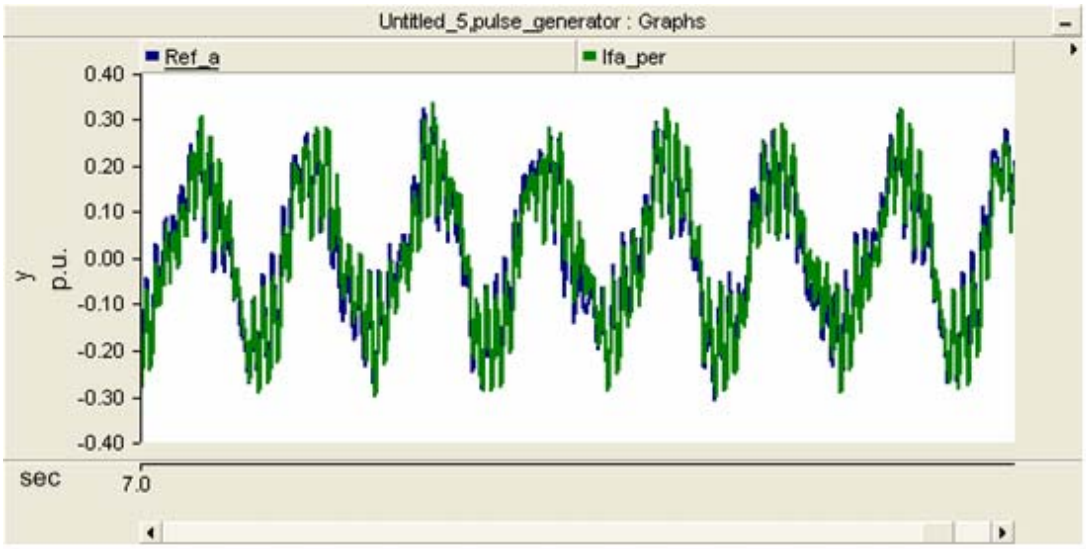

Figure 6.37 Reference signal and APF current signal

6.3 Case 3

The induction furnace works with only shunt active power filter. There is no passive filter in the network. The active filter works to only compensate the harmonic content. There is no reactive current control in the control circuit of the active power filter.

The three phase compensated source current waveforms and distorted furnace current waveforms are shown in figure 6.38 and figure 6.39 respectively.

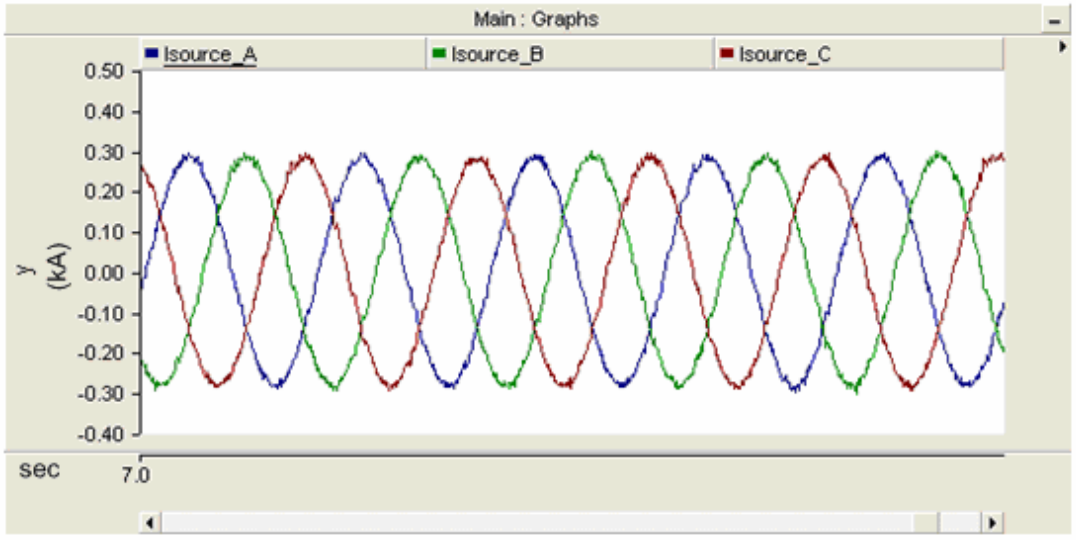

Figure 6.38 Three phase source current of the network

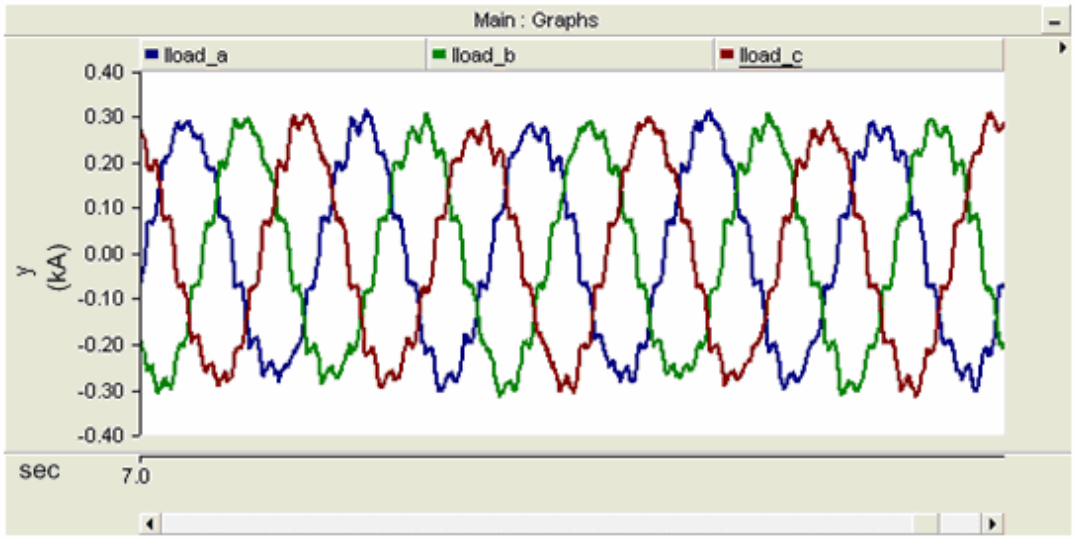

Figure 6.39 Three phase load current of the network

Figure 6.40 shows the compensated phase A source current. Phase A distorted furnace current is shown in figure 6.41. In figure 6.42, the compensated phase A current and the distorted furnace current is shown at the same graphic. It is clearly seen that the furnace current and the source current is overlap in figure 6.42.Because there is no reactive current control in the system.

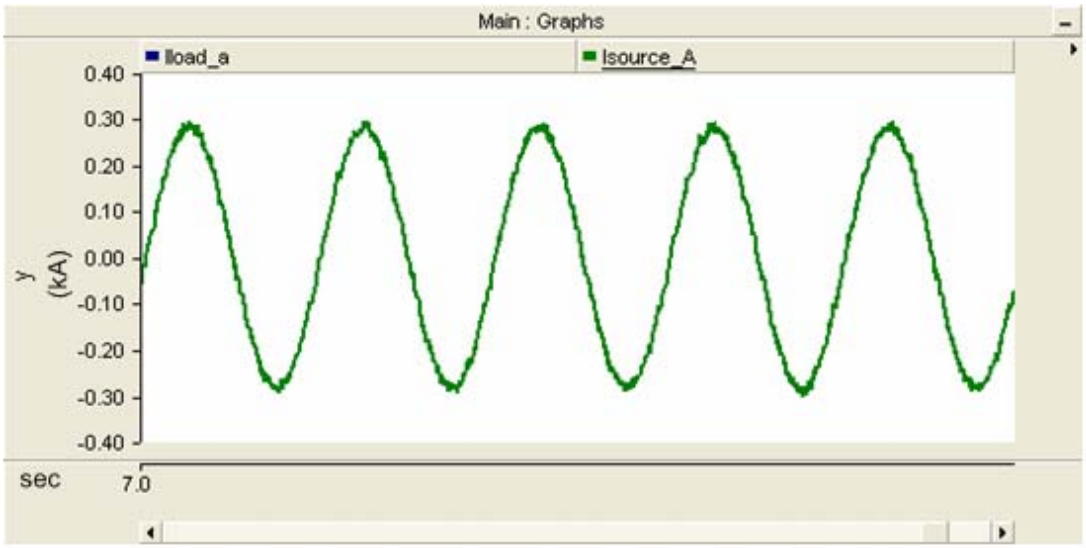

Figure 6.40 Phase A source current of the network

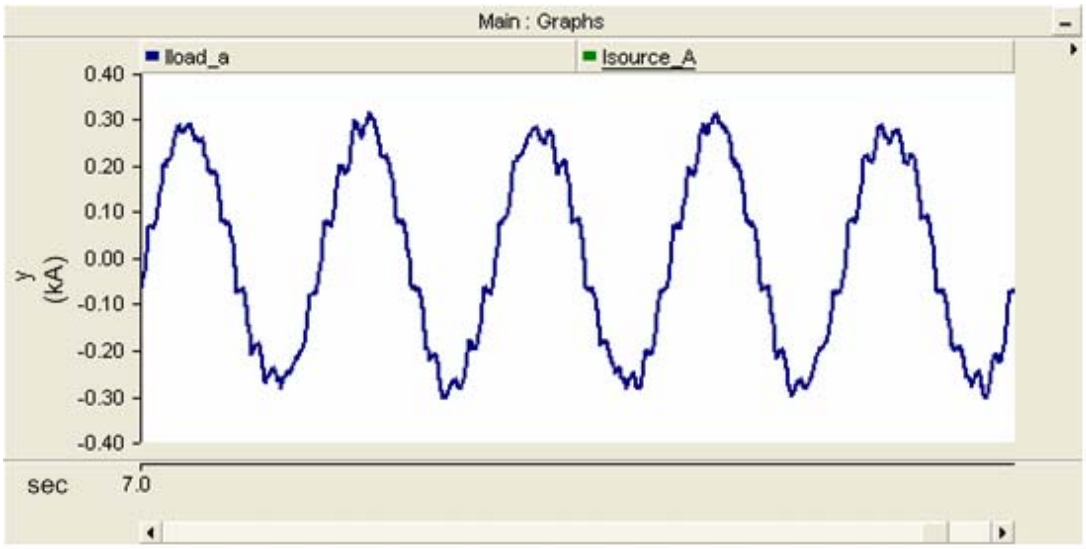

Figure 6.41 Phase A load current of the network

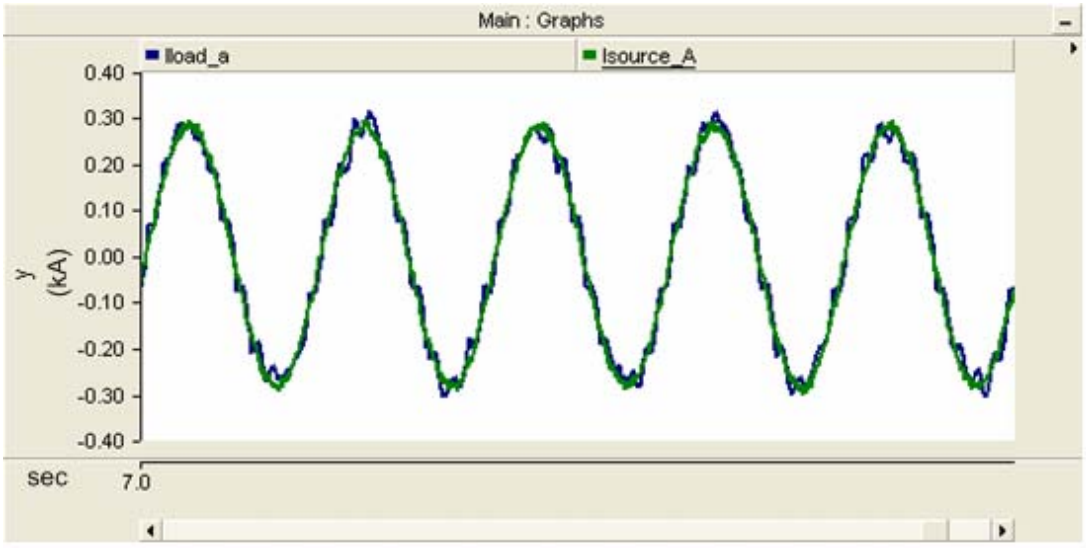

Figure 6.42 Phase A load and source current of the network

Three phase source voltage is shown in figure 6.43 and phase A source voltage is shown in figure 6.44. It is clearly seen that there is no distortion in the voltage waveforms.

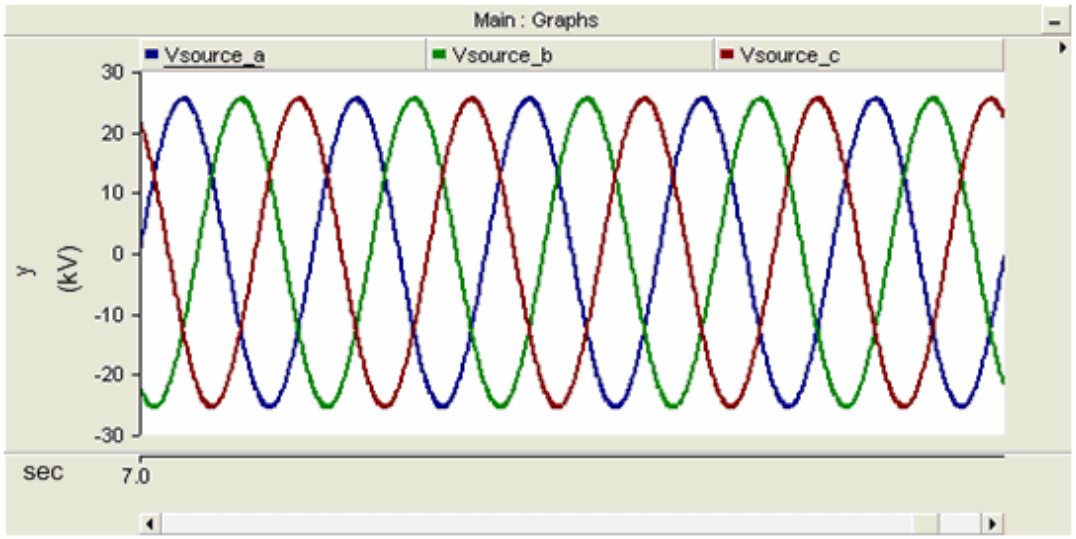

Figure 6.43 Three phase source voltage of the network

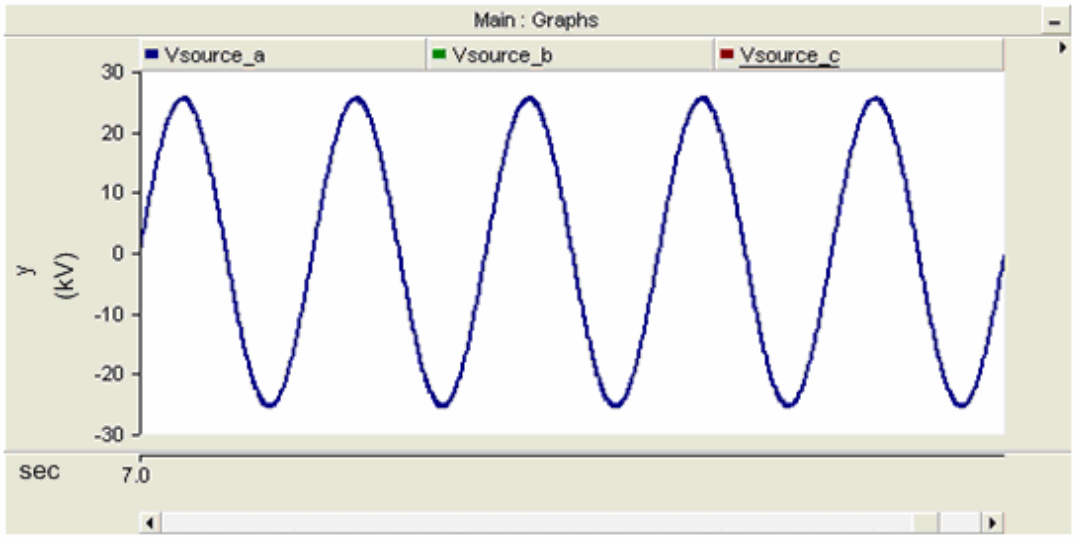

Figure 6.44 Phase A source voltage of the network

Like the previous cases, the trend of load current THD is changed between 10% and 20% as shown in figure 6.45 and Shunt APF decreases the source current THD below 4% as shown in figure 6.46.

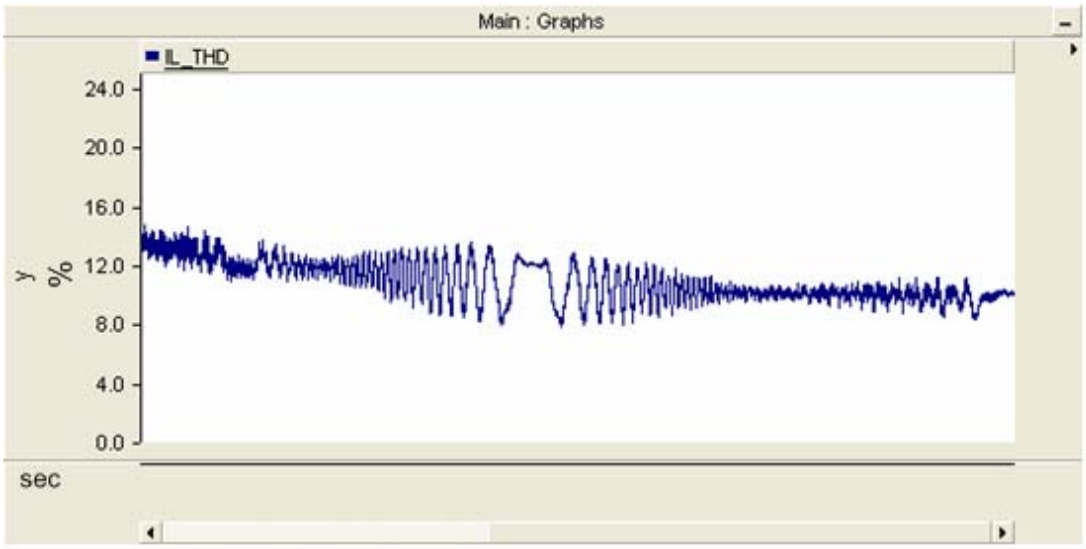

Figure 6.45 Total Harmonic Distortion of load current of the network

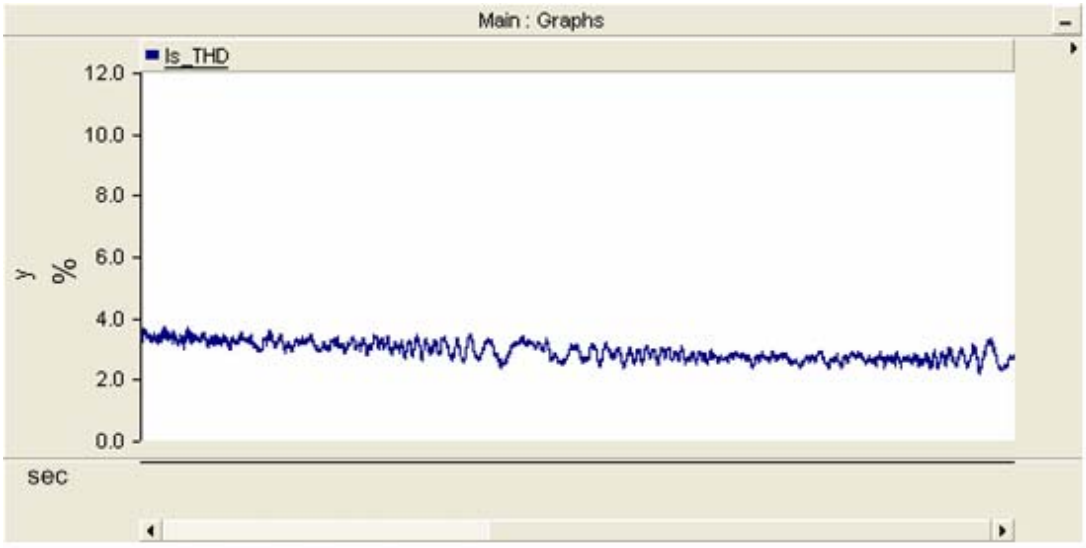

Figure 6.46 Total Harmonic Distortion of source current of the network

The DC link capacitor voltage is set to 3000V and its trend is shown in figure 6.47.

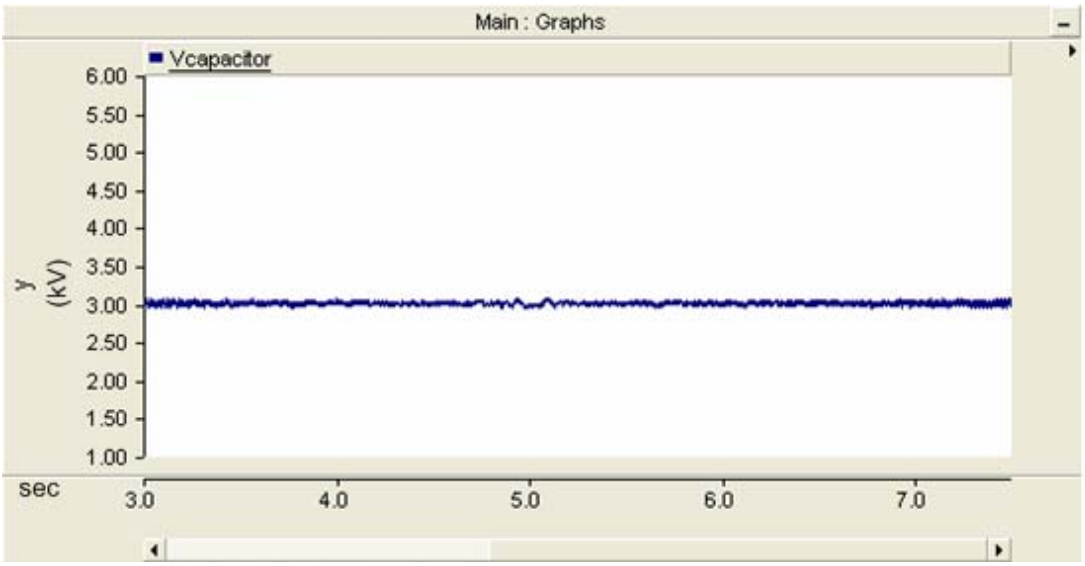

Figure 6.47 The DC Link voltage of the Active power filter

As shown in figure 6.48, the reactive power of furnace increases up to 2.25 MVAR with the increase of operating frequency of furnace. Because of the lack of the reactive current control, reactive power of source increases in parallel to furnace.

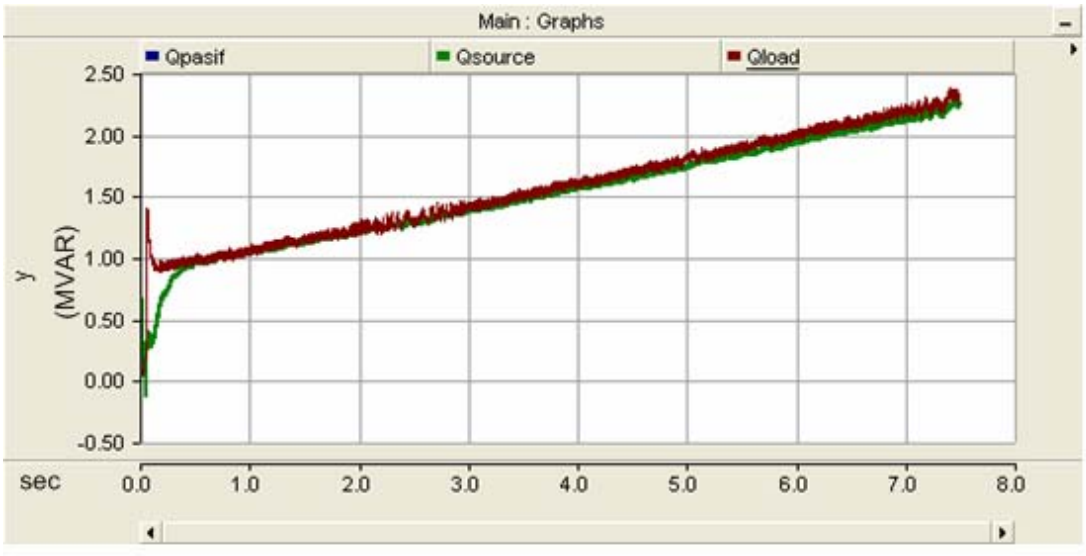

Figure 6.48 The reactive power of the source and load waveform

The rms trend of injected current of APF is shown in figure 6.49 and figure 6.50. The Shunt APF injects approximately 20A from 31.5kV side of transformer.

The 1 kV side of the transformer approximately 550A is injected by the shunt active power filter. It is seen that first case injected current graphic resembles figure 49 and figure 6.50.

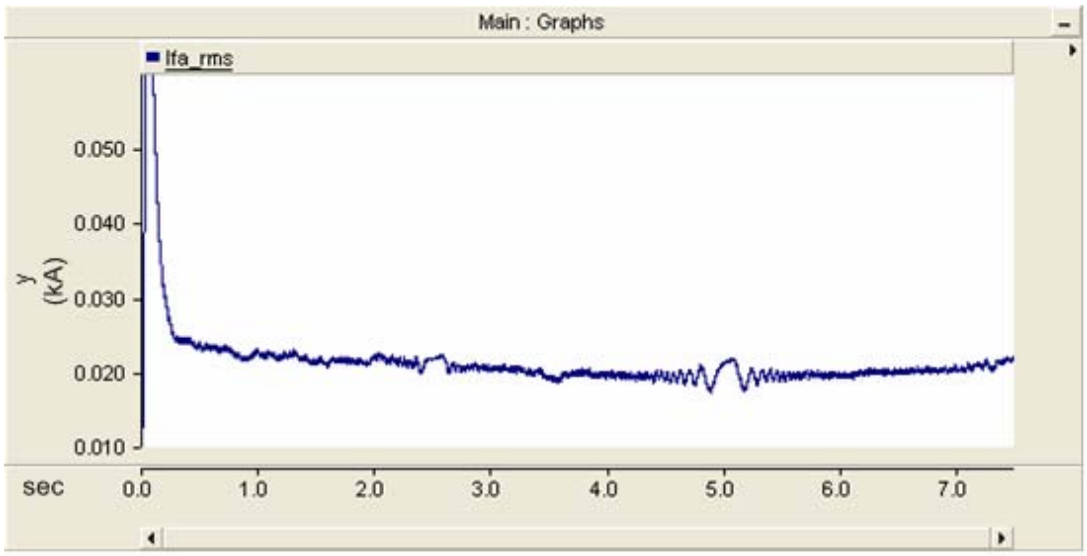

Figure 6.49 The Secondary side injected current RMS value of APF

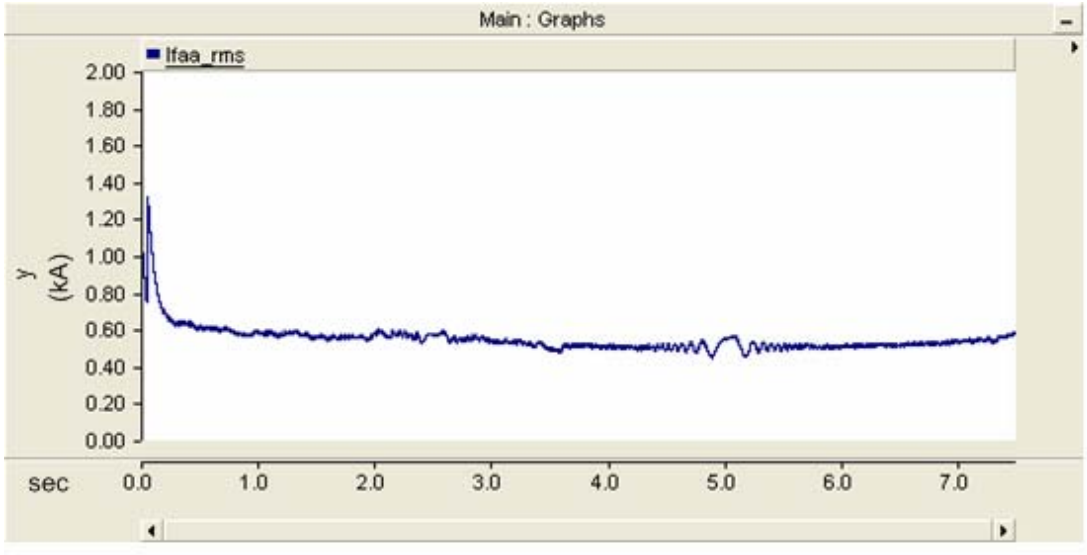

Figure 6.50 The Primary side injected current RMS value of APF

The figure 6.51, figure 6.52 and figure 6.53 shows the simulation results of EPLL used in Shunt APF. The load current measurement in figure 6.51 is applied to the input of EPLL and EPLL creates the fundamental components of input signal in figure 6.53 and harmonic components of input signal in figure 6.52.

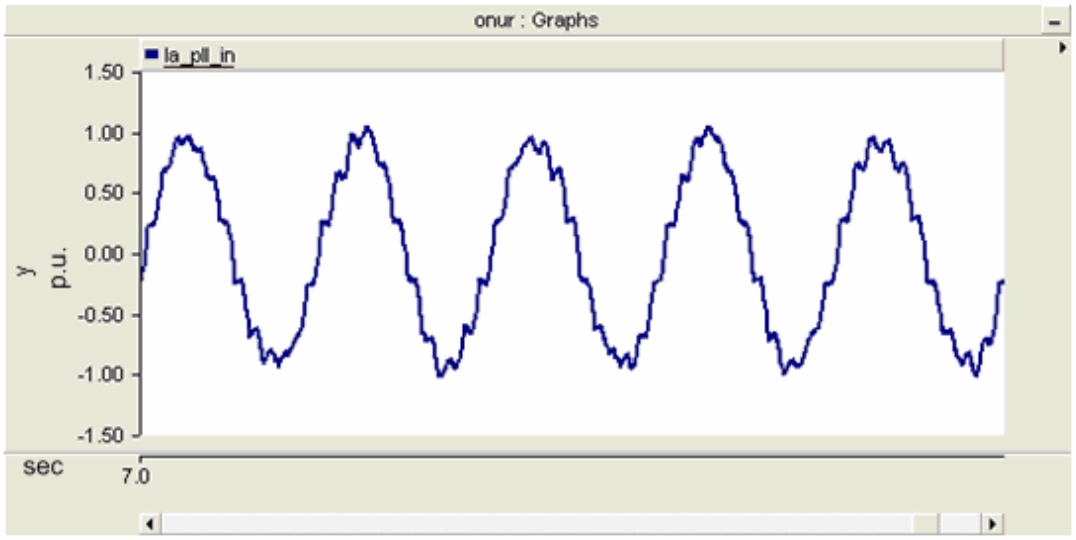

Figure 6.51 Input signal of EPLL circuit

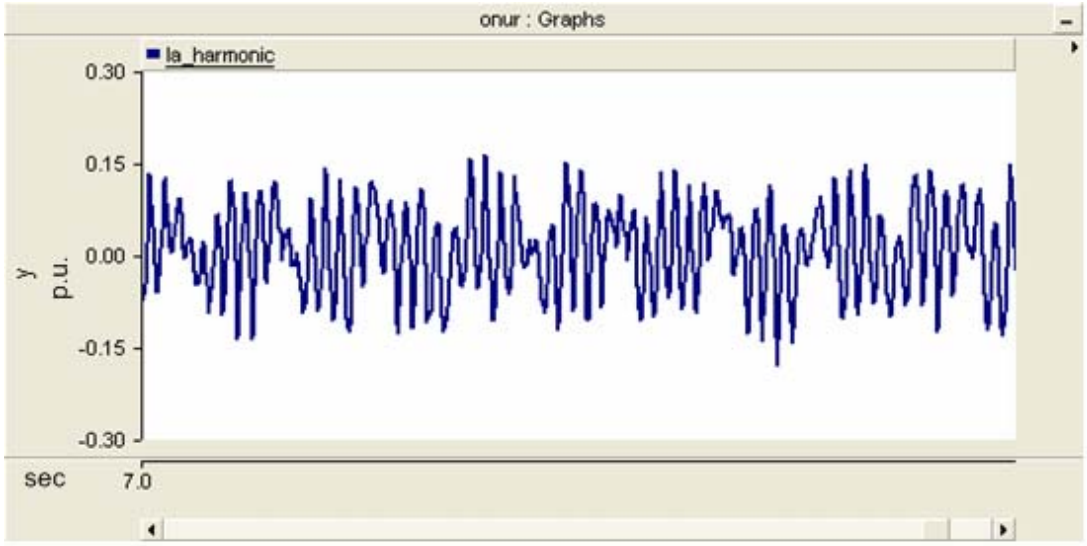

Figure 6.52 Error signal calculated by EPLL

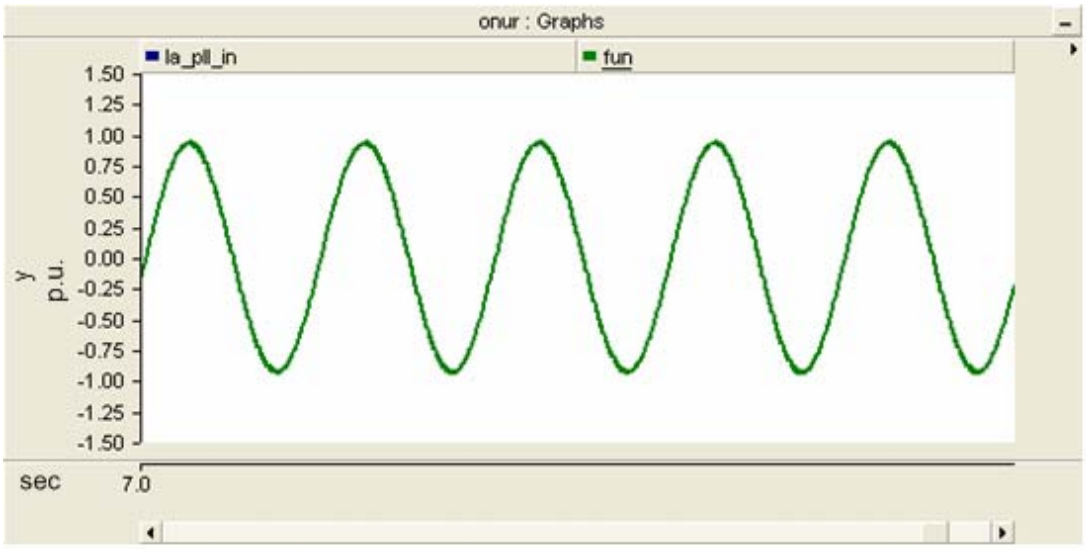

Figure 6.53 Output signal of EPLL circuit

The reference signal created by the controller is shown in figure 6.54. The injected currents of APF and reference signal created by controller of APF are shown in figure 6.55.

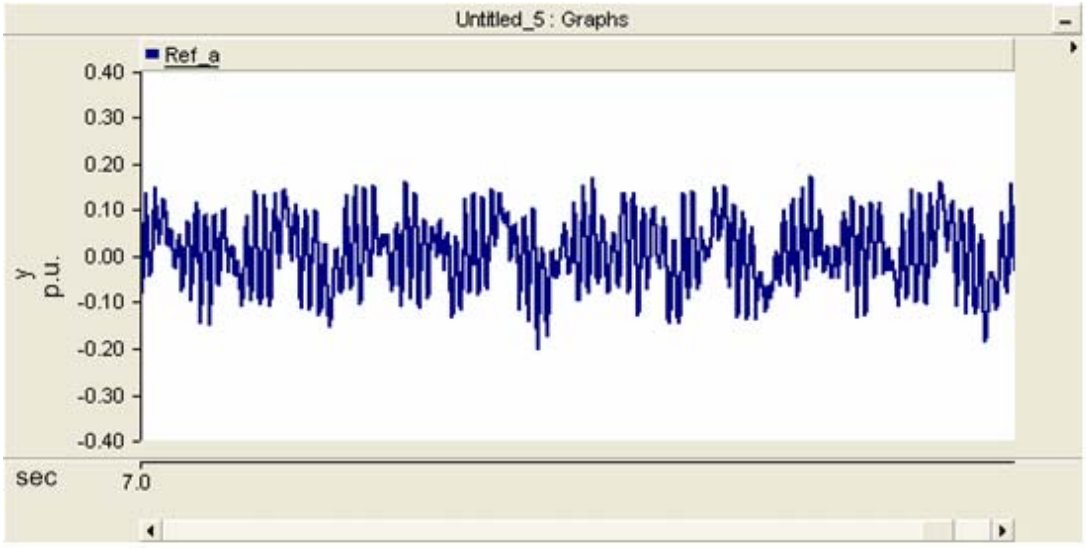

Figure 6.54 Reference signal generated by the control circuit

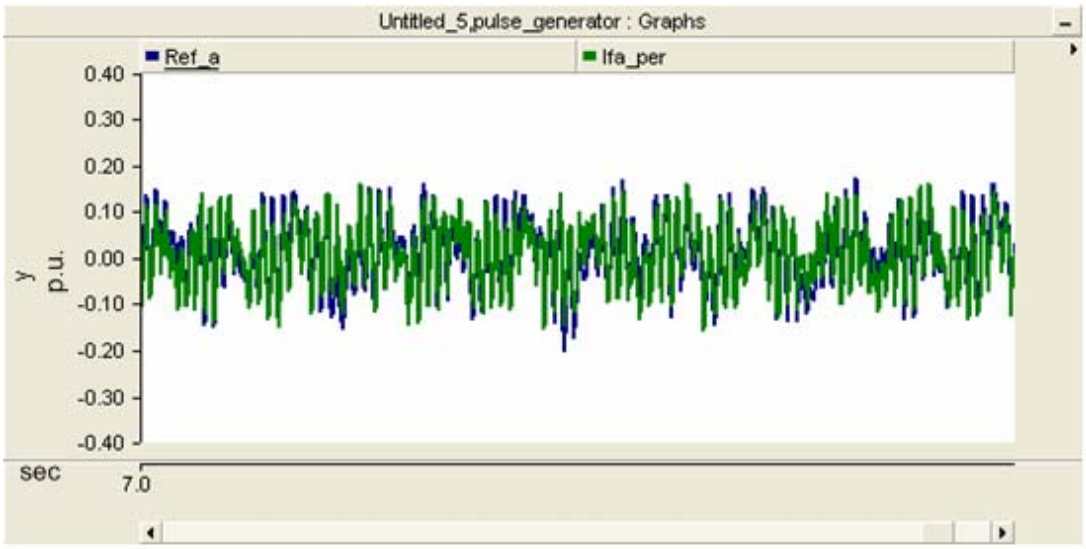

Figure 6.55 Reference signal and APF current signal

6.4 Discussions

In the chapter 4 of thesis, the operating principles and power quality problems of current source induction furnace is presented clearly with simulation results. The varying harmonics and interharmonics of induction furnace are indicated with a few different operating frequency examples.

In the proposed power quality compensation system, shunt APF is capable of both harmonic and reactive power compensation ability. However, passive filters are used for reactive power compensation to decrease the power ratings of shunt APF.

In order to compare the case studies results achieved by power quality compensation system, Table 6.1 shows the some quantities.

Table 6.1 Performance comparisons among study cases

Parameter	Case 1	Case 2	Case 3
Furnace THD (%)	20-25	20-25	20-25
Source THD (%)	3	3	3
Power Rating of APF (MVA)	1.4	2.5	1.1
Compensated reactive power by APF(MVAR)	0.3	2.25	0
DC Link Voltage (kV)	3	3	3
H Bridge inverter frequency(Hz)	150-300	150-300	150-300
Simulation Time (s)	7.5	7.5	7.5

As shown from Table 6.1 the proposed Shunt APF can compensate easily the varying harmonics and interharmonics and reactive power of current source induction furnace without passive filters. The furnace current THD is decreased from 20-25% to below 4% and 2.25 MVAR rated reactive power of furnace is compensated. . The rated power of Shunt APF is 2.5MVA for alone operation.

When the shunt APF and passive Filters operate together, shunt APF compensates only the 0.3MVAR reactive power and the power rating of shunt APF decreases to 1.4 MVA. The power ratings of APF are directly related to the installation cost of APF.

On the other hand, the power circuit of proposed APF becomes inadequate for the high power applications. Multilevel inverter topologies are preferred for high power applications because of the capabilities of power electronic switching devices.

The THD level of source voltage is always kept below the standard limits by using proposed control strategy without reactive current control. Without reactive current control, the rated power of shunt APF is 1.1 MVA.

In all cases the DC link voltage of the shunt APF is the set 3000V. The DC link control circuit keeps the voltage desired level as shown table 6.1.

7. CONCLUSIONS

The aim of the thesis is to introduce the induction furnace system and develop the power quality compensation system for current source coreless induction furnace.

The iron and steel market is large and set to grow further. Automotive, household durables and machinery & equipment comprise the main sectors to trigger this growth. The steel industry actively manages the use of energy. For this reason the comprehensive literature research was carried out in order to introduce the iron and steel industry to chapter two.

One of the most economic ways of producing steel is made through the use of induction furnaces. Induction furnaces are most widely used type of furnace and have become a quite popular choice for melting iron. The induction heating power supply sends alternating current through the induction coil, which generates a magnetic field. Induction furnaces work on the principle of a transformer. An alternative electromagnetic field induces eddy currents in the metal which converts the electric energy to heat without any physical contact between the induction coil and the work piece. Induction furnace capacities range from less than one kilogram to one hundred tones capacity. With increasing the capacity of Induction furnace cause to draw larger currents from supply and that current also cause power quality problems particularly weak distribution systems. Those furnaces are also major contributors in the harmonic arena. In addition to the harmonics that are normally expected from different pulse rectifiers large furnaces operating at a few hundred hertz can generate significant non-characteristic harmonics. These harmonics, which fluctuate with the frequency of the furnace resonant circuit, are usually not multiples of the supply frequency, making them difficult to filter In chapter three induction furnace operation principle is explained. Power quality problems generated by the induction furnace in and their solution of major problems have been investigated by inclusive survey. Power quality problems of current source induction furnaces are very strange and there exist fewer researches on power quality problems on current source induction furnaces.

In chapter four of thesis the power quality problems of induction furnace is clearly explained with the simulation results. In this chapter only the induction furnace is connected to the network. Normal operation mode of furnace is simulated. Our furnace operating frequency has changed between 150Hz and 300Hz.According to melting iron the furnace operating frequency changes. The non characteristic harmonic is observed to the $2f_0 \pm 50$ Hz frequency where f_0 shows the induction furnace operating frequency

As a result of the study on power quality problems of induction furnace a new power quality conditioner has been proposed as a solution and it is introduced in chapter five. The varying harmonics and interharmonics problem of induction furnace are not solved with passive filter combinations or selective harmonics elimination based APFs. In the proposed power quality system passive filter and shunt APF combination is used. Such a combination with the passive filter makes it possible to reduce the rating of the active filter. The main advantage of this configuration is to reduce initial costs and to improve efficiency. Our passive filter is only designed to compensate the reactive power. Passive filters are tuned below the operating frequency of furnace to shift the resonance frequency of system. In order to increase performance of active power filter enhanced phase loop lock (EPLL) technique has been used to track distortion and generate reference signal for pulse width modulator (PWM). Shunt APF has both harmonic and interharmonic compensation and reactive power compensation ability.

The simulation has been performed under the carefully chosen four cases in thirteen different conditions by using PSCAD/EMTDC to verify the performance and operation of proposed model. The simulation results show that full reactive power compensation, proper elimination of harmonics and control of the DC Link voltage of the shunt active power filter is achieved. The current total harmonic distortion values that have been obtained by simulation are in a very good level and less than required standards. Using PSCAD/EMTDC as a simulation tool gives many advantages and the most important advantages were rapid simulation response and very easy operation due to visual quality.

In the first case the combination of shunt active filter and shunt passive filter was connected to the system. Connected passive filter consists of four levels. First step compensates 950kVAR and other steps compensate 300kVAR reactive power. All steps of passive filters are tuned to 215 Hz. Remaining reactive power is compensated by the active power filter. The system harmonic, reactive current compensation and DC link control of the active power filter has been achieved satisfactorily, the total harmonic distortion is decreased approximately to %3.5.Because of the reactive power compensation is made by the passive filter the injected current size is acceptable level as shown chapter 6 table 6.1.

In the second case only the shunt active power filter is connected to the network. All of the compensation is made by active filter. The system harmonic, reactive current compensation and DC link control of the active power filter has been achieved satisfactorily; the total harmonic distortion is decreased approximately to %3.5.In this case all of the reactive power compensation was done by the shunt active power filter.

In the third case the shunt active power filter is connected to the system and control circuit of the active filter is set to compensate the harmonics and control the DC link voltage of the active filter. There is no reactive power compensation in the network. The system harmonic current compensation and DC link control of the active power filter has been achieved satisfactorily.

Induction furnace is modeled in detail at first time in the literature. The varying harmonics and interharmonics problem of induction furnace is presented with simulation results. To solve these power quality problems, the shunt active power filter with EPLL controller is proposed. Passive filter which is formed from 4 - step is designed for reactive power compensation to reduce the ratings of shunt active power filter. Shunt active power filters and proposed power compensation system is tested in three case studies. The simulation results show the ability and success of compensation system for induction furnace. The main advantage of the proposed control system extracts harmonic and reactive current components independently; its structure is adaptive with respect to frequency. And also control the DC link voltage of active power filter smoothly.

Finally according to all literature research and simulation results, proposed model is very suitable for implementation to 10 MVA induction furnace systems.

REFERENCES

AHMED M.M., MASOUD M., EL-SHARKAWY A.M., 2009, Design of a Coreless Induction Furnace for Melting Iron, International Conference on Communication, Computer and Power (ICCCP'09)

AL–SHAİKHLİ A.K.M., ABOUD A.A. , 2009, Stirring of Coreless Induction Furnaces, Australian Journal of Basic and Applied Sciences, 3(3): 2926–2934

AMERICAN IRON AND STEEL INDUSTRY INSTITUTE, 2005, A New Roadmap for Transformation of Steelmaking Process

ANNEX I EXPERT GROUP, 2001. An Initial View on Methodologies for Emission Baselines: Iron and Steel Case Study. Organization for Economic Co-operation and Development 2001 International Energy Agency

ANONYMOUS, 2006. Iron and Steel Industry

ANONYMOUS, 2003. Overview of Iron And Steel Industry

ASIMINOAEI L., BLAABJERG. F. , HANSEN S.,2005, Evaluation of Harmonic Detection Methods for Active Power Filter Applications, APEC 2005. Twentieth Annual IEEE, 1:635-641

BALA K.C., 2005, Design Analysis of an Electric Induction Furnace for Melting Aluminum Scrap, AU Journal of Technology, 9, 2:83-88

BAYINDIR, K.C., 2006. Modeling Of Custom Power Devices

BURCH R.F., 2008, Thoughts on Improving the Electric Arc Furnace Model, IEEE Power and Energy Society General Meeting - Conversion and Delivery of Electrical Energy in the 21st Century: 1-5

CHEN D., XİE S., 2004, Review of the control strategies applied to active power filters. IEEE International Conference on Electric Utility Deregulation, Restructuring and Power Technologies (DRPT2004)

DIXON J. W, GARCIA J. J., MORAN L, 1995, Control System For Three-Phase Active Power Filter Simultaneously Compensates Power Factor and Unbalanced Loads, IEEE Transactions on Industrial Electronics, 42, 6:636-641

DUGAN R.C.,CONRAD L.E., 1999, Impact of Induction Furnace Interharmonics on Distribution Systems, IEEE Transmission and Distribution Conference, 2:791-796

ECOFYS, 2009, Methodology for the free allocation of emission allowances in the EU ETS post 2012 .Sector report for the iron and steel industry, Fraunhofer Institute for Systems and Innovation Research

FENTON M.D., 2005. Mineral Commodity Profiles-Iron and Steel.U.S. Geological Survey, Reston, Virginia

GONZALEZ D., BALCELLS J., LOVERA S., LİMA R, 1998, Comparison between Unity Power Factor and Instantaneous Power Theory Control Strategies applied to a Three Phase Active Power Filter, Industrial Electronics Society. Proceedings of the 24th Annual Conference of the IEEE, 2:843- 847

HALPIN S.M., 2005, Comparison of IEEE and IEC Harmonic Standards, IEEE Power Engineering Society General Meeting: 3, 2214-2216

JAIN S.K., AGARWAL P.H.O., 2007, Design Simulation and Experimental Investigations, on a Shunt Active Power Filter for Harmonics, and Reactive Power Compensation, Electric Power Components and Systems 13 10:672-692

IAGAR A., POPA G.N., DINIS C.M, 2009, Assessment of Power Quality for Line Frequency Coreless Induction Furnaces, WSEAS Transactions on Circuits and Systems, 1, 8:115-124

IRAVANİ M.R.,KARİMİ M,GHARTEMANİ, 2003, Online estimation of Steady state and instantaneous symmetrical components, Generation, Transmission and Distribution, IEE Proceedings 150, 5:616-622

ISTANBUL CHAMBER OF COMMERCE, 2008. Turkey's Iron and Steel Industry

IZHAR, HADZER M., MASRI C.M., S.IDRIS, S., 2003, A Study of The Fundamental Principles to Power System Harmonic, Proceedings on National Power and Energy Conference: 223 - 231

KARIMI, GHARTEMANI, M. BAKHSHAI, A.R. MOJIRI, M. 2005, Estimation of Power System Frequency Using Adaptive Notch Filters, IEEE Instrumentation and Measurement Technology Conference, 2:1494-1497

KARIMI,GHARTEMANİ, M. IRAVANİ, M.R., FELLOW, 2004, A Method for Synchronization of Power Electronic Converters in Polluted and Variable-Frequency Environments, IEEE Transactions on Power Systems, 19, 3:1263:1270

KARIMI,GHARTEMANİ, M. IRAVANİ ,M.R., KATİRAEİ F.,2004, Extraction of signals for harmonics, reactive current and network-Unbalance compensation, IEE Proceedings- Generation, Transmission and Distribution, 152,1:137-143

KARIMI,GHARTEMANİ, M.MOKHTARİ, H. IRAVANİ,M.R. SEDİGHY,M 2004,A Signal Processing System for Extraction of Harmonics and Reactive Current of Single- Phase Systems, IEEE Transactions on Power Delivery, 19, 3:979-986

KIYOUMARSI,A. HOUSHMAND,R.-O.-A. ZARGAR, A., R. HASSANZADEH, 2008.Closed Loop Power Control of an Induction Furnace, IEEE Proceedings of the 2008 International Conference on Electrical Machines: 1377, 1-6

LANKFORD, W.T. JR; SAMWAYS, N.L.;CRAVEN, R.F.; MCGANNON, H.E., 1985,The Making, Shaping and Treating of Steel, 10th edition; United States Steel

LINDROOS T.J., 2009.Sectoral Approaches in the Case of the Iron and Steel Industry. VTT Working Papers VTT-WORK–111: 58 p. + app. 11 p.

LUPİ S., 2003. Modeling for research and industrial development in induction heating, Proceedings of the Electromagnetic Processing of Materials International Conference 2003

MARQUES, G.D. 1998, A Comparison of Active Power Filter Control Methods in Unbalanced and Nonsinusoidal Conditions, Industrial Electronics Society. Proceedings of the 24th Annual Conference of the IEEE, 1:444-449

MEO S., PERFETTO A., 2002, Comparison of different Control Techniques for Active Filter Applications, Fourth IEEE International Caracas Conference on Devices, Circuits and Systems, 016:1-6

MOLEYKUTTY G. and KARTİK P B., 2008, Three-Phase Shunt Active Power Filter, American Journal of Applied Sciences 5, 8: 909-916

MONTERO,M.I.M.,CADAVAL,E.L.GONZALEZ,F.B.,2007,Comparison of Control Strategies for Shunt Active Power Filters in Three-Phase Four-Wire Systems, IEEE Transactions On Power Electronics, 22, 1:229-236

MORAN L.,DİXON J., ESPİNOZA J.,WALLACE R.,1999, Using Active Power Filters To Improve Power Quality, 5th Brazilian Power Electronics Conference, COBEP'99:501–511

MOUTTOU S., NGANDUI E., SICARD P., 2001, A novel PWM Current Control Method for AC Harmonic Elimination by Active Power Filter, Electrical and Computer Engineering, Canadian Conference,2:793-797

QUASS U. X, FERMAN M. BRÖKER G, 2007, European Dioxin Inventory. Electric furnace steel plant; Results: pg135-143

PRİCE L., SİNTON J., WORRELL E., PHYLİPSEN D., HU X., Lİ. J., 2001.Energy use and carbon dioxide emissions from steel production in China. Published in Energy 27:429-446

RUDNEV V.,LOVELESS D.,COOK R.,BLACK M.,1999, Power Quality for Induction Melting in Metal Production, TechCommentary Electric Power Research Institute, U.S.A

RUDNICK, H., MORAN, L., J., DIXON, 2003, Active power filters as a solution to power quality problems in distribution Networks, IEEE Power and Energy Magazine: 32-40

SALOR, O. GULTEKIN, B. BUHAN, S. BOYRAZOGLU, B. INAN, T. ATALIK, T. ACIK, A. TERCIYANH, A. UNSAR, O. ALTINTAS, E. AKKAYA, Y. OZDEMIRCI, E. CADIRCI, I. ERMIS, M., 2010. Electrical Power Quality of Iron and steel Industry in Turkey, IEEE Transactions on Industry Applications, 46,1:60-80

SINGH B., AL-HADDAD K., CHANDRA A., 1999, A Review of Active Filters for Power Quality Improvement, IEEE Transactions On Industrial Electronics, 46,5:960-971

SMS MEVAC, The Heart of Steel Making Secondary Metallurgy

TREMAYNE J. F., 1983, Impedance and Phase Balancing of Mains – Frequency Induction Furnaces, IEE Proceedings on Electric Power Applications, 130, (3), pp. 161 – 170.

UNNİKRİSHNAN A.K.,JOSEPH A.,SUBHASH J.T.G.,2006,Three level STATCOM Based Power Quality Solution for a 4 MW Induction Furnace, Power Electronics, Drives and Energy Systems International Conference 1-5

USTA Ö., OZDEMİR E., YUMAK K., Design and Implementation of a Three Phase Four Wire Shunt Active Power Filter

ZAMORA I., ALBİZU I., MAZON A.J.,SAGASTABEİTİA K.J.,FERNANDEZ E., 2003, Harmonic distortion in a steel plant with induction Furnaces, International Conference on Renewable Energies and Power Qualıty'03

CIRRICULUM VITAE

Can Onur TOKUNÇ was born in Adana, Turkey, in 1983.He completed the high school education in Adana. He received his BSc degree in Electrical and Electronics Engineering from Çukurova University in 2005. After completion his B.S training, he has started MSc degree in the department of Electrical and Electronics Engineering in Çukurova University. He has been working in ISDEMIR as electric automation maintenance engineer. His research interests are power quality, power quality devices and control of power converters.